Dissertation

Measuring and Controlling Critical Process Parameters of Pharmaceutical Manufacturing by PAT

to obtain the academic degree of

'Doktor der technischen Wissenschaften'

Graz University of Technology

DI Patrick Wahl

Graz, 2014

Institute of Process and Particle Engineering

Graz University of Technology

Graz, Austria

Research Center Pharmaceutical Engineering GmbH

Graz, Austria

Patrick Wahl

Measuring and Controlling
Critical Process Parameters of
Pharmaceutical Manufacturing by PAT

Dissertation

First assessor

Univ.-Prof. Dr. Johannes G. Khinast
Institute for Process and Particle Engineering
Graz University of Technology, and
Research Center Pharmaceutical Engineering GmbH

Second assessor

Prof. Dr. Thomas De Beer
Laboratory of Pharmaceutical Process Analytical Technology
Ghent University

STATUTORY DECLARATION

I declare that I have authored this thesis independently, that I have not used other than the declared sources / resources, and that I have explicitly marked all material which has been quoted either literally or by content from the used sources.

(Ich erkläre an Eides statt, dass ich die vorliegende Arbeit selbstständig verfasst, andere als die angegebenen Quellen/Hilfsmittel nicht benutzt, und die den benutzten Quellen wörtlich und inhaltlich entnommenen Stellen als solche kenntlich gemacht habe.)

March, 2014 ……

DI Patrick Wahl

Unfortunately,
the work of chemometricians
is still often viewed by the uninitiated
as arcane magic [1].

Acknowledgement

I am grateful for the scientific supervision of Prof. Johannes Khinast throughout my thesis. The discussions gave valuable insights how to properly tackle difficult problems and how to communicate the results to the scientific community.

I also thank Prof. Thomas De Beer for being the second assessor of this thesis and for providing me the opportunity to conduct research at the laboratory for pharmaceutical process analytical technology, with the support of Lien Saerens.

The first principle component for successfully surviving "the struggle through the jungle of my PhD studies" are the colleagues of the formerly PAT group, formerly QbD/PAT group, now known as the CPQC group at RCPE GmbH. I would like to thank Daniel Koller, Nikolaus Balak, Otto Scheibelhofer, Roland Hohl, Daniel Markl, Elena Stocker, Stephan Sacher and Hannah Greiner (in order of appearance) as well as students and interns for the good times and the great support, whenever needed. Especially pointing out over and again "what PhD students need to know" broadened my knowledge of *things*.

Lastly, but most important to me, is the invaluable support throughout the entire "career" as a (PhD) student by Nelly and the whole family – Denise, Reinhard, Nicole, Christa, Marcel, Marianne and Georg. Thank you!

Abstract

Pharmaceutical companies are strongly pushed by regulatory agencies to develop their products and processes according to Quality by Design (QbD) principles ("quality has to be built in by design"). Here Process Analytical Technology (PAT) can significantly help to better understand the processes and their impact on final product quality.

For monitoring of an extrusion process a near-infrared (NIR) probe was located in the die section to measure the active pharmaceutical ingredient (API) concentration profile. By analyzing the API profile the criticality of the influential factors (feeders, screw design and screw speed) on content homogeneity was determined. Using extrusion in conjunction with a hot die face pelletizer pellets were manufactured. A photometric stereo imaging system was used to monitor the pellet size and shape. Different implementations into the product stream were compared, concerning representativeness of the results. Additionally, a broader view how PAT tools are integrated in an extrusion process, its downstream processes and into computerized systems, is presented. This allowed monitoring of process data as well as qualitative and quantitative process state determination.

In the feed frame of an industrial tablet press a NIR probe was implemented for inline monitoring of the content uniformity (API and two main excipients). Significant segregation effects in the last minutes of the process were found and confirmed by UV-Vis analysis of drawn tablets.

Kurzfassung

Regulatorische Agenturen fordern von Pharma-Firmen, dass sie ihre Produkte und Prozesse nach den „Quality by Design“ (QbD) Prinzipien entwickeln. Das bedeutet, dass Qualität bereits durch entsprechende Produktentwicklung sichergestellt werden muss. Hier können Prozessanalytische Technologien (PAT) zu einem besseren Verständnis der Prozesse und deren Auswirkungen auf die Endproduktqualität beitragen.

Zur Überwachung einer Schmelzextrusion (HME) wurde eine Nah-Infrarot (NIR) Sonde zwischen Schnecken und Lochplatte positioniert. Anhand des zeitlichen Verlaufs des Wirkstoffgehalts war es möglich die Kritikalität der Einflussfaktoren (Dosierer, Schneckendesign, Drehzahl) auf die Mischhomogenität zu bewerten. Mittels eines HME-Prozesses und Heißstranggranulierung wurden Pellets hergestellt. Dabei wurde ein Bildanalyse System verwendet um die Pelletgröße und -form zu überwachen. Verschiedene inline Implementierungen wurden hinsichtlich Repräsentativität verglichen. Ferner wird gezeigt, wie PAT in den HME-Prozess, nachgelagerte Formgebungsprozesse und in Computersysteme eingebunden werden kann. Das ermöglichte die Überwachung von Prozessdaten als auch eine Bestimmung des Prozesszustandes.

Im Füllschuh einer Tablettenpresse wurde eine NIR Sonde positioniert um so die Formulierung (Wirkstoff und zwei Hilfsstoffe) zu überwachen. Dabei wurden signifikante Segregationserscheinungen in den letzten Minuten des Prozesses beobachtet und mittels UV-Vis Analyse bestätigt.

Contents

1. Introduction 1

1.1 Motivation 1

1.2 Process Analytical Technology (PAT) 4

1.2.1 Near-Infrared Spectroscopy 6

1.2.2 Raman Spectroscopy 9

1.2.3 Chemical Imaging 10

1.3 Manufacturing Processes and PAT Implementations 11

1.3.1 Tablet Compaction 11

1.3.2 Extrusion 15

1.4 Thesis Content 20

1.5 References 21

2. Inline Monitoring and a PAT Strategy for Pharmaceutical Hot Melt Extrusion 34

2.1 Introduction 34

2.2 Materials and Methods 36

2.2.1 Materials 36

2.2.2 NIR Spectroscopy 37

2.2.3 Chemometric Model 37

2.2.4 HPLC Offline Analysis 40

2.2.5 Extruder 41

2.2.6 Experimental Design 42

2.3 Results and Discussion 43

2.3.1 Selecting a Correct NIR Probe Position 43

2.3.2 Validation of the NIR Model 48

2.3.3 Influential Factors on API Content Uniformity 50

2.4 Conclusion 53

2.5 References 55

3. Hot Melt Extrusion as a Continuous Pharmaceutical Manufacturing Process 58

3.1 Continuous Processing in the Pharmaceutical Industry 58

3.1.1 Continuous HME 60

3.2 Downstream Processing 64

3.2.1 Direct Shaping of Final Product 65

3.2.2 Intermediate Products 68

3.3 PAT Analyzers and Integration 71

3.3.1 Overview of Available PAT Analyzers 72

3.3.2 Integration in the Extruder 76

3.4 Process Integration into Computerized Systems 80

3.4.1 Introduction to Computerized Systems 81

3.4.2 Architecture of Supervisory Control Systems 83

3.4.3 Monitoring the Hot Melt Extrusion Process via SIMATIC SIPAT 86

3.5 Continuous Process Analysis 90

3.5.1 Monitoring of Process Parameters 91

3.5.2 Qualitative Process Analysis 93

3.5.3 Quantitative Spectral Analysis 95

3.6 Conclusion 99

3.7 References 100

4. In-line Implementation of an Image-based Particle Size Measurement Tool to Monitor Hot Melt Extruded Pellets 105

4.1 Introduction 105

4.2 Materials and Methods 107

4.2.1 Materials 107

4.2.2 Methods 108

4.2.3 Reference Particle Analysis 111

4.2.4 Implementation 112

4.3 Results and Discussion 114

4.3.1 Applicability to Pellet Analysis 114

4.3.2 Implementation Evaluation 116

4.3.3 Application to In-line Process Monitoring 120

4.3.4 Application to Process Development ... 124
4.4 Conclusion ... 125
4.5 Literature ... 126

5. PAT for Tableting: Inline Monitoring of API and Excipients via NIR Spectroscopy ... 129
5.1 Introduction ... 129
5.2 Materials and Methods ... 132
5.2.1 Materials ... 132
5.2.2 Tablet Press ... 132
5.2.3 NIR Spectroscopy ... 133
5.2.4 Probe Position in Feed Frame ... 133
5.2.5 UV-Vis Reference Analytics ... 134
5.2.6 Chemometric Model and Mixture Design ... 134
5.3 Results and Discussion ... 137
5.3.1 PCA Analysis to Detect Process Irregularities ... 137
5.3.2 Confirmation of Deviations with UV-Vis ... 138
5.3.3 Inline Monitoring of the Powder Composition ... 139
5.3.4 Quality Improvement Opportunities by Inline Analysis ... 140
5.4 Conclusion ... 141
5.5 References ... 143

6. Summary and Outlook ... 147
6.1 Summary of Major Findings ... 147
6.2 Outlook ... 149
6.3 References ... 151

7. Publications ... 152

List of Abbreviations

Abbreviation	*Meaning*
AOTF	acusto-optical tunable filters
ASA	acetylsalicylic acid
BCS	biopharmaceutics classification system
CARS	coherent anti-Stokes Raman scattering
CU	content uniformity
(C)PP	(critical) process parameter
(C)QA	(critical) quality attribute
EMSC	extended multiplicative signal correction
FDA	United States Food and Drug Administration
HME	hot-melt extrusion
IVR	intra-vaginal ring
LCTF	liquid crystal tunable filters
LIF	laser induced fluorescence
MCR-ALS	multivariate curve resolution – alternating least squares
NCE	new chemical entity
NDA	new drug application
NIR-CI	near infrared-chemical imaging
OCT	optical coherence tomography
PAT	process analytical technology
PCA	principal component analysis
PE	polyethylene
PLS	partial least squares (also: projection to latent structures)
PP	polypropylene
PSD	particle size distribution
QbD	quality by design
RTD	residence time distribution
RTR	real-time release
SIS	spectral interference subtraction
SRS	spatially resolved spectroscopy
SD	standard deviation
THz	terahertz

The connected mathematical problems are rather simple.
Today, 1994, I would like to add:
'as the statistical problems usually are'.

Svante Wold

1. Introduction

1.1 Motivation

The progress of the pharmaceutical industry in developing drugs for many pressing diseases, including cancer and HIV, is tremendous. This is strongly nurtured by advances in the understanding of the complex interactions within the human body, and DNA sequencing. Still, the common manufacturing methods are far behind other industries, when talking about failure rate, efficacy and control. This is expressed in an article published in *The Wall Street Journal* in 2003 [2]:

> *The pharmaceutical industry has a little secret: Even as it invents futuristic new drugs, its manufacturing techniques lag far behind those of potato-chip and laundry-soap makers.*

Although this statement is fairly sensational, it does not fail to fit the facts. When the article was written, the lifecycle of a drug, from a manufacturing point of view, was similar to the following short description. A NCE was developed with lab-scale reactions or bio-cell cultures and had proven efficacy in pre-clinical trials. As the drug (slowly) moved through the clinical phases, optimization of the chemical or biological processes and scale-up were important. For filing of the NDA, prior to marketing of the drug, the capability of repeatable manufacturing of in-spec products had to be proven with three batches. If the end product tests of all three batches were within

predefined specifications, the manufacturing process was accepted. All subsequent changes to an NDA, including (1) components and composition, (2) manufacturing sites, (3) manufacturing process, (4) specifications, (5) container closure system, and (6) labeling, as well as (7) miscellaneous changes and (8) multiple related changes had to be filed again [3].

Because change filings were (and still are) costly and time consuming the manufacturing process was usually frozen, even if improvement possibilities in e.g. cost, quality and raw-materials were known. Hence, the continuous improvement programs, typically applied in most other industries like food, chemistry, petroleum and electronics were not in place.

But, since the appearance of this article a paradigm shift in the pharmaceutical industry has begun. Starting in 2004, the FDA released a series of guidelines, with the aim to promote "a risk based approach" [4] to pharmaceutical development and manufacturing. As part of this approach, the PAT initiative deals with inline process analytics, as opposed to traditional end of line testing. This should ultimately lead to RTR of manufactured drugs. The PAT framework is described as a mechanism to design, analyze, and control pharmaceutical manufacturing processes through the measurement of CPPs which affect CQAs [5]. Thereby a sound scientific knowledge of the processes and their impact on the products needs to be gained. Only by then, an engineering approach of designing pharmaceutical processes such that the final products meet the CQAs, in contrast to a trial-and-error approach, will be possible. This is condensed in the QbD paradigm: "quality cannot be tested into products, it should be built-in or should be by design" [5]. With ICH Q8R [6] the ability to freely operate processes within a design space was introduced, which is important for process control. Thus, by showing profound scientific understanding of the process, optimizations became possible. In order to fully take advantage of this freedom, control strategies based on inline measurements are needed, as stated by ICH Q10 [7]. Now, ten years later, the acceptance of these concepts in industry is still progressing too slow.

Along with the PAT initiative comes continuous manufacturing. As opposed to batch manufacturing, in continuous usually only a small product volume is processed at

once. Here even short fluctuations might impact the final product quality [8]. Therefore PAT is necessary to monitor the process state in real-time and control strategies have to be in place to keep the process within a desired range of operation.

A vision of the desired future of pharmaceutical manufacturing was termed *Plantopia* by McKinsey & Co [9].

> *This version of pharma Plantopia would require full integration, beyond QbD, as well as standard platforms in design and operations. The plant would be highly automated, with Six Sigma performance levels on all key quality parameters. Process controls would be well known and continuously refined. Equipment would be highly precise and ultra fast. Product quality would be built in, and truly scientific process knowledge would exist in both the development and manufacturing groups. Highly skilled technicians would propel continuous improvement in process controls and product design.*

There is still a long road ahead, since regulations are strict, the number and diversity of raw materials is enormous, important PAT sensors are still missing (e.g. powder mass flow rate), the complex influences of process parameters on the measured value (e.g. NIR spectrum) are not fully understood and integration of existing sensors in standard manufacturing equipment is slow. Additionally, control strategies are rather scarce and often a lack of mechanistic understanding of the involved processes is apparent.

The author of this thesis aims to contribute his share to applied research in the area of PAT. Especially the use of spectroscopic tools to inline monitoring of chemical composition and physical parameters of the processed materials shall be pushed forward.

1.2 Process Analytical Technology (PAT)[1]

PAT is a mechanism to design, analyze, and control pharmaceutical manufacturing processes through the measurement of CPPs which affect CQAs, as stated by the FDA [5]. Therefore PAT does not only deal with sensors, but with analysis of data as stated above. By using the knowledge of correlations between CPPs and CQAs, a statistical process model can be obtained. By integrating sensors into the process the necessary data for the models can be obtained to predict the current process state. This should allow tight control of the process. By then PAT can have a significant impact on manufacturing: constant highest quality resulting in higher yield, lower labor costs, as well as faster and leaner processes leading to reduced energy and/or chemicals consumption [9].

For process analysis a wide range of sensors is available. These sensors can be divided in several groups, according to their integration in the process (inline, online, atline) and the number of output variables and interpretation (uni- and multivariate), as shown in Figure 1 and Figure 2. Often multivariate data have a low information density. Exemplarily, a spectrum can consist of 500 measured wavelengths for the prediction of a single variable (e.g. API content). Therefore MVDA is needed for multivariate data.

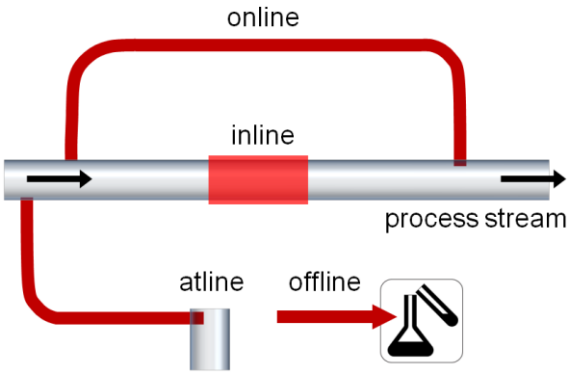

Figure 1: Classification of sensor integration possibilities into the process stream.

PAT is often associated with spectroscopic techniques (NIR, Raman, LIF, UV-Vis, …) and MVDA, because unique real-time information about mixing

[1] Parts of this section are to some extent based on section 15.4 "PAT Analyzers and Integration", which was solely written by the author of this thesis, of the book chapter: D. Treffer, P. Wahl, D. Markl, G. Koscher, E. Roblegg, and J. Khinast, "Hot Melt Extrusion as a Continuous Pharmaceutical Manufacturing Process," in *Melt Extrusion: Equipment and Pharmaceutical Applications*, M. Repka, Ed. Springer Publishers, 2013, pp. 363–396.

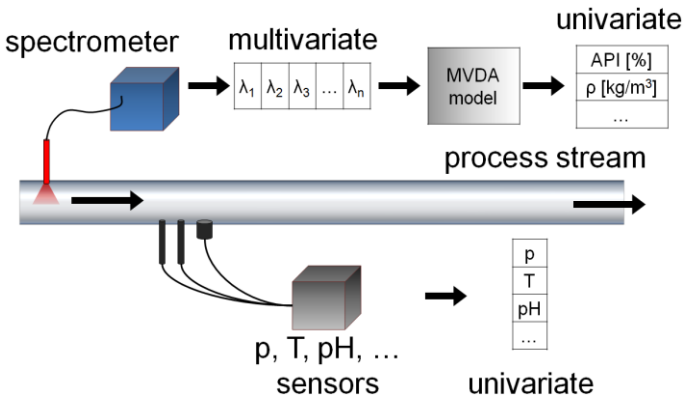

Figure 2: Differentiating between multivariate and univariate sensors. A typical multivariate sensor is spectroscopy, as opposed to univariate sensors for pressure, temperature, pH-value among others.

homogeneity, material composition and physical properties (e.g. crystalline form [10], [11], particle size [12]) is accessible. These techniques cover the wavelength range from UV to NIR (Figure 3). But PAT is by no means limited to that. Classical univariate process sensor, e.g. moisture, pH-value, conductivity, temperature, pressure, torque, energy consumption, microwave dampening, rheology, capacitance among many others can be utilized to determine the state of the process. In contrast to spectroscopic techniques, univariate sensors often have the distinct advantage of measuring a specific property, independent of all others. Thus, in the author's opinion, if a (cheap) univariate sensor for a desired material property is available, it should be preferred to spectroscopic sensors and MVDA models, for its simplicity of use and robustness. Additionally the univariate data (e.g. temperature) can be utilized to correct for its influences on the obtained spectra.

The following sections deal with the two most important and common spectroscopic techniques, NIR and Raman, with a focus on NIR. Both have been extensively reviewed in literature [13]–[16]. In pharmaceutical industry they have mainly been applied to measure homogeneity during blending and

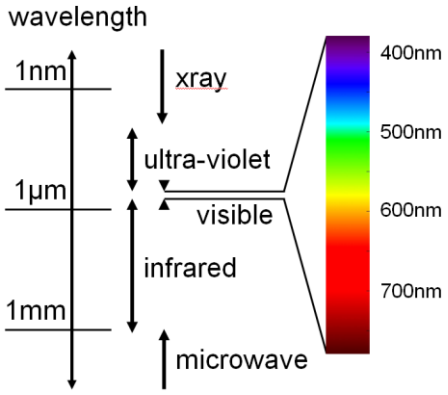

Figure 3: The electromagnetic spectrum of light.

moisture content during granulation and drying, to study chemical or physical interactions (e.g. drug-matrix interactions) and to perform coating analysis. Exemplarily, for blending the homogeneity was assessed by NIR [17], NIR-CI [18], [19] and Raman [20].

NIR and Raman can be used to obtain the spectrum of a single spot, which is the common mode of operation for nearly all inline probes, and to derive a 2D set of spectra from a surface, termed CI. The methods to obtain chemical images with NIR and Raman are different, though.

1.2.1 Near-Infrared Spectroscopy

NIR diffuse reflection spectra are the result of both absorption and scattering [21]–[24]. The sample is irradiated with light in the wavelength range of about 1000 nm – 2500 nm, depending on the spectrometer system. The light photons can be absorbed by the sample's molecules to excite higher vibrational states. Thus, the chemical composition and structure as well as interactions (e.g. H-bonds) define the obtained absorption spectrum. Wavelengths of the incident light, that excite such vibrational states, are absorbed. Therefore less intensity at these wavelengths is reflected back to the detector.

Only molecular vibrations, which result in a change of dipole moment, are NIR active [25]. Therefore, polar bonds show stronger absorption of NIR radiation. Additionally, bonds with a pronounced difference in atomic mass have stronger NIR absorption. Hence, the most prominent bands belong to -CH, -OH and -NH functional groups [26]. For water both criteria are fulfilled, resulting in intense absorption peaks. Within the NIR region mainly overtones and combination vibrations of these functional groups are present, as depicted in Figure 4. An exemplary NIR spectrum of ASA is given in Figure 5. The spectral pattern is also influenced by further physical rules, i.e., Fermi resonance [26], [27].

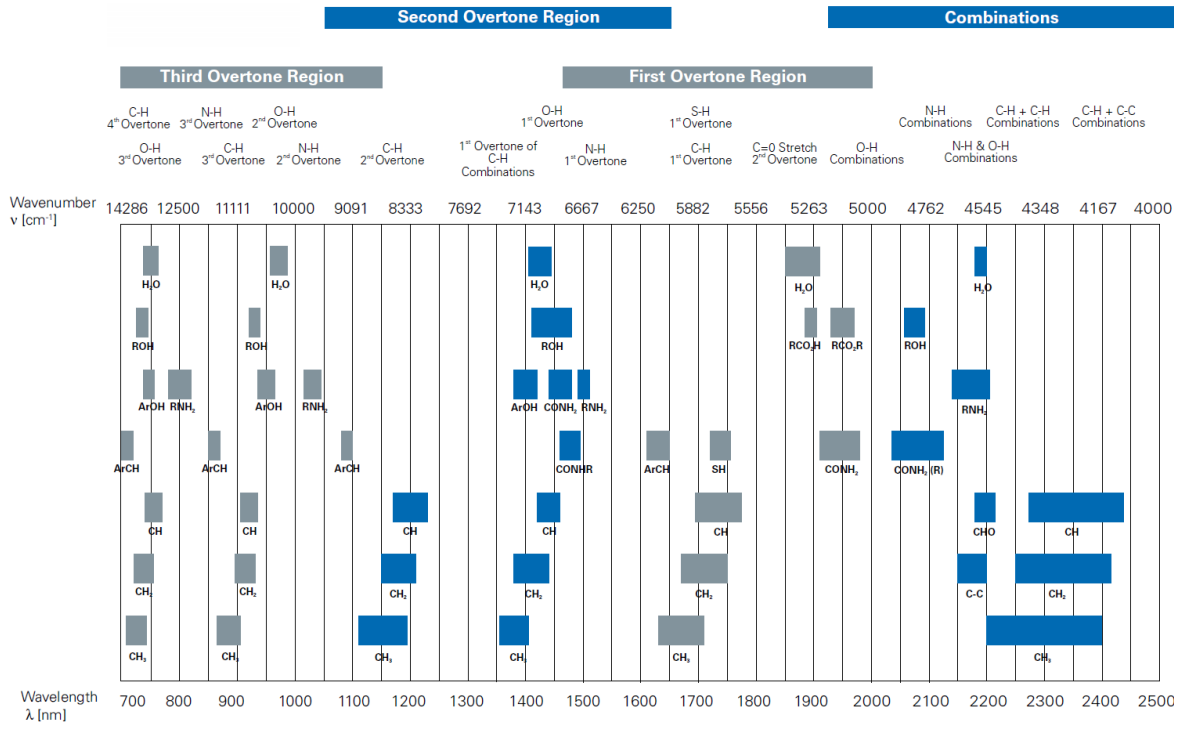

Figure 4: NIR band assignment table (courtesy of Bruker Optics [144]*)*

Absorption and scattering have different physical causes. The absorption spectrum is defined by the vibrational states of a molecule, as stated above. Which vibrational state is occupied or empty depends on temperature, according to the Boltzmann distribution. By changing the temperature, the transition probability between peaks is altered, which in turn changes the relative intensity of peaks in the spectrum. Additionally, peaks can shift by altering the bonding energy ("spring-constant") by molecular interactions. In contrast, scattering is a boundary / inhomogeneity effect in the material's refractive index. Influencing parameters of scattering are particle size, porosity or density of the bulk, as well as surface roughness. Thus, NIR spectra carry chemical and physical information, which ideally are separated for correct interpretation.

Several approaches to separate different aspects of spectra have been published. Burger *et al.* introduces the concept of measuring both, diffuse reflectance and transmittance spectra, to separate scattering and absorption coefficients. For signal acquisition an integrating sphere was used [28]. These separated spectra were used to

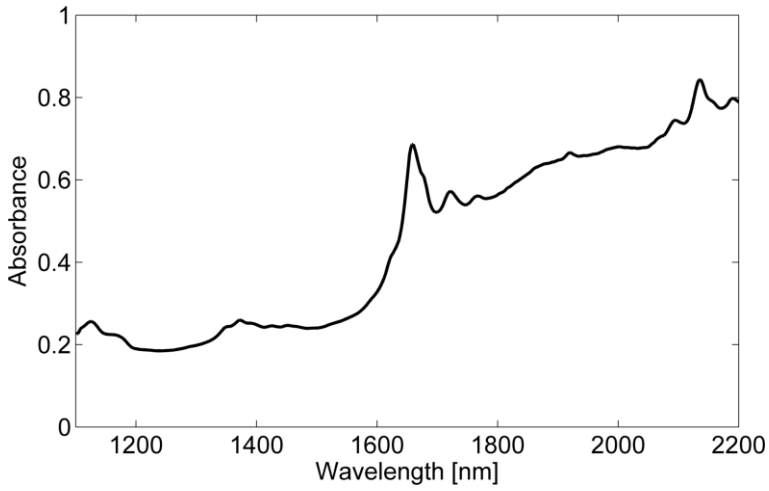

Figure 5: NIR spectrum of ASA, the API of Aspirin®.

predict a binary mixture of paracetamol and lactose with different particle sizes [29]. Often transmittance measurements are not possible, especially inline. Therefore EMSC, a preprocessing method, was used. EMSC allows using prior-knowledge about the spectra of the analytes and interference effects [30], [31]. Thus, for inline measurements obtaining diffuse reflectance spectra is sufficient. For EMSC several extension were developed, including polynomial extension, constituent spectra and orthogonal subspace models [32]. In contrast to EMSC, a method is proposed, which performs reflection and transmission measurements of a single tablet once, using an integrating sphere. The scattering and absorption spectra are then used as hard model constraints of an MCR-ALS modeling algorithm [33]. This approach should result in better predictions and a more robust model, compared to EMSC. For the penetration of light into scattering media (e.g. powders or tablets), important simulation work was also presented and compared to measurements. Equations are derived for the depth origin of reflection and the depth profile of absorption. Data are presented for different scattering and absorption coefficients, arbitrary layer thicknesses, collimated and diffused irradiation, and anisotropic forward scattering [34]. The determination of the depth origin of reflection, which defines the effective sample size, is also discussed by Berntsson *et al.* [35].

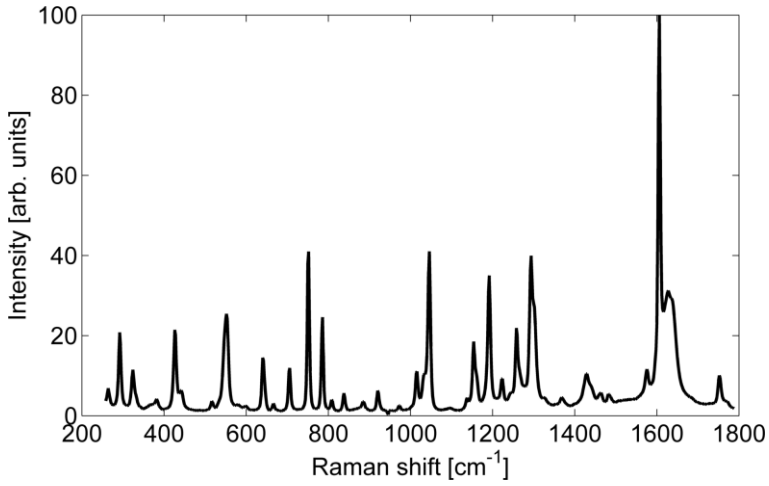

Figure 6: Raman spectrum of ASA.

1.2.2 Raman Spectroscopy

Raman spectroscopy is based on frequency shifts of the reflected light compared to an incident monochromatic laser light. These shifts are caused by inelastic scattering of photons on a molecule. The energy of the frequency shift is used to induce transitions between vibrational states.

There are two types of Raman shifts: Stokes and Anti-Stokes radiation. For Stokes radiation parts of the incident energy is converted to excite higher vibrational states and the scattered light shifts to lower frequencies. At room temperature this is the most commonly observed effect in Raman spectroscopy [26]. At elevated temperatures excited vibrational states can be occupied, according to the Boltzmann distribution [36]. Thus molecules can relax back to the ground state, and a shift towards higher frequencies of the scattered light occurs (Anti-Stokes radiation).

A molecule is Raman active, if the polarizability changes with the inter-atomic distance of a bond [37]. For high polarizability the electrons of the molecule need high mobility. Thus, Raman is well suited to measure non-polar bonds, i.e., C-C, C=C, S-S, N=N [25], like carbon chains and aromatic rings. Raman is well suited to monitor suspensions or slurries, because the spectra are not affected by the presence of water, which is highly polar. In contrast to Raman, the NIR absorbance of polar bonds is

strong, and the two spectroscopic techniques can be used complementary. Additionally the peaks in Raman spectra are much narrower than NIR spectra, because fundamental vibrations are observed, as can be seen by comparing the NIR spectrum (Figure 5) and the Raman spectrum (Figure 6) of the same substance (ASA).

1.2.3 Chemical Imaging

Chemical imaging can be performed with a wide range of spectroscopic techniques and wavelength regions: Raman, IR, NIR, UV-Vis and LIF [38]. The sensors are used to obtain spatially resolved (2D) information of the chemical composition, e.g., the API distribution of a tablet surface. The 2D image cannot be taken in one shot, but via the following approaches: (1) Filter techniques: 2D images of the complete surface, but at a specific wavelength, are taken by a detector chip, using optical band-pass filters for wavelength selection. A 2D image is obtained by wavelength variation using single wavelength filters, AOTF, LCTF or monochromatic illumination [38]. Recent advances using tunable Bragg filters have been made [39]. During acquisition of a chemical image the sample under scrutiny must not move. (2) Pushbroom principle: A 1D line is projected onto a detector chip. The second dimension of the chip is used for wavelength separation by a grating. If the sample is moving in relation to the detector, the surface can be mapped as a function of time (Figure 7). The "surface" can also refer to

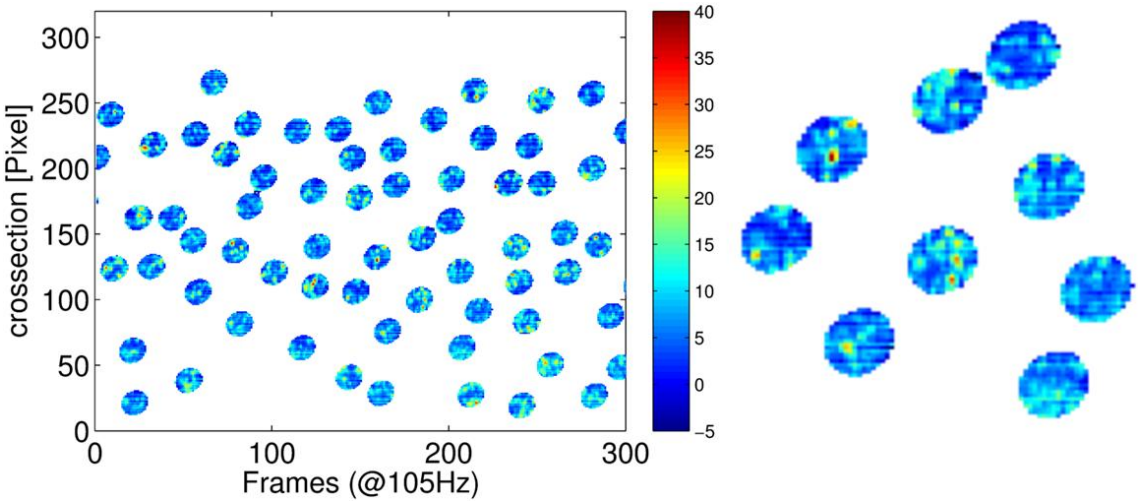

Figure 7: Chemical imaging of tablets consisting of 7% ASA and 93% cellulose. Note the visible aggregation of ASA crystals, indicating non-ideal mixing performance.

the time evolution of the process. For this technique NIR camera systems are used. (3) Rasterizing the surface (whiskbroom principle): The surface is scanned point by point (0D) in x and y direction, resulting in a 2D image. During acquisition the sample must not move. Moreover, measurements are time consuming compared to other methods: to map a tablet with 300x300 pixels, a typical resolution of comparable pushbroom imaging systems, 90,000 single point measurements are necessary.

To map a non-moving sample with high resolution filter techniques are the methods of choice. If a stop-motion is possible, they can be used inline as well. But usually for inline measurements the sample will be in motion, and pushbroom chemical imagers should be preferred. In the author's opinion, tunable filter techniques will replace whiskbroom imaging in lab uses, because of its by far faster acquisition rates.

1.3 Manufacturing Processes and PAT Implementations

Secondary manufacturing of solid pharmaceutical dosage forms relies on many different processes. These include powder handling, mixing, granulation, milling, spray drying, extrusion, pelletizing, spheronization, tablet compaction and coating among many others. It is an elaborate list, even if processes for liquids, pastes, injectables and of primary manufacturing (chemical synthesis and biotech) are still excluded. In this section the emphasis shall be put on those processes, used to perform the experiments for this thesis. Therefore tablet compaction and hot melt extrusion will be dealt with in more detail.

1.3.1 Tablet Compaction

1.3.1.1 Description of the Process

Tablets are still by far the most common and important dosage form. Reasons for this success can be attributed to patient compliance of oral administration and a long shelf life [40]. A definition loosely according to Münzel [41]: tablets are rigid aggregates, manufactured under pressure of a tablet press, which consist of powders, crys-

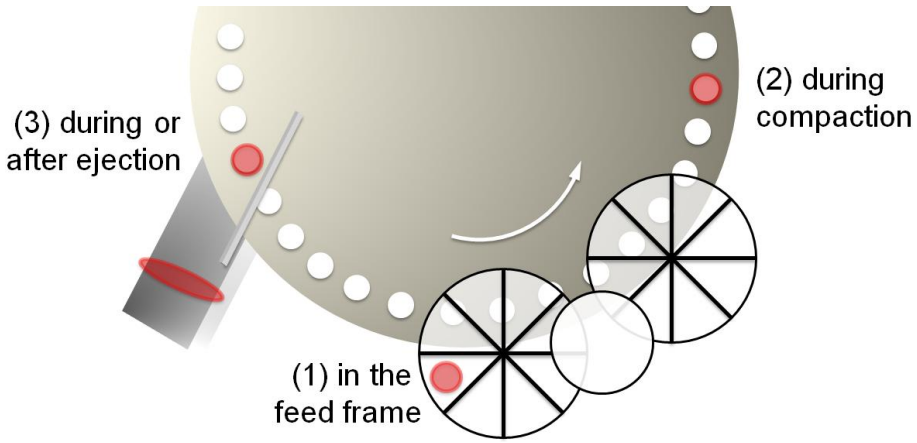

Figure 8: Potential integration positions of PAT monitoring for tablet compaction: (1) in the feed frame, (2) during compaction and (3) during or after ejection.

tals and/or granules and contain an API; commonly radial-symmetric or mirror-symmetric.

This definition does not communicate the complexity of tablet formulations. Many different excipients are necessary to achieve the targeted release characteristics and bioavailability. These include: fillers, binders, adsorbants, glidants, lubricants, disintegrants, flavors and coating [42]. Exemplarily, a time controlled release can be achieved by a drug-matrix system, or an enteric coating is used to protect the drug from the gastric juices. Very likely API and excipients do not have the same material properties like PSD, shape and cohesion, resulting in different flowability and behavior during mixing. Thus, these formulations might be prone to segregation and monitoring the blend composition is important.

1.3.1.2 PAT Applications

From a PAT point of view there are several process steps of potential interest to monitor during compaction: (1) in the feed frame, (2) during compaction, and (3) during or after ejection of the tablets (Figure 8).

Firstly, in the feed frame measuring the homogeneity of the powder was recently published [43]. Here the powder can be monitored as close to filling of the dies as possible, as suggested by [44]. Additionally the analysis of powder with spectral tech-

niques is well known [45]–[49]. This approach was also taken by the author of this thesis [50].

Secondly, during compaction the basic tools of analysis are force-displacement measurements [51], [52]. Important information about particle interaction, i.e. friction and bonding, and plastic properties can be obtained. Also relations to properties of the final tablets can be found, concerning surface structure, crushing strength, friability and disintegration time, as shown by [53]. With ultrasound probes built into the dies, the velocity of wave propagation and ultrasound spectrum during compaction can be obtained [54]–[56]. Thereby the density, mechanical behavior of tablets and possible defects can be detected. Due to the necessity of wiring, up until now ultrasound is not applied to a rotary tablet press.

Lastly, for tablets during or after ejection often spectroscopy (NIR, Raman, LIF, THz) was applied. NIR was used to monitor the homogeneity [57] in combination with physical properties (e.g. hardness) [58]–[62] of tablets. This was also tested during ejection of tablets from the dies [63], at a speed of 6000 tablets/hour. Using NIR-CI techniques the distribution of excipients and API within each tablet can be assessed [64], [65]. Additionally to NIR, the chemical composition of tablets can be measured with LIF [66], [67], for APIs which fluoresce, THz [68], [69] and Raman [70].

Each measurement position and approach has its advantages and drawbacks, which shall be discussed based on NIR spectroscopy. When the powder prior to compaction is measured, clearly, only a small fraction of the overall powder will be sampled. Presuming a proper exchange of powder in the field of view of the probe and an approximately uniform composition of powder in the feed frame, the determined API content should still be representative. However the measurements can be influenced by the density of the powder in front of the probe. Periodic density changes are introduced by the rotating paddle wheel, which can be corrected by appropriate integration times. Towards the process end density changes of the powder itself is an issue [43]. The feed frame approach has no limitations concerning the maximum throughput. Also with NIR-CI very high throughputs can be achieved with reported speeds up to 720.000 tablets/hour [71]. Thereby an inspection of the surface composition of

every single manufactured tablet is possible. This vast amount of data can give additional (visual and statistical) information about the mixing homogeneity or clustering of API and excipients [65].

The ability of NIR to derive information about physical properties is "a blessing and a curse" at the same time. One the one hand tablet hardness is an important QA and therefore valuable information to obtain, but on the other hand this extra degree of freedom of the spectrum has to be included in the model. By successfully separating scattering and absorption effects, a model can be obtained, which is independent of tablet hardness. Otherwise changes in tablet hardness might be misinterpreted as changes in composition.

Another challenge of surface scanning, as opposed to transmission measurements, is the sample volume, which is defined by the penetration depth of NIR radiation into tablets. According to the supplementary data of [72], the transmitted intensity I at λ = 1000 nm in a tablet of 1mm thickness is around $I = I_0/1000$. Thus, only a small fraction of a tablet can be measured, which raises the question of representativeness. In the author's opinion this disadvantage, can be compensated for by appropriate averaging of spectra. Hence, an average volume in the amount of a unit-dose can be obtained, with valuable extra information regarding the mixing homogeneity and tablet-to-tablet variability.

Let's summarize the vast amount of PAT possibilities for tablet compaction. Spectroscopic determination of the formulation composition is an important aspect, which will be essential for RTR strategies. Here NIR is the most wide-spread solution. In the author's opinion two measurement positions for NIR are most beneficial: (1) feed frame monitoring, and (2) surface scanning of the final tablets. For both positions the influence of physical properties (powder density or tablet hardness) shall not be underestimated and need to be taken into account during model development.

1.3.2 Extrusion

1.3.2.1 Description of the Process

Extrusion is a continuous manufacturing process, which processes pellets, powders and/or liquids to form a material of homogeneous composition. A typical formulation for HME comprises of an API, a matrix and functional additives like plasticizers, pore formers or disintegrants. By embedding the drug in a matrix (polymers, lipids or waxes) and by proper selection of plasticizers and process settings unique properties can be achieved. These matrix systems have significant potential to control the drug release profile from immediate to retarded release [73]–[77] and is therefore increasingly gaining interest in the pharmaceutical industry.

On the one hand the bioavailability of poorly soluble drugs can be improved by solid solutions, where the drug is molecularly dispersed in the matrix [76], [78]. This is of great importance because most NCEs are classified as poorly soluble (BCS class II and IV), which is a major challenge to overcome in formulating these NCEs. And on the other hand the release can be retarded for highly soluble drugs by solid dispersions, where the drug is embedded in crystalline form in a slowly dissolving matrix [73]–[75], [79]. Thereby the number of tablets per day needed to maintain certain blood-plasma levels can be reduced, which can be beneficial in pain therapy [77].

Several downstream process are available to form the melt-stream into intermediates or final products: direct shaping via (1) injection molding, (2) shaping calander, (3)

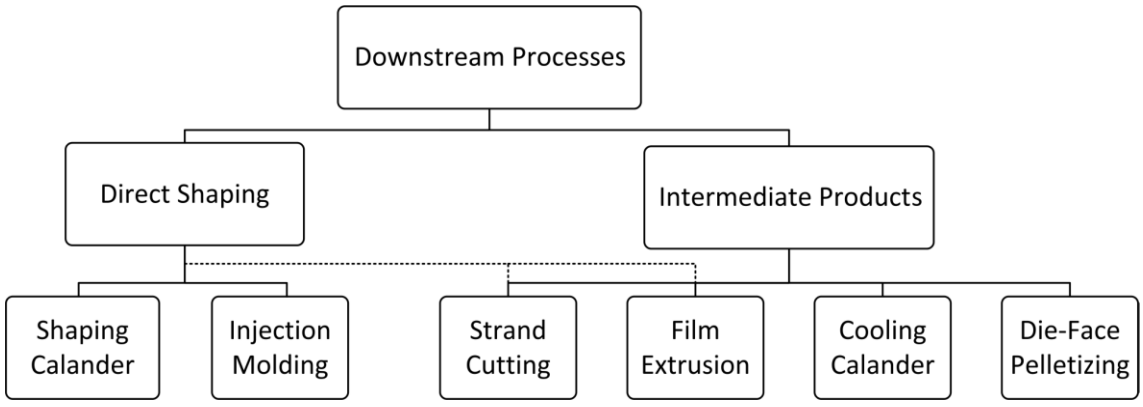

Figure 9: Overview of common downstream processes for extrusion.

co-extrusion or manufacturing of intermediates via (4) strand cutting, (5) die-face pelletizing, (6) film extrusion, (7) cooling calander followed by milling or pelletizing with subsequent spheronization (Figure 9).

With combinations of extrusion and downstream processes many different dosage forms are possible, including pellets [80]–[83] (e.g. for capsules), milled powder [84]–[86] or granules [87]–[89] (e.g. for tablets), foams [90], [91] and directly shaped products like tablets [92], IVRs [93]–[95], implants [96]–[98] and films [99], [100].

1.3.2.2 PAT Applications

For pharmaceutical extrusion several positions for PAT sensors are of interest: (1) Monitoring the powder homogeneity after mixing or during feeding. (2) Along the barrels in proximity of the screw typically univariate sensors are used to monitor temperatures and pressures. Some applications to monitor the RTD or drug-matrix interactions are published. (3) In the die section, or in a custom-made slit die, that can accommodate several sensors. Alternatively bypasses are used to monitor the melt before it is forced through the dies. Typically temperatures and pressures are monitored as well. (4) Monitoring of intermediate or final products, including formulation composition and physical properties like particle size of pellets or the width of films

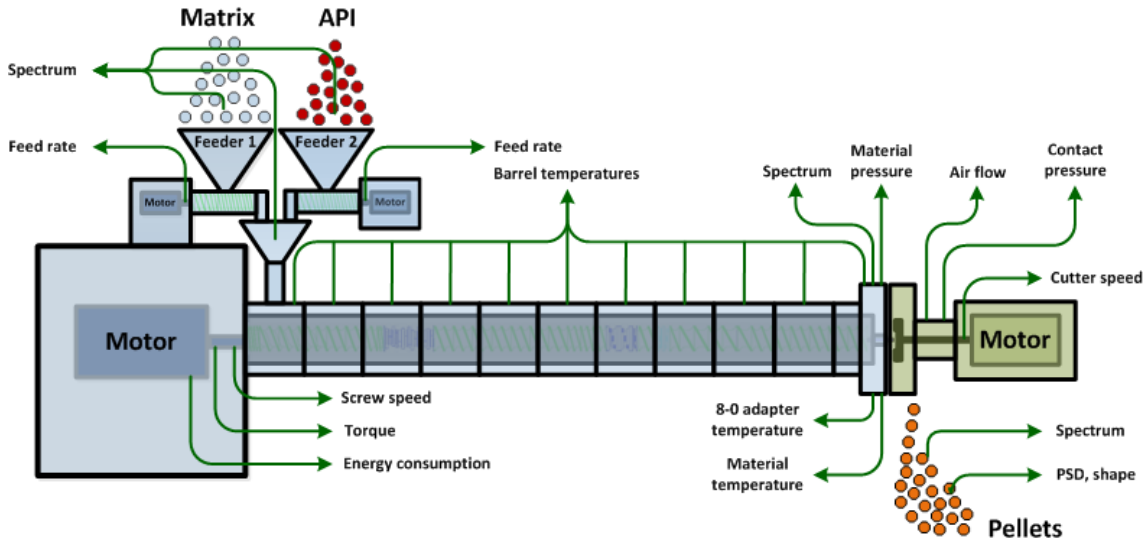

Figure 10: Potential sources of PAT data for a continuous manufacturing line of pellets: HME followed by die-face pelletizing. Here all five mentioned positions for PAT sensors are included.

or layers for co-extrusion. (5) Parameters which can be obtained by the electronic system of the extruder like torque, energy consumption and feed rates (Figure 10).

Most PAT tools for pharmaceutical extrusion were adopted from plastics industry for polymer extrusion [101]. Thus early an application of NIR spectroscopy was published to monitor PE/PP blends during polymer extrusion [102]. Often simultaneous measurement of NIR, Raman, ultrasound [103], [104] and dielectric spectroscopy [105] were performed. A recent review by Alig *et al.* additionally covers small-angle light scattering, to detect process-induced structures during compounding of incompatible polymers, and conductivity to detect conductive fillers [106]. A simple method to separate absorption and scattering spectra is given, by subtracting the pure polymer signal from the spectrum of polymer/clay. Also, the in-line monitoring of morphology of multiphase polymer systems (composites and blends) by means of NIR and ultrasonic spectroscopy is shown [106], [107]. In addition to morphology, the mechanical properties of polymer nanocomposites were monitored with NIR and ultrasonic spectroscopy. The spectra were correlated with off-line rheological measurements, transmission electron microscopy and mechanical tests [108].

With regard to pharmaceutical extrusion, NIR has been used to determine the API content (clotrimazole) of extruded PE oxide films [109] and the API (metoprolol tartrate) content as well as polymer-API interaction [110]. By monitoring the temporal variations of the API (paracetamol) content a mixing homogeneity can be defined. Here different screw designs can be compared on a rational basis [111]. Raman spectroscopy has been applied to determine the API (clotrimazole and ketoprofen) content of melt extruded films [112] and for solid state characterization of the melt to differentiate solid solutions and solid dispersions of metoprolol tartrate [113].

Most of the presented papers either use lab-scale extruders or custom-made slit dies to host the sensors. Without customization of the extrusion equipment, the applicability to monitoring at manufacturing scale is limited. An attempt to monitor the melt composition inline in the extrusion die is published by the author of this thesis [111]. Here the die section had to be modified to ensure high shear forces in the vicinity of the probe to avoid window fouling.

Aside from spectroscopy, rheometers are of interest. The viscosity strongly influences the processability by downstream processes [114]. Several publications deal with the application of on-/atline rheometers. Most of them rely on drawing a sample to measure it, exemplarily with a rotational rheometer [115], [116], or capillary rheometer [117], as the rotating screws do not allow inline measurements.

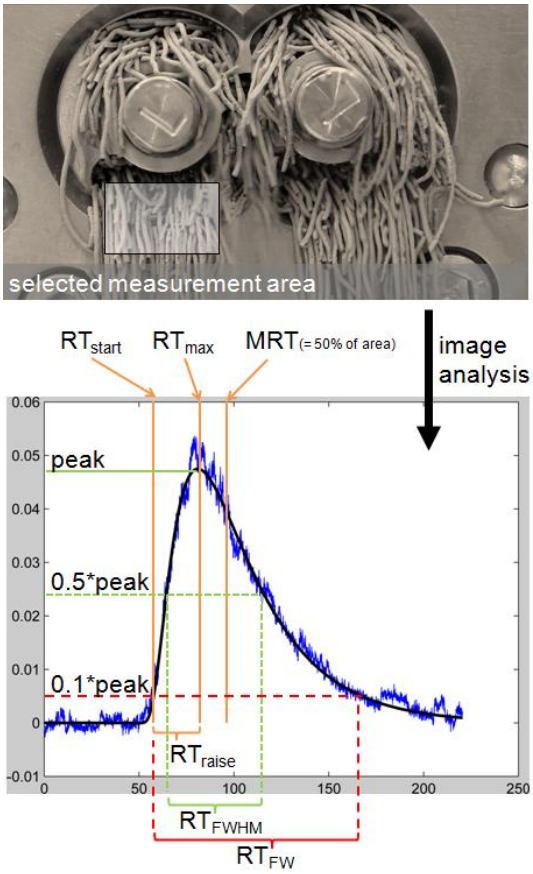

Figure 11: The RTD and several key properties including minimal residence time (RT_{start}) and full width at half maximum of the distribution (RT_{FWHM}) were derived by image analysis of the extruded strands.

Different mixing characteristics of screw configurations result in changes of the RTD. By analysing the RTD curve for each experiment of a DoE, the influence of the process parameters (screw configuration, screw speed, feed rate) can be well understood. Techniques to measure the RTD inline are fluorescence [117]–[119], ultrasound [120], [121], magnetic susceptibility [122], color [123] and NIR-CI [124]. Poulesquen *et al*. mounted three fluorescence probes along the extruder to measure to RTD of the whole extruder, and to derive the local RTD of separate screw sections. The results were successfully compared to simulations of these sections [119]. Most applications of color measurements or digital image processing were offline [125]–[127]. The author of this thesis has developed an inline color measurement method by digital image processing of videos taken from the extruded strands (Figure 11). The RGB values were converted in the LAB color space and the resulting curve was fit by an analytical solution of the RTD for twin screw extruders, by Todd *et al*. [128]. Compared to inline spectrometers this method is less susceptible to window fouling and it uses inexpensive equipment.

For twin screw wet granulation PSD and water content are typical CPPs. PSD determination of granules is still mainly performed by sieve analysis (e.g. [129]–[131]), despite capable in/online analyzers are readily available. A very suitable tool for pellets is based on photometric stereo image analysis, as shown by Fonteyne *et al.* [132], [133] and the author of this thesis (see chapter 4). With changes in PSD the flowability of the granules changes as well [133].

NIR is well suited to determine water content, as shown by early publications [134], [135]. In granulation NIR can be applied to monitor the amount of granulation liquid in the extrudate [133], [136], [137]. Recently the time and space resolved distribution of water in granules was monitored with NIR-CI. Periodic accumulations of water in the granules were found at low water addition rates. By monitoring the temporal change in water content, the RTD could be determined [124]. Complementary to inter granular changes in granulation liquid, the intra-granular distribution of binder was evaluated by hyperspectral CARS microscopy [138].

Final dosage forms manufactured by extrusion also include films and implants. Both can consist of a multilayered structure. Here the layer thickness is of importance, because it either determines the mass of the film and thus the amount of API, or the release characteristics. The thickness of the membrane, to control the API release of an implant, and the API distribution within the core was measured by Raman chemical imaging [98]. Other nondestructive methods to measure layer thickness are OCT and THz, which do not rely on prior model building as long as the refractive indices are known. The coating of tablets was monitored with OCT [139], [140] and THz [141]–[143], but it can be directly transferred to extruded films and implants as well.

In summary, PAT for extrusion monitoring is rapidly gaining interest and several inline applications have been shown. Still, extrusion is a very complex process, which poses difficulties for analytical tools (as well as simulation). Exemplarily, the influences of material temperature, moisture and pressure on spectroscopic and ultrasound measurements is known, but not yet fully understood [111]. Here further research is essential to ensure accurate model performance across a larger operating space. A more complete understanding of the actual process state can only be ob-

tained by combining spectroscopy, PSD analysis and film thickness determination with process data (e.g., torque and material temperature). In the author's opinion, this combination of multi- and univariate data will be of major interest for future developments and could be called a must-have for advanced process control strategies.

1.4 Thesis Content

The thesis deals with the application of PAT tools to pharmaceutical manufacturing of solid dosage forms.

Chapter one introduces the main concepts of QbD and PAT, as well as the driving forces behind this initiative. The necessity of applying PAT to manufacturing should become clear, which is a driving force behind this thesis. The physical principles behind spectroscopy (NIR and Raman), which is commonly associated as the typical PAT tool, are introduced. Their applicability to tablet compaction and extrusion is discussed among other analytical technologies.

Chapter two encompasses inline monitoring of a HME process by NIR spectroscopy. By analyzing the timely varying API content the influential factors (feeders, screw design and screw speed) on content homogeneity were determined and rated according to their criticality.

Chapter three gives a broader view how PAT is embedded in computerized systems, and utilized for monitoring of a continuous HME process and its downstream processes. The variety of available processes is discussed as well.

In chapter four different implementations of a photometric stereo imaging system to monitor pellets produced by HME and die-face pelletizing are compared. Here the focus is put on representativeness of the results.

The monitoring of an industrial tablet press with NIR is shown in chapter five. By monitoring the composition (API and two main excipients) in the feed frame, signifi-

cant segregation effects were observed in the last minutes of the process. These deviations were confirmed by UV-Vis analysis of drawn tablets.

1.5 References

[1] S. J. Doherty and A. J. Lange, "Avoiding pitfalls with chemometrics and PAT in the pharmaceutical and biotech industries," *TrAC Trends Anal. Chem.*, vol. 25, no. 11, pp. 1097–1102, Dec. 2006.

[2] L. Abboud and S. Hensley, "New Prescription For Drug Makers: Update the Plants," *The Wall Street Journal*, 2003. [Online]. Available: http://online.wsj.com/news/articles/SB10625358403931000.

[3] U.S. Food and Drug Administration, "Guidance for Industry. Changes to an approved NDA or ANDA," 2004.

[4] U.S. Food and Drug Administration, "Pharmaceutical cGMPs for the 21st century – A risk based approach; Final Report," 2004.

[5] U.S. Food and Drug Administration, "Guidance for Industry. PAT - a framework for innovative pharmaceutical development, manufacturing, and quality assurance," US Department of Health, Rockville, MD., 2004.

[6] ICH, "ICH Q8(R2), Pharmaceutical Development, Part I: Pharmaceutical development, and Part II: Annex to pharmaceutical development," 2009.

[7] ICH, "ICH Q10, Pharmaceutical Quality System," 2008.

[8] L. Schenck, G. M. Troup, M. Lowinger, L. Li, and C. McKelvey, "Achieving a Hot melt extrusion design space for the production of solid solutions," in *Chemical Engineering in the Pharmaceutical Industry: R&D to Manufacturing*, D. J. am Ende, Ed. John Wiley & Sons Ltd., 2011, pp. 819–836.

[9] A. Gonce and U. Schrader, "Plantopia? A mandate for innovation in pharma manufacturing," in *Operations for the Executive Suite*, D. Keeling and U. Schrader, Eds. 2012, pp. 9–22.

[10] G. Buckton, E. Yonemochi, J. Hammond, and A. Moffat, "The use of near infra-red spectroscopy to detect changes in the form of amorphous and crystalline lactose," *Int. J. Pharm.*, vol. 168, no. 2, pp. 231–241, 1998.

[11] T. Norris, P. K. Aldridge, and S. Sonja Sekulic, "Determination of End-points for Polymorph Conversions of Crystalline Organic Compounds Using On-line Near-infrared Spectroscopy," *Analyst*, vol. 122, no. 6, pp. 549–552, Jan. 1997.

[12] M. C. Pasikatan, J. L. Steele, C. K. Spillman, and E. Haque, "Near infrared reflectance spectroscopy for online particle size analysis of powders and ground materials," *J. Near Infrared Spectrosc.*, vol. 9, pp. 153–164, 2001.

[13] Y. Roggo, P. Chalus, L. Maurer, C. Lema-Martinez, A. Edmond, and N. Jent, "A review of near infrared spectroscopy and chemometrics in pharmaceutical technologies.," *J. Pharm. Biomed. Anal.*, vol. 44, no. 3, pp. 683–700, Jul. 2007.

[14] C. Gendrin, Y. Roggo, and C. Collet, "Pharmaceutical applications of vibrational chemical imaging and chemometrics: a review.," *J. Pharm. Biomed. Anal.*, vol. 48, no. 3, pp. 533–53, Nov. 2008.

[15] T. Vankeirsbilck, A. Vercauteren, W. Baeyens, G. Van der Weken, F. Verpoort, G. Vergote, and J. P. Remon, "Applications of Raman spectroscopy in pharmaceutical analysis," *Trends Anal. Chem.*, vol. 21, no. 12, pp. 869–877, 2002.

[16] T. De Beer, A. Burggraeve, M. Fonteyne, L. Saerens, J. P. Remon, and C. Vervaet, "Near infrared and Raman spectroscopy for the in-process monitoring of pharmaceutical production processes.," *Int. J. Pharm.*, vol. 417, no. 1–2, pp. 32–47, Sep. 2011.

[17] M. Jamrógiewicz, "Application of the near-infrared spectroscopy in the pharmaceutical technology," *J. Pharm. Biomed. Anal.*, vol. 66, pp. 1–10, Jul. 2012.

[18] H. Ma and C. A. Anderson, "Optimisation of magnification levels for near infrared chemical imaging of blending of pharmaceutical powders," *J. Near Infrared Spectrosc.*, vol. 15, no. 3, pp. 137–151, 2007.

[19] A. A. Gowen, C. P. O'Donnell, P. J. Cullen, and S. E. J. Bell, "Recent applications of chemical imaging to pharmaceutical process monitoring and quality control.," *Eur. J. Pharm. Biopharm.*, vol. 69, no. 1, pp. 10–22, May 2008.

[20] T. De Beer, C. Bodson, B. Dejaegher, B. Walczak, P. Vercruysse, A. Burggraeve, A. Lemos, L. Delattre, Y. Vander Heyden, J. P. Remon, C. Vervaet, and W. R. G. Baeyens, "Raman spectroscopy as a process analytical technology (PAT) tool for the in-line monitoring and understanding of a powder blending process.," *J. Pharm. Biomed. Anal.*, vol. 48, no. 3, pp. 772–9, Nov. 2008.

[21] O. Berntsson, L.-G. Danielsson, B. Lagerholm, and S. Folestad, "Quantitative in-line monitoring of powder blending by near infrared reflection spectroscopy," *Powder Technol.*, vol. 123, no. 2, pp. 185–193, 2002.

[22] H. C. Van De Hulst, *Light scattering by small particles*. New York: Dover Publications, Inc., 1981.

[23] C. F. Bohren and D. R. Huffman, *Absorption and scattering of light by small particles*. Weinheim: Wiley-VCH Verlag GmbH & Co. KGaA, 2007.

[24] M. I. Mishchenko, L. D. Travis, and A. A. Lacis, *Scattering, absorption, and emission of light by small particles*. Cambridge: Cambridge University Press, 2002.

[25] M. Reichenbächer and J. Popp, "Schwingungsspektroskopie," in *Strukturanalytik organischer und anorganischer Verbindungen*, Wiesbaden: B.G. Teubner Verlag / GWV Fachverlage GmbH, 2007, pp. 61–118.

[26] H. W. Siesler, "Basic principles of near-infrared spectroscopy," in *Handbook of Near-Infrared Analysis*, 3rd ed., D. A. Burns and E. W. Ciurczak, Eds. Boca Raton: CRC Press, Taylor & Francis Group, 2007, pp. 7–20.

[27] H. W. Siesler, Y. Ozaki, S. Kawata, and H. . Heise, Eds., *Near-Infrared Spectroscopy: Principles, Instruments, Applications*. Weinheim: Wiley-VCH, 2002.

[28] T. Burger, H. J. Ploss, J. Kuhn, S. Ebel, and J. Fricke, "Diffuse reflectance and transmittance spectroscopy for the quantitative determination of scattering and absorption coefficients in quantitative powder analysis," *Appl. Spectrosc.*, vol. 51, no. 9, pp. 1323–1329, 1997.

[29] T. Burger, J. Kuhn, R. Caps, and J. Fricke, "Quantitative Determination of the Scattering and Absorption Coefficients from Diffuse Reflectance and Transmittance Measurements: Application to Pharmaceutical Powders," *Appl. Spectrosc.*, vol. 51, no. 3, pp. 309–317, 1997.

[30] H. Martens and E. Stark, "Extended multiplicative signal correction and spectral interference subtraction: new preprocessing methods for near infrared spectroscopy," *J. Pharm. Biomed. Anal.*, vol. 9, no. 8, pp. 625–635, 1991.

[31] H. Martens, J. P. Nielsen, and S. B. Engelsen, "Light scattering and light absorbance separated by extended multiplicative signal correction. Application to near-infrared transmission analysis of powder mixtures," *Anal. Chem.*, vol. 75, no. 3, pp. 394–404, Feb. 2003.

[32] N. K. Afseth and A. Kohler, "Extended multiplicative signal correction in vibrational spectroscopy, a tutorial," *Chemom. Intell. Lab. Syst.*, vol. 117, pp. 92–99, Aug. 2012.

[33] W. Kessler, D. Oelkrug, and R. Kessler, "Using scattering and absorption spectra as MCR-hard model constraints for diffuse reflectance measurements of tablets.," *Anal. Chim. Acta*, vol. 642, no. 1–2, pp. 127–34, May 2009.

[34] D. Oelkrug, M. Brun, K. Rebner, B. Boldrini, and R. Kessler, "Penetration of light into multiple scattering media: model calculations and reflectance experiments. Part I: the axial transfer.," *Appl. Spectrosc.*, vol. 66, no. 8, pp. 934–43, Aug. 2012.

[35] O. Berntsson, T. Burger, S. Folestad, L. G. Danielsson, J. Kuhn, and J. Fricke, "Effective sample size in diffuse reflectance Near-IR spectrometry.," *Anal. Chem.*, vol. 71, no. 3, pp. 617–23, Feb. 1999.

[36] I. V. Hertel and C.-P. Schulz, "Zweiatomige Moleküle," in *Atome, Moleküle und optische Physik 2*, Heidelberg, 2010, pp. 1–88.

[37] I. V. Hertel and C.-P. Schulz, "Molekülspektroskopie," in *Atome, Moleküle und optische Physik 2*, Heidelberg, 2010, pp. 247–327.

[38] R. W. Kessler, "Chemical imaging," 2013. [Online]. Available: http://www.reutlingen-university.de/uploads/media/chemical_imaging_2013.pdf. [Accessed: 09-Jan-2014].

[39] S. Marcet, M. Verhaegen, S. Blais-Ouellette, and R. Martel, "Raman spectroscopy hyperspectral imager based on Bragg tunable filters," in *Photonics North 2012*, 2012, p. 84121J.

[40] A. Bauer-Brandl and W. A. Ritschel, *Die Tablette*, 3rd ed. Aulendorf: Editio Cantor Verlag, 2012.

[41] K. Münzel, J. Büchi, and O.-E. Schultz, *Galenisches Praktikum*. Stuttgart, 1959, p. 727.

[42] J. G. Khinast, "Pharmaceutical Engineering II: Drug Products and Manufacturing Science." Graz University of Technology, 2013.

[43] H. W. Ward, D. O. Blackwood, M. Polizzi, and H. Clarke, "Monitoring blend potency in a tablet press feed frame using near infrared spectroscopy," *J. Pharm. Biomed. Anal.*, vol. 80, pp. 18–23, 2013.

[44] R. Mendez, F. Muzzio, and C. Velazquez, "Study of the effects of feed frames on powder blend properties during the filling of tablet press dies," *Powder Technol.*, vol. 200, no. 3, pp. 105–116, Jun. 2010.

[45] S. S. Sekulic, H. W. Ward II, D. R. Brannegan, E. D. Stanley, C. L. Evans, S. T. Sciavolino, P. A. Hailey, and P. K. Aldridge, "On-line monitoring of powder blend homogeneity by near-infrared spectroscopy," *Anal. Chem.*, vol. 68, no. 3, pp. 509–513, 1996.

[46] O. Scheibelhofer, N. Balak, P. R. Wahl, D. M. Koller, B. J. Glasser, and J. G. Khinast, "Monitoring Blending of Pharmaceutical Powders with Multipoint NIR Spectroscopy.," *AAPS PharmSciTech*, vol. 14, no. 1, pp. 234–44, Mar. 2013.

[47] O. Scheibelhofer, N. Balak, D. M. Koller, and J. G. Khinast, "Spatially resolved monitoring of powder mixing processes via multiple NIR-probes," *Powder Technol.*, vol. 243, pp. 161–170, 2013.

[48] Y. Sulub, B. Wabuyele, P. Gargiulo, J. Pazdan, J. Cheney, J. Berry, A. Gupta, R. Shah, H. Wu, and M. Khan, "Real-time on-line blend uniformity monitoring using near-infrared reflectance spectrometry: A noninvasive off-line calibration approach," *J. Pharm. Biomed. Anal.*, vol. 49, no. 1, pp. 48–54, 2009.

[49] C. V. Liew, A. D. Karande, and P. W. S. Heng, "In-line quantification of drug and excipients in cohesive powder blends by near infrared spectroscopy," *Int. J. Pharm.*, vol. 386, no. 1, pp. 138–148, 2010.

[50] P. R. Wahl, G. Fruhmann, S. Sacher, G. Straka, S. Sowinski, and J. G. Khinast, "PAT for tabletting: inline monitoring of API and excipients with NIR spectroscopy," *J. Cargo Cult Sci.*, 2041.

[51] G. Ragnarsson and J. Sjögren, "Force-displacement measurements in tableting," *J. Pharm. Pharmacol.*, vol. 37, no. 3, pp. 145–150, Mar. 1985.

[52] C. J. de Blaey and J. Polderman, "Compression of pharmaceuticals. I. The quantitative interpretation of force-displacement curves.," *Pharm. Weekbl.*, vol. 105, no. 9, pp. 241–50, Feb. 1970.

[53] M. Riippi, O. Antikainen, T. Niskanen, and J. Yliruusi, "The effect of compression force on surface structure, crushing strength, friability and disintegration time of erythromycin acistrate tablets," *Eur. J. Pharm. Biopharm.*, vol. 46, no. 3, pp. 339–345, 1998.

[54] J. T. T. Leskinen, S.-P. Simonaho, M. Hakulinen, and J. Ketolainen, "In-line ultrasound measurement system for detecting tablet integrity," *Int. J. Pharm.*, vol. 400, no. 1–2, pp. 104–13, Nov. 2010.

[55] J. T. T. Leskinen, S.-P. Simonaho, M. Hakulinen, and J. Ketolainen, "Real-time tablet formation monitoring with ultrasound measurements in eccentric single station tablet press," *Int. J. Pharm.*, vol. 442, no. 1–2, pp. 27–34, Feb. 2013.

[56] J. D. Stephens, M. V Lakshmaiah, B. R. Kowalczyk, B. C. Hancock, and C. Cetinkaya, "Wireless transmission of ultrasonic waveforms for monitoring drug tablet properties and defects.," *Int. J. Pharm.*, vol. 442, no. 1–2, pp. 35–41, Feb. 2013.

[57] W. Li, L. Bagnol, M. Berman, R. A. Chiarella, and M. Gerber, "Applications of NIR in early stage formulation development. Part II. Content uniformity evaluation of low dose tablets by principal component analysis," *Int. J. Pharm.*, vol. 380, no. 1, pp. 49–54, 2009.

[58] P. Schoenmakers, R. Smits, A. Townshend, M. Blanco, and M. Alcalá, "Content uniformity and tablet hardness testing of intact pharmaceutical tablets by near infrared spectroscopy," *Anal. Chim. Acta*, vol. 557, no. 1, pp. 353–359, 2006.

[59] M. Blanco, M. Alcalá, J. M. González, and E. Torras, "A process analytical technology approach based on near infrared spectroscopy: tablet hardness, content uniformity, and dissolution test measurements of intact tablets.," *J. Pharm. Sci.*, vol. 95, no. 10, pp. 2137–44, Oct. 2006.

[60] R. P. Cogdill, C. A. Anderson, M. Delgado-Lopez, D. Molseed, R. Chisholm, R. Bolton, T. Herkert, A. M. Afnán, and J. K. Drennen, "Process analytical

technology case study, part I: feasibility studies for quantitative near-infrared method development.," *AAPS PharmSciTech*, vol. 6, no. 2, pp. E262–72, Jan. 2005.

[61] R. P. Cogdill, C. A. Anderson, M. Delgado, R. Chisholm, R. Bolton, T. Herkert, A. M. Afnan, and J. K. Drennen, "Process analytical technology case study, part II: development and validation of quantitative near-infrared calibrations in support of a process analytical technology application for real-time release.," *AAPS PharmSciTech*, vol. 6, no. 2, pp. E273–83, Jan. 2005.

[62] S. H. Tabasi, R. Fahmy, D. Bensley, C. O'Brien, and S. W. Hoag, "Quality by design, part I: application of NIR spectroscopy to monitor tablet manufacturing process.," *J. Pharm. Sci.*, vol. 97, no. 9, pp. 4040–51, Sep. 2008.

[63] A. D. Karande, P. W. S. Heng, and C. V. Liew, "In-line quantification of micronized drug and excipients in tablets by near infrared (NIR) spectroscopy: Real time monitoring of tabletting process.," *Int. J. Pharm.*, vol. 396, no. 1–2, pp. 63–74, Aug. 2010.

[64] J. M. Amigo and C. Ravn, "Direct quantification and distribution assessment of major and minor components in pharmaceutical tablets by NIR-chemical imaging," *Eur. J. Pharm. Sci.*, vol. 37, no. 2, pp. 76–82, 2009.

[65] J. M. Prats-Montalbán, J. I. Jerez-Rozo, R. J. Romañach, and A. Ferrer, "MIA and NIR chemical imaging for pharmaceutical product characterization," *Chemom. Intell. Lab. Syst.*, vol. 117, pp. 240–249, 2012.

[66] R. Domike, S. Ngai, and C. L. Cooney, "Light induced fluorescence for predicting API content in tablets: sampling and error," *Int. J. Pharm.*, vol. 391, no. 1–2, pp. 13–20, May 2010.

[67] C. K. Lai, A. Zahari, B. Miller, W. E. Katstra, M. J. Cima, and C. L. Cooney, "Nondestructive and on-line monitoring of tablets using light-induced fluorescence technology," *AAPS PharmSciTech*, vol. 5, no. 1, p. E3, Jan. 2004.

[68] H. Wu, E. J. Heilweil, A. S. Hussain, and M. A. Khan, "Process analytical technology (PAT): effects of instrumental and compositional variables on terahertz spectral data quality to characterize pharmaceutical materials and tablets," *Int. J. Pharm.*, vol. 343, no. 1–2, pp. 148–58, Oct. 2007.

[69] H. Wu, E. J. Heilweil, A. S. Hussain, and M. A. Khan, "Process analytical technology (PAT): quantification approaches in terahertz spectroscopy for pharmaceutical application," *J. Pharm. Sci.*, vol. 97, no. 2, pp. 970–984, 2008.

[70] H. Wikström, S. Romero-Torres, S. Wongweragiat, J. A. Stuart Williams, E. R. Grant, and L. S. Taylor, "On-line content uniformity determination of tablets using low-resolution Raman spectroscopy," *Appl. Spectrosc.*, vol. 60, no. 6, pp. 672–681, 2006.

[71] visiotec GmbH, "Technical description, VisioNIR AS," 2008. [Online]. Available: http://www.visiotec.info/fileadmin/Redakteure_VisioTec/Info_Download/Produktinfo/EN/visionirsolid.pdf.

[72] M. C. Hennigan and A. G. Ryder, "Quantitative polymorph contaminant analysis in tablets using Raman and near infra-red spectroscopies," *J. Pharm. Biomed. Anal.*, vol. 72, pp. 163–171, 2013.

[73] N. Follonier, E. Doelker, and E. T. Cole, "Evaluation of hot-melt extrusion as a new technique for the production of polymer-based pellets for sustained release capsules containing high loadings of freely soluble drugs," *Drug Dev. Ind. Pharm.*, vol. 20, no. 8, pp. 1323–1339, Oct. 1994.

[74] N. Follonier, E. Doelker, and E. T. Cole, "Various ways of modulating the release of diltiazem hydrochloride from hot-melt extruded sustained release pellets prepared using polymeric materials," *J. Control. Release*, vol. 36, no. 3, pp. 243–250, Oct. 1995.

[75] F. Zhang and J. W. McGinity, "Properties of sustained-release tablets prepared by hot-melt extrusion.," *Pharm. Dev. Technol.*, vol. 4, no. 2, pp. 241–50, May 1999.

[76] J. Breitenbach, "Melt extrusion: from process to drug delivery technology.," *Eur. J. Pharm. Biopharm.*, vol. 54, no. 2, pp. 107–17, Sep. 2002.

[77] E. Roblegg, E. Jäger, A. Hodzic, G. Koscher, S. Mohr, A. Zimmer, and J. Khinast, "Development of sustained-release lipophilic calcium stearate pellets via hot melt extrusion.," *Eur. J. Pharm. Biopharm.*, vol. 79, no. 3, pp. 635–645, Nov. 2011.

[78] D. A. Miller, J. T. McConville, W. Yang, R. O. Williams, and J. W. McGinity, "Hot-melt extrusion for enhanced delivery of drug particles.," *J. Pharm. Sci.*, vol. 96, no. 2, pp. 361–76, Feb. 2007.

[79] C. De Brabander, C. Vervaet, and J. . Remon, "Development and evaluation of sustained release mini-matrices prepared via hot melt extrusion," *J. Control. Release*, vol. 89, no. 2, pp. 235–247, Apr. 2003.

[80] C. Vervaet, L. Baert, and J. P. Remon, "Extrusion-spheronisation: a literature review," *Int. J. Pharm.*, vol. 116, no. 2, pp. 131–146, Mar. 1995.

[81] C. R. Young, J. J. Koleng, and J. W. McGinity, "Production of spherical pellets by a hot-melt extrusion and spheronization process," *Int. J. Pharm.*, vol. 242, no. 1–2, pp. 87–92, Aug. 2002.

[82] E. Roblegg, S. Ulbing, S. Zeissmann, and A. Zimmer, "Development of lipophilic calcium stearate pellets using ibuprofen as model drug.," *Eur. J. Pharm. Biopharm.*, vol. 75, no. 1, pp. 56–62, May 2010.

[83] S. Bialleck and H. Rein, "Preparation of starch-based pellets by hot-melt extrusion.," *Eur. J. Pharm. Biopharm.*, vol. 79, no. 2, pp. 440–448, Oct. 2011.

[84] G. Verreck, K. Six, G. Van den Mooter, L. Baert, J. Peeters, and M. E. Brewster, "Characterization of solid dispersions of itraconazole and hydroxypropylmethylcellulose prepared by melt extrusion—part I," *Int. J. Pharm.*, vol. 251, no. 1, pp. 165–174, 2003.

[85] G. P. Andrews, D. S. Jones, O. A. Diak, C. P. McCoy, A. B. Watts, and J. W. McGinity, "The manufacture and characterisation of hot-melt extruded enteric tablets," *Eur. J. Pharm. Biopharm.*, vol. 69, no. 1, pp. 264–273, 2008.

[86] J. Albers, R. Alles, K. Matthée, K. Knop, J. S. Nahrup, and P. Kleinebudde, "Mechanism of drug release from polymethacrylate-based extrudates and milled strands prepared by hot-melt extrusion," *Eur. J. Pharm. Biopharm.*, vol. 71, no. 2, pp. 387–394, 2009.

[87] P. Kleinebudde and H. Lindner, "Experiments with an instrumented twin-screw extruder using a single-step granulation/extrusion process," *Int. J. Pharm.*, vol. 94, no. 1, pp. 49–58, 1993.

[88] B. Van Melkebeke, C. Vervaet, and J. P. Remon, "Validation of a continuous granulation process using a twin-screw extruder," *Int. J. Pharm.*, vol. 356, no. 1, pp. 224–230, 2008.

[89] E. I. Keleb, A. Vermeire, C. Vervaet, and J.-P. Remon, "Twin screw granulation as a simple and efficient tool for continuous wet granulation," *Int. J. Pharm.*, vol. 273, no. 1, pp. 183–194, 2004.

[90] M. R. Thompson, S. Weatherley, R. N. Pukadyil, and P. J. Sheskey, "Foam granulation: new developments in pharmaceutical solid oral dosage forms using twin screw extrusion machinery.," *Drug Dev. Ind. Pharm.*, vol. 38, no. 7, pp. 771–84, Jul. 2012.

[91] K. E. Rocca, S. Weatherley, P. J. Sheskey, and M. R. Thompson, "Influence of filler selection on twin screw foam granulation.," *Drug Dev. Ind. Pharm.*, Oct. 2013.

[92] J. Breitenbach, "Melt extrusion can bring new benefits to HIV therapy," *Am. J. Drug Deliv.*, vol. 4, no. 2, pp. 61–64, 2006.

[93] M. R. Clark, T. J. Johnson, R. T. McCabe, J. T. Clark, A. Tuitupou, H. Elgendy, D. R. Friend, and P. F. Kiser, "A hot-melt extruded intravaginal ring for the sustained delivery of the antiretroviral microbicide UC781.," *J. Pharm. Sci.*, vol. 101, no. 2, pp. 576–87, Feb. 2012.

[94] D. R. Friend, "Intravaginal rings: controlled release systems for contraception and prevention of transmission of sexually transmitted infections," *Drug Deliv. Transl. Res.*, vol. 1, no. 3, pp. 185–193, Apr. 2011.

[95] N. T. T. Dang, M. S. Turner, and A. G. A. Coombes, "Development of intra-vaginal matrices from polycaprolactone for sustained release of antimicrobial agents.," *J. Biomater. Appl.*, vol. 28, no. 1, pp. 74–83, Jul. 2013.

[96] A. Loxley, "Devices and implants prepared using hot melt extrusion," in *Melt Extrusion: Materials, Technology and Drug Product Designs*, vol. 9, M. A. Repka, N. Langley, and J. DiNunzio, Eds. New York, NY: Springer New York, 2013, pp. 281–298.

[97] A. Rothen-Weinhold, K. Besseghir, E. Vuaridel, E. Sublet, N. Oudry, F. Kubel, and R. Gurny, "Injection-molding versus extrusion as manufacturing technique for the preparation of biodegradable implants," *Eur. J. Pharm. Biopharm.*, vol. 48, no. 2, pp. 113–121, 1999.

[98] F. Krier, J. Mantanus, P.-Y. Sacré, P.-F. Chavez, J. Thiry, A. Pestieau, E. Rozet, E. Ziemons, P. Hubert, and B. Evrard, "PAT tools for the control of co-extrusion implants manufacturing process," *Int. J. Pharm.*, vol. 458, no. 1, pp. 15–24, 2013.

[99] C. R. Palem, S. Kumar Battu, S. Maddineni, R. Gannu, M. A. Repka, and M. R. Yamsani, "Oral transmucosal delivery of domperidone from immediate release films produced via hot-melt extrusion technology.," *Pharm. Dev. Technol.*, vol. 18, no. 1, pp. 186–95, Feb. 2013.

[100] J. O. Morales and J. T. McConville, "Manufacture and characterization of mucoadhesive buccal films," *Eur. J. Pharm. Biopharm.*, vol. 77, no. 2, pp. 187–199, 2011.

[101] L. Saerens, C. Vervaet, J. P. Remon, and T. De Beer, "Process monitoring and visualization solutions for hot-melt extrusion: a review," *J. Pharm. Pharmacol.*, Aug. 2013.

[102] D. Fischer, T. Bayer, K. J. Eichhorn, and M. Otto, "In-line process monitoring on polymer melts by NIR-spectroscopy," *Fresenius J. Anal. Chem.*, vol. 359, no. 1, pp. 74–77, 1997.

[103] P. D. Coates, S. E. Barnes, M. G. Sibley, E. C. Brown, H. G. M. Edwards, and I. J. Scowen, "In-process vibrational spectroscopy and ultrasound measurements in polymer melt extrusion," *Polymer (Guildf).*, vol. 44, no. 19, pp. 5937–5949, Sep. 2003.

[104] S. E. Barnes, E. C. Brown, M. G. Sibley, H. G. M. Edwards, I. J. Scowen, and P. D. Coates, "Vibrational spectroscopic and ultrasound analysis for in-process characterization of high-density polyethylene/polypropylene blends during melt extrusion.," *Appl. Spectrosc.*, vol. 59, no. 5, pp. 611–619, 2005.

[105] I. Alig, D. Fischer, D. Lellinger, and B. Steinhoff, "Combination of NIR, Raman, ultrasonic and dielectric spectroscopy for in-line monitoring of the extrusion process," *Macromol. Symp.*, vol. 230, pp. 51–58, 2005.

[106] I. Alig, B. Steinhoff, and D. Lellinger, "Monitoring of polymer melt processing," *Meas. Sci. Technol.*, vol. 21, no. 6, Jun. 2010.

[107] M. P. Villanueva, L. Cabedo, E. Giménez, J. M. Lagarón, P. D. Coates, and A. L. Kelly, "Study of the dispersion of nanoclays in a LDPE matrix using microscopy and in-process ultrasonic monitoring," *Polym. Test.*, vol. 28, no. 3, pp. 277–287, 2009.

[108] D. Fischer, J. Müller, S. Kummer, and B. Kretzschmar, "Real time monitoring of morphologic and mechanical properties of polymer nanocomposites during extrusion by near infrared and ultrasonic spectroscopy," *Macromol. Symp.*, vol. 305, no. 1, pp. 10–17, Jul. 2011.

[109] V. S. Tumuluri, S. Prodduturi, M. M. Crowley, S. P. Stodghill, J. W. McGinity, M. A. Repka, and B. A. Avery, "The use of near-infrared spectroscopy for the quantitation of a drug in hot-melt extruded films.," *Drug Dev. Ind. Pharm.*, vol. 30, no. 5, pp. 505–511, 2004.

[110] L. Saerens, L. Dierickx, T. Quinten, P. Adriaensens, R. Carleer, C. Vervaet, J. P. Remon, and T. De Beer, "In-line NIR spectroscopy for the understanding of polymer-drug interaction during pharmaceutical hot-melt extrusion.," *Eur. J. Pharm. Biopharm.*, vol. 81, no. 1, pp. 237–230, Jan. 2012.

[111] P. R. Wahl, D. Treffer, S. Mohr, E. Roblegg, G. Koscher, and J. G. Khinast, "Inline monitoring and a PAT strategy for pharmaceutical hot melt extrusion.," *Int. J. Pharm.*, vol. 455, no. 1–2, pp. 159–68, Oct. 2013.

[112] V. S. Tumuluri, M. S. Kemper, I. R. Lewis, S. Prodduturi, S. Majumdar, B. A. Avery, and M. A. Repka, "Off-line and on-line measurements of drug-loaded hot-melt extruded films using Raman spectroscopy.," *Int. J. Pharm.*, vol. 357, no. 1–2, pp. 77–84, Jun. 2008.

[113] L. Saerens, L. Dierickx, B. Lenain, C. Vervaet, J. P. Remon, and T. De Beer, "Raman spectroscopy for the in-line polymer-drug quantification and solid state characterization during a pharmaceutical hot-melt extrusion process.," *Eur. J. Pharm. Biopharm.*, vol. 77, no. 1, pp. 158–63, Jan. 2011.

[114] D. Treffer, P. Wahl, D. Markl, G. Koscher, E. Roblegg, and J. Khinast, "Hot melt extrusion as a continuous pharmaceutical manufacturing process," in *Melt Extrusion: Equipment and Pharmaceutical Applications*, M. Repka, Ed. Springer Publishers, 2013, pp. 363–396.

[115] R. Williams, K. Walters, J. A. Covas, J. M. Maia, A. V. Machado, and P. Costa, "On-line rotational rheometry for extrusion and compounding operations," *J. Nonnewton. Fluid Mech.*, vol. 148, no. 1, pp. 88–96, 2008.

[116] S. Mould, J. Barbas, A. V. Machado, J. M. Nóbrega, and J. A. Covas, "Measuring the rheological properties of polymer melts with on-line rotational rheometry," *Polym. Test.*, vol. 30, no. 6, pp. 602–610, 2011.

[117] J. A. Covas, O. S. Carneiro, P. Costa, A. V. Machado, and J. M. Maia, "Online monitoring techniques for studying evolution of physical, rheological and chemical effects along the extruder," *Plast. Rubber Compos.*, vol. 33, no. 1, pp. 55–61, Jan. 2004.

[118] O. S. Carneiro, J. A. Covas, J. A. Ferreira, and M. F. Cerqueira, "On-line monitoring of the residence time distribution along a kneading block of a twin-screw extruder," *Polym. Test.*, vol. 23, no. 8, pp. 925–937, 2004.

[119] A. Poulesquen, B. Vergnes, P. Cassagnau, A. Michel, O. S. Carneiro, and J. A. Covas, "A study of residence time distribution in co-rotating twin-screw extruders. Part II: Experimental validation," *Polym. Eng. Sci.*, vol. 43, no. 12, pp. 1849–1862, Dec. 2003.

[120] R. Gendron, L. E. Daigneault, J. Tatiboueut, and M. M. Dumoulin, "Residence time distribution in extruders determined by in-line ultrasonic measurements," *Adv. Polym. Technol.*, vol. 15, no. 2, pp. 111–125, Jan. 1996.

[121] Z. Sun, C.-K. Jen, C.-K. Shih, and D. A. Denelsbeck, "Application of ultrasound in the determination of fundamental extrusion performance: Residence time distribution measurement," *Polym. Eng. Sci.*, vol. 43, no. 1, pp. 102–111, Jan. 2003.

[122] J. P. Puaux, G. Bozga, and A. Ainser, "Residence time distribution in a corotating twin-screw extruder," *Chem. Eng. Sci.*, vol. 55, no. 9, pp. 1641–1651, May 2000.

[123] C. Gilmor, S. T. Balke, F. Calidonio, and A. Rom-Roginski, "In-line color monitoring of polymers during extrusion using a charge coupled device spectrometer: Color changeovers and residence time distributions," *Polym. Eng. Sci.*, vol. 43, no. 2, pp. 356–368, Feb. 2003.

[124] J. Vercruysse, M. Toiviainen, M. Fonteyne, N. Helkimo, J. Ketolainen, M. Juuti, U. Delaet, I. Van Assche, J. P. Remon, C. Vervaet, and T. De Beer, "Visualization and understanding of the granulation liquid mixing and distribution during continuous twin screw granulation using NIR chemical imaging.," *Eur. J. Pharm. Biopharm.*, Nov. 2013.

[125] G. R. Ziegler and C. A. Aguilar, "Residence time distribution in a co-rotating, twin-screw continuous mixer by the step change method," *J. Food Eng.*, vol. 59, no. 2, pp. 161–167, 2003.

[126] A. Kumar, G. M. Ganjyal, D. D. Jones, and M. A. Hanna, "Digital image processing for measurement of residence time distribution in a laboratory extruder," *J. Food Eng.*, vol. 75, no. 2, pp. 237–244, Jul. 2006.

[127] C. Bi, B. Jiang, and A. Li, "Digital image processing method for measuring the residence time distribution in a plasticating extruder," *Polym. Eng. Sci.*, vol. 47, no. 7, pp. 1108–1113, Jul. 2007.

[128] D. B. Todd, "Residence time distribution in twin-screw extruders," *Polym. Eng. Sci.*, vol. 15, no. 6, pp. 437–443, Jun. 1975.

[129] J. Vercruysse, D. Córdoba Díaz, E. Peeters, M. Fonteyne, U. Delaet, I. Van Assche, T. De Beer, J. P. Remon, and C. Vervaet, "Continuous twin screw granulation: influence of process variables on granule and tablet quality.," *Eur. J. Pharm. Biopharm.*, vol. 82, no. 1, pp. 205–11, Sep. 2012.

[130] D. Djuric, B. Van Melkebeke, P. Kleinebudde, J. P. Remon, and C. Vervaet, "Comparison of two twin-screw extruders for continuous granulation.," *Eur. J. Pharm. Biopharm.*, vol. 71, no. 1, pp. 155–60, Jan. 2009.

[131] K. T. Lee, A. Ingram, and N. A. Rowson, "Comparison of granule properties produced using Twin Screw Extruder and High Shear Mixer: A step towards understanding the mechanism of twin screw wet granulation," *Powder Technol.*, vol. 238, pp. 91–98, Apr. 2013.

[132] M. Fonteyne, J. Vercruysse, D. C. Díaz, D. Gildemyn, C. Vervaet, J. P. Remon, and T. De Beer, "Real-time assessment of critical quality attributes of a continuous granulation process," Dec. 2012.

[133] M. Fonteyne, S. Soares, J. Vercruysse, E. Peeters, A. Burggraeve, C. Vervaet, J. P. Remon, N. Sandler, and T. De Beer, "Prediction of quality attributes of continuously produced granules using complementary pat tools.," *Eur. J. Pharm. Biopharm.*, vol. 82, no. 2, pp. 429–36, Oct. 2012.

[134] J. E. Sinsheimer and N. M. Poswalk, "Pharmaceutical applications of the near infrared determination of water," *J. Pharm. Sci.*, vol. 57, no. 11, pp. 2007–2010, Nov. 1968.

[135] E. Ciurczak, "Uses of Near-Infrared Spectroscopy in Pharmaceutical Analysis," *Appl. Spectrosc. Rev.*, vol. 23, no. 1–2, pp. 147–163, Mar. 1987.

[136] N. Sandler, J. Rantanen, J. Heinämäki, M. Römer, M. Marvola, and J. Yliruusi, "Pellet manufacturing by extrusion-spheronization using process analytical technology.," *AAPS PharmSciTech*, vol. 6, no. 2, pp. E174–83, Jan. 2005.

[137] L. Chablani, M. K. Taylor, A. Mehrotra, P. Rameas, and W. C. Stagner, "Inline real-time near-infrared granule moisture measurements of a continuous granulation-drying-milling process.," *AAPS PharmSciTech*, vol. 12, no. 4, pp. 1050–5, Dec. 2011.

[138] M. Fonteyne, A. L. Fussell, J. Vercruysse, C. Vervaet, J. P. Remon, C. Strachan, T. Rades, and T. De Beer, "Distribution of binder in granules produced by means of twin screw granulation.," *Int. J. Pharm.*, vol. 462, no. 1–2, pp. 8–10, Dec. 2013.

[139] D. M. Koller, G. Hannesschläger, M. Leitner, and J. G. Khinast, "Non-destructive analysis of tablet coatings with optical coherence tomography.," *Eur. J. Pharm. Sci.*, vol. 44, no. 1–2, pp. 142–8, Sep. 2011.

[140] A. Nemeth, R. Gahleitner, G. Hannesschläger, G. Pfandler, and M. Leitner, "Ambiguity-free spectral-domain optical coherence tomography for determining the layer thicknesses in fluttering foils in real time," *Opt. Lasers Eng.*, vol. 50, no. 10, pp. 1372–1376, Oct. 2012.

[141] A. J. Fitzgerald, B. E. Cole, and P. F. Taday, "Nondestructive analysis of tablet coating thicknesses using terahertz pulsed imaging.," *J. Pharm. Sci.*, vol. 94, no. 1, pp. 177–83, Jan. 2005.

[142] L. Ho, R. Müller, M. Römer, K. C. Gordon, J. Heinämäki, P. Kleinebudde, M. Pepper, T. Rades, Y. C. Shen, C. J. Strachan, P. F. Taday, and J. A. Zeitler, "Analysis of sustained-release tablet film coats using terahertz pulsed imaging.," *J. Control. Release*, vol. 119, no. 3, pp. 253–61, Jun. 2007.

[143] R. K. May, M. J. Evans, S. Zhong, I. Warr, L. F. Gladden, Y. Shen, and J. A. Zeitler, "Terahertz in-line sensor for direct coating thickness measurement of individual tablets during film coating in real-time.," *J. Pharm. Sci.*, vol. 100, no. 4, pp. 1535–44, Apr. 2011.

[144] Bruker Optics, "Guide for Infrared Spectroscopy," 2011.

Wise men speak,
because they have something to say;
fools because they have to say something.

Plato

2. Inline Monitoring and a PAT Strategy for Pharmaceutical Hot Melt Extrusion[2]

2.1 Introduction

Over last hundred years and longer, batch processing was the prevailing way to produce pharmaceuticals. However, continuous manufacturing may reduce the required investment capital, labour costs and product waste and can in many cases offer a better product quality [1]. Especially the last point, i.e., the control of product quality makes continuous manufacturing an attractive alternative to current production paradigms. However, continuous manufacturing needs strict process control, since end-of-pipe testing is not feasible in such an environment. Moreover, due to the typically small product volume even short process upsets (e.g., during hopper refilling) can lead to significant output fluctuations [2]. As such, to ensure constant product quality, an adequate control strategy of the entire process must be established.

[2] This chapter is based on: P.R. Wahl, D. Treffer, S. Mohr, E. Roblegg, G. Koscher, and J.G. Khinast, "Inline monitoring and a PAT strategy for pharmaceutical hot melt extrusion.," Int. J. Pharm., vol. 455, no. 1–2, pp. 159–68, 2013.

Hot melt extrusion (HME) is a continuous process that has significant potential for the manufacturing of different dosage forms with an improved control of the drug release profile [3], [4]. The process is well-known and commonly used in plastics industries. HME combines several unit operations in one process to produce homogeneous strands of molten material. The material is typically fed with volumetric or loss-in-weight feeders in the intake zone of the extruder. The solids melt in the plastification zone due to high shear forces and to a lesser extent due to heat transfer via the extruder barrel. Next, the melt is devolatized and subsequently forced into an extrusion die. Depending on the screw configuration, the extruder has a certain mixing capability. Mixing occurs between the plastification zone and the extrusion die, and the extent of mixing depends on the screw design. Cross-sectional mixing is driven by drag flow and back (axial) mixing is driven by pressure flow [5]. Acting as a low pass filter, an extruder can compensate for short-time feeder disturbances in the order of seconds. However, long-term disturbances can affect the product [2], [6]. Feeding is another aspect that depends on many factors [2]. Thus, tight process control, e.g., via spectroscopic tools, is essential for a successful implementation.

Near-Infrared (NIR) and Raman spectroscopy have been extensively reviewed in literature and have been commonly used in the pharmaceutical industry [7]–[9]. They have mainly been applied to measure uniformity during blending and moisture content during granulation and drying, to study chemical or physical interactions and to perform coating analysis. With regard to extrusion, NIR has been used to determine the active pharmaceutical ingredient (API) content of extruded films [10] and the API content and polymer-API interaction directly in the die [11]. Raman spectroscopy has been applied to determine the API content of a melt extruded film [12] and for solid state characterization of the melt [13]. Both spectroscopic techniques were applied to monitor PE/PP (polyethylene/polypropylene) blends during polymer extrusion [14] (often in combination with ultrasound analysis for blend composition of PE/PP [15], [16]. For details concerning advantages and drawbacks of each method see [17].

Many measurement approaches that are successfully used for research purposes (e.g., a custom-made slit die to hold the probes or at-line measurements) can be difficult to

implement for industrial downstream processes, such as die-face pelletizing or calendaring. But the FDA increasingly suggests in-line monitoring and process control of manufacturing processes via the Process Analytical Technology (PAT) initiative [18]. Therefore PAT tools (e.g., spectroscopy) are required, which are not restricted to research only, but can be implemented in a manufacturing environment. Hence in-line NIR spectroscopy can be a valuable tool for process control strategies.

The current study presents a PAT strategy for the production of an API (paracetamol) embedded in a calcium stearate matrix via HME. The API content of the melt was assessed with an NIR probe mounted in-line, close to the extrusion die. Using this setup the extrusion process was monitored to gain a better understanding of the factors impacting content uniformity (CU), as well as API content. Experiments were performed and the extrudate concentration was analyzed with the NIR probe, according to an experimental design involving different API concentrations, screw speeds and screw designs.

2.2 Materials and Methods

2.2.1 Materials

The matrix carrier for the extrusion was calcium stearate CaSt (Werba-Chem GmbH, Austria; mean particle size 16.62 µm) and API was paracetamol (GL Pharma GmbH, Austria, mean particle size 139.2 µm). The paracetamol crystals were embedded in CaSt resulting in a solid dispersion. At the processing temperature CaSt is within its smectic liquid crystalline state and paracetamol remains crystalline. The formulation of calcium stearate and paracetamol, including different plasticizers, introduced by Roblegg et al. [4], offers a versatile system for controlling the API release with a tailored release profile, depending on the material and mass fraction of the plasticizer.

In this study, to reduce the complexity of the system, only API and matrix without additional plasticizers were investigated.

2.2.2 NIR Spectroscopy

NIR spectra were collected in the transflexion mode with a process spectrometer SentroPAT FO (Sentronic GmbH, Germany). The diode array spectrometer has a spectral range of 1100 nm - 2200 nm with a resolution of 2 nm. For in-line monitoring of the melt a fiber-optic Dynisco NIR probe was mounted close to the extrusion die, after the screws. The die section had to be significantly modified to obtain spectra that reflect the existing bulk composition of the melt. Although the Dynisco ports above the screws could also be used for NIR measurements, they were inferior with regard to sample presentation (see below).

For calibration runs the software SentroSuite was used to control the spectrometer and store the data. For each saved measurement 120 spectra were averaged, with an integration time of 0.014 s per spectrum, resulting in the total integration time of 1.68 s per measurement. For runs according to the experimental design, the spectrometer was controlled directly via SIPAT (Siemens AG, Belgium), with spectra taken exactly every 5 s and the integration time of 1.68 s.

2.2.3 Chemometric Model

The chemometric model was developed with the software Simca P+ 12.0 (Umetrics, Sweden). A premix of each API concentration (0% to 60% with 10% increments) was prepared and mixed in the Turbula T2F tumbler blender (Maschinenfabrik Willy A. Bachofen AG, Switzerland) for 20 min at 50 Hz.

Essential for the development of a good model is the API homogeneity of the melt. In HME homogeneity mostly depends on feeding accuracy, which is strongly impacted by the powder properties. Non-cohesive powders with different particle size tend to segregate when agitated [19], [20]. The mean particle size of paracetamol is around eight times larger than that of CaSt. Furthermore, since feeders have a built-in agitator to break up powder bridges for better performance, segregation or local demixing might be an issue. However, CaSt is cohesive, with a flow function of 3.5, as determined with a rotational shear cell FT4 (Freeman Technology, UK). Thus, segre-

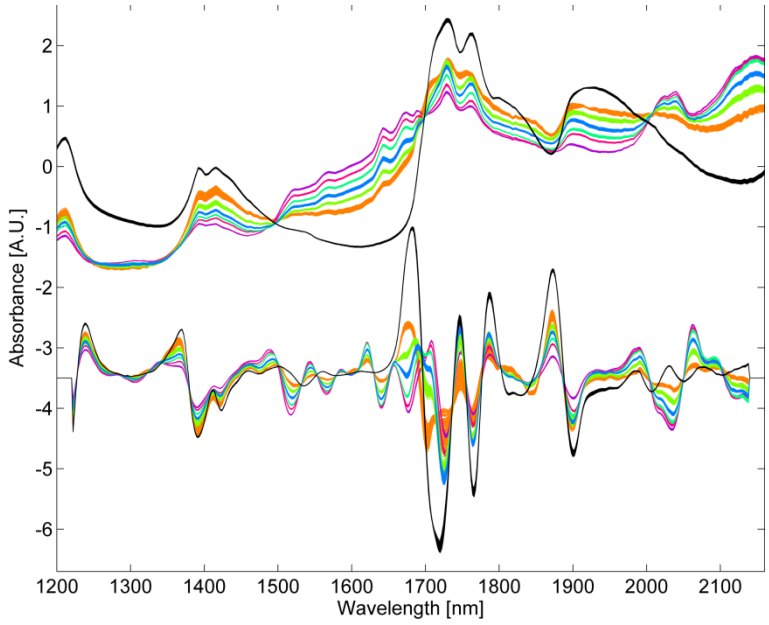

Figure 1: Calibration model spectra after pre-treatment: SNV (above) followed by second-order derivative with Savitzky-Golay smoothing (below, baseline shifted by -3.5). Only 0% paracetamol (black line) had a very different spectrum. The model was developed for the spectral ranges of 1500 nm – 1580 nm, 1860 nm – 1880 nm and 1970 nm – 2050nm.

gation is unlikely to occur. Additionally, to ensure that all spectra used for model development reflect the desired API content (e.g., 30%), the following procedure was established: for each extruded premix around 500 spectra of the melt were collected in-line. After preprocessing, a Principal Component Analysis (PCA) was performed and about 300 of the central spectra were selected. These spectra were expected to represent the bulk API content, assuming deviations (e.g., by local de-mixing) are distributed around a correct mean value. A Partial Least Squares (PLS) model to predict the paracetamol content was established.

The pretreatment methods were standard normal variate (SNV, 1200nm - 2160nm) followed by second-order derivative with Savitzky-Golay smoothing (1200nm - 2160nm, second order polynomial, kernel: 23 points), as shown in Figure 1. The model was developed in the spectral ranges of 1500 nm – 1580 nm, 1860 nm – 1880 nm and 1970 nm – 2050 nm, within which the API groups were well-separated and nearly equidistant. A PCA analysis of the model spectra was performed and the first two PCs are shown in Figure 2. The PLS model consisted of four latent variables, with an R^2 = 0.999 for prediction, Q^2 = 0.974 for validation and a root mean square

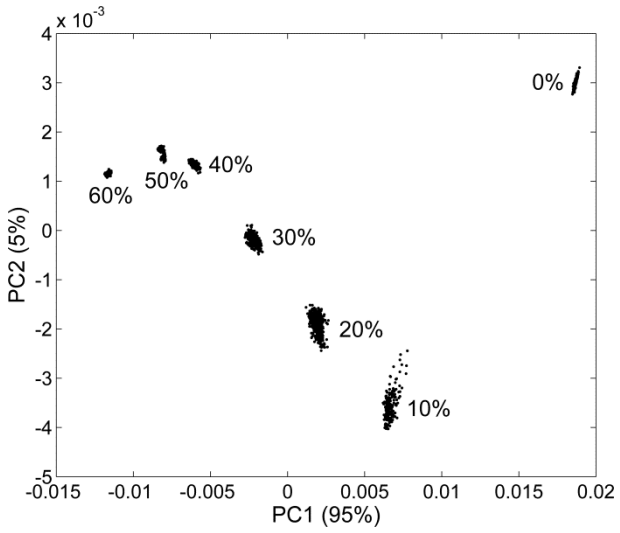

Figure 2: PC1 and PC2 of the model spectra. The PCA was performed in the same spectral range as the model.

error of prediction RMSEP = 0.53% (Figure 3), suggesting a suitable accuracy for process dynamics monitoring. Q^2 for validation was determined by excluding one group of the API content (e.g., 30% premix) from the model and predicting the excluded group.

For cross validation the predictions of the 0% API group were off (around -9% of the correct value), which resulted in a lower $Q^2 = 0.974$ which is still a good overall result. The reason for incorrect predictions was the influence of the API on the optical properties of the melt, which led to different spectral patterns (Figure 1). The embedded API crystals change the melt opacity: pure matrix is more translucent than the matrix with embedded API. Adding only 10% crystalline API made the melt opaque, which significantly lowered the penetration depth of NIR, and thus, reduced the measured volume. Consequently the strongly scattering API had a dominating influence on the diffuse reflected NIR signal, compared to the translucent matrix. Therefore, the spectrum of the 0% API was notably different from the others and could not be predicted without being included in the model, leading to a lower Q^2. By including the 0% premix the predictions of model spectra are correct throughout the whole range from 0% to 60%.

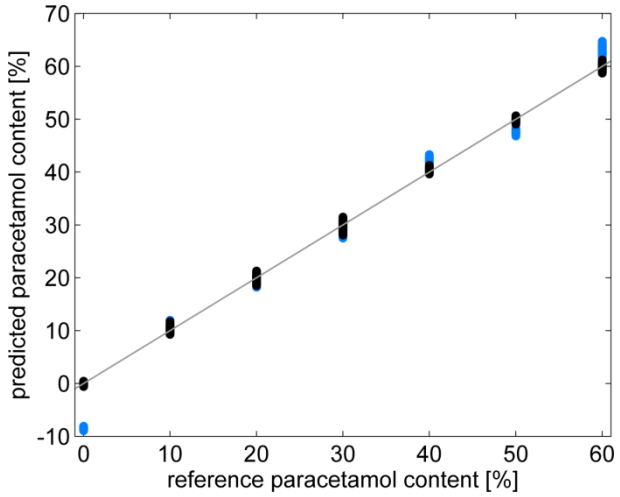

Figure 3: The chemometric model from 0% to 60% API (paracetamol) content in the melt with R^2 = 0.999 (black), Q^2 = 0.974 (blue), RMSEP = 0.53% and four latent variables. Due to the nonlinear behaviour at a low API content, the cross validation (blue) of the 0% group failed. Nevertheless, the predictive capabilities of the model, including 0%, were high.

The change of the spectrum from 0% to 10% is pronounced. Based on these significant differences it was concluded that an API mass fraction of 1% should be accurately detectable. Generally the NIR signal of a solid dispersion, which changes the opacity of a translucent matrix in the low API regime, should be sensitive to concentration changes. This is useful, for example, for monitoring high-potential APIs. The model was used to analyze the temporal changes in the API content for different runs, according to the experimental design (see below).

2.2.4 HPLC Offline Analysis

The extruded strands were collected for five seconds, which corresponds to a sample mass of 833 mg and ground prior to further analysis. 100mg of the ground extrudate were dissolved in 50ml EtOH.

HPLC analysis was carried out with a HP 1090 Liquid Chromatography System (Hewlett Packard, USA) equipped with a diode array detector. A reversed-phase ODS silica column (125x4 mm, PurospherSTAR®, 5 µm RP-18e, VWR international) was used as stationary phase. The mobile phase consisted of an aqueous solution containing 7.6 mM ammonium hydrogenphosphate and 5.4 mM ammonium dihydrogenphosphate adjusted with phosphoric acid 85% to pH 2.6 and methanol (60:40). The mo-

bile was pre-filtered through a 0.2 µm cellulose nitrate filter (Sartorius, Germany) and degassed with helium 5.0 for 10 min. The samples were injected automatically with an autosampler (5 µl), and the flow rate was 0.6 ml/min. Quantification was performed, using a linear regression equation of a four-point calibration.

2.2.5 Extruder

The HME was performed with a co-rotating twin-screw extruder (ZSK 18, Coperion GmbH, Germany). The extruder had a screw diameter of Da=18mm, a ratio of Da/Di = 1.55 and a barrel length of 40 x Da. Fig. 3 illustrates the experimental setup. The raw material was fed with two twin-screw loss-in-weight feeders (K-PH-CL-24-KT20 & K-CL-KT20, K-Tron, Switzerland) into the first barrel. The extruder had eleven barrels, each one individually heated and cooled, except for the first one in the feeding zone. The temperatures of every barrel were set in the beginning of an experiment and kept constant throughout the experiment (see Figure 4). The material properties, NIR-spectrum, pressure (Gefran SPA, Italy, Model: 1E0-A-6-M-B01C-1-4-0, 100 bar) and temperature (Gräff, Troisdorf, Pt-100 sensor, Model: 7143) were measured in the "8-0 adapter" at the end of the extruder, which is a connector between the eight-shaped extruder barrel and a circular, 0-shaped die section.

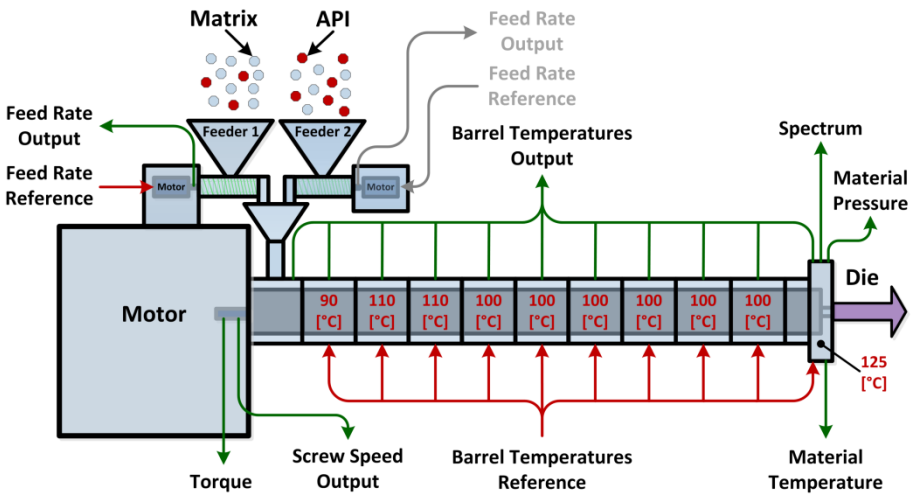

Figure 4: Overview of monitored (green, output), controlled (red, input) and manually controlled (grey) parameters of the extruder and the NIR spectrum close to the die.

2.2.6 Experimental Design

In the experimental study step changes of the concentration were performed to validate the NIR measurements and concentration predictions. The experiments were conducted at a constant throughput of 0.6 kg/h. Due to inferior flowability of the pure substances, which would have resulted in poor feeding accuracy, the feeders were filled with premixes. Feeder 1 was filled with a 20% paracetamol / 80% CaSt premix and feeder 2 with a 50% paracetamol / 50% CaSt premix. The experimental design included (1) a start-up procedure, (2) concentration levels at 20, 30, 40 and 50% mass fraction for 30 minutes and (3) a screw speed change from 150 rpm to 250 rpm. Figure 5 shows the preset concentration profile (black and gray) and the rotational speed of the screw (green). In addition, samples of the extruded strands were collected for offline HPLC analysis every 5 min. The samples were taken at the extrusion die. As such, the strands were cut and the emerging material was collected for 5 s.

Two screw designs were used: a mixing screw with three kneading elements and a conveying screw with conveying elements only (see Figure 6). The kneading elements improve the mixing behaviour of the API and matrix carrier and compensate for feeder dosing fluctuations (e.g., pulsating streams that decrease the product's content homogeneity). The mixing ability of conveying elements is lower compared to kneading elements, which should become evident by higher fluctuations in the predicted API content.

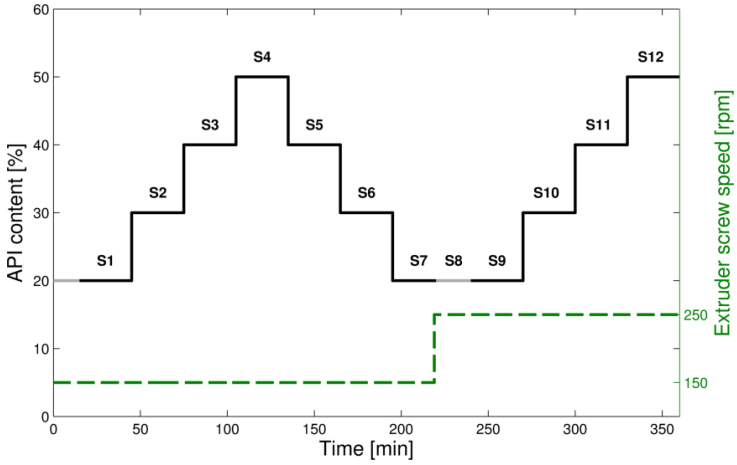

Figure 5: Experimental design that was used for each screw configuration. API concentration steps from 20% to 50% and a change in the screw speed from 150 rpm to 250 rpm.

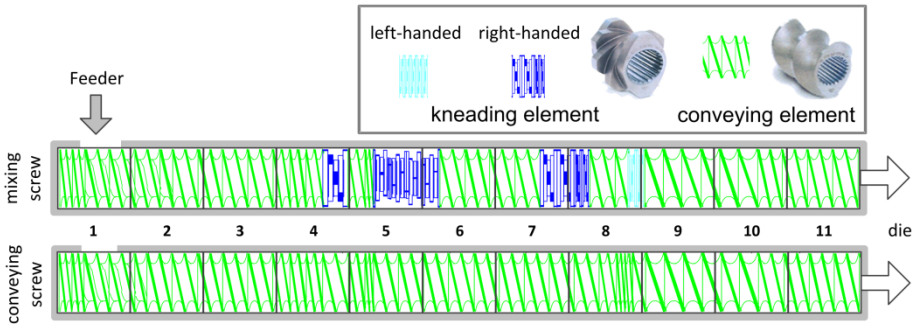

Figure 6: Illustration of the conveying and mixing screw designs.

2.3 Results and Discussion

2.3.1 Selecting a Correct NIR Probe Position

2.3.1.1 Theory of Sampling Considerations

Sampling, either by classical thief sampling based on offline analysis or performed in-line with PAT sensors, is critical for correct measurements. The practical rules defined by the theory of sampling (TOS) [21] were applied to evaluate different measurement positions of the in-line PAT sensor during the extrusion process.

For this purpose the material stream in the 8-0 adapter was approximated as a pressure-driven flow through a pipe. For a material flowing through a pipe it would be ideal to sample an entire cross section [21]. If the API content is a function of the radius, a segment of the circle provides the correct sampling. However, collecting samples close to the barrel wall (which is typically done when using spectroscopic techniques) is only valid when the melt API concentration is completely uniform throughout the entire cross-section. Therefore, the likelihood of a uniform cross section must be analyzed.

Intrinsic fluctuations in the API content are due to feeding fluctuations or content inhomogeneity in the premixes. Thus, a uniform cross section is only possible for a perfect plug flow pattern, which typically is not achieved in the laminar channel flows of viscous melts. By simplifying the die section of the extruder to a single cylinder

with laminar flow of a Newtonian liquid, the flow velocity u can be described using the Hagen–Poiseuille equation as

$$u(r) = -\frac{1}{4\eta}\frac{\Delta P}{\Delta x}(R^2 - r^2) \qquad (1)$$

Here u depends on the viscosity η, the pressure drop ΔP, the length of the cylinder Δx, the cylinder radius R and the radius r of the section in which the flow velocity is calculated. Figure 7 compares the velocity profiles of a perfect plug flow (red) and the one of a laminar Newtonian flow (black) in a tube at the steady state without slip. While the perfect plug has the same velocity u_{av} at every point in the tube, the laminar profile shows a parabolic shape with the maximum velocity u_{max} in the center. The velocity profile for a shear-thinning non-Newtonian liquid is somewhere between the ideal plug flow and the Hagen-Poiseuille profile. The shape of the real profile in the die section of the extruder depends on the rheology [5], [22] and the pulsation of the inlet stream.

As can be seen from Figure 7, the material exchange at the barrel wall, where the probe is typically situated, is small compared to the exchange in the core of the melt, especially if the NIR signal has a low penetration depth. Because of this flow pattern, a sample taken close to the barrel wall does not necessarily represent the overall concentration, but rather the local concentration at the barrel wall.

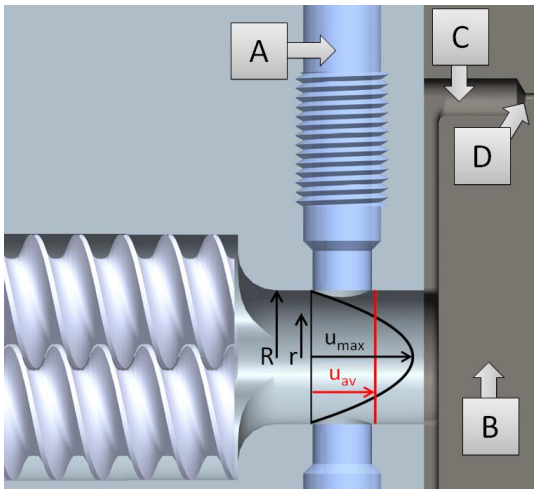

Figure 7: Die section of the extruder where the (A) NIR probe is situated. The figure shows the velocity profile of (red) a perfect plug with constant velocity uav and (black) a Newtonian melt with parabolic shape and a maximum velocity umax in the center. With (B) the die plate, (C) the extrudate channel and (D) the die hole.

2.3.1.2 Application to Spectroscopic Measurements

The TOS rules for thief sampling can be applied to in-line PAT measurements. For in-line spectroscopic sensors the sample volume is defined by several factors: first, by the irradiated volume, which depends on the spot size and penetration depth of the material [23], second, by the transportation velocity of the material in front of the sensor and, third, by the integration time. The sample volume is approximated by

$$V_{Sample} = \frac{d^2}{4} \cdot \pi \cdot \lambda + t \cdot d \cdot \int_{R-\lambda}^{R} v(r) \cdot dr \qquad (2)$$

with the diameter of the illuminating spot d, the penetration depth λ, the velocity of the material $v(r)$, the radius of the die section R and the integration time t. The first term corresponds to the irradiated volume defined by the spot size, while the second term is defined by the movement of the melt through the irradiated volume during the integration time. The integral was solved assuming a circular flow channel, ignoring the plane probe surface.

To calculate the sample volume the mean penetration depth is needed. In pharmaceutical powders the penetration depth is roughly between 100 and 200 µm, strongly depending on particle size and wavelength. However, to our best knowledge, the penetration depth of NIR radiation in CaSt melt is not reported in literature. The penetration depth in melts should be higher compared to powders. Melts have less pronounced scattering centers, because the difference in refractive index between crystal and melt is lower than between crystal and air. For solid dispersions the penetration depth will be highest for a pure matrix. Thus, while raising the drug loading the number of scattering centers (particle-melt boundaries) increases. Therefore, the mean penetration depth was assumed to be λ = 500 µm for an opaque CaSt-paracetamol melt with a high drug loading. This assumption was made to exemplarily study the influence of the flow profile and the penetration depth on the measured volume. The velocity profile $v(r)$ was calculated by assuming a fully developed Newtonian flow. For the setup (d = 3 mm, λ = 500 µm, R = 9 mm, t = 1.68 s, $\dot{M}$ = 0.6 kg/h, ρ = 1100 kg/m^3) with the mass flow $\dot{M}$ and the melt density ρ, the sample volume was estimated as V_{sample} = 3.7 mm^3, according to equation (2). Here the first term domi-

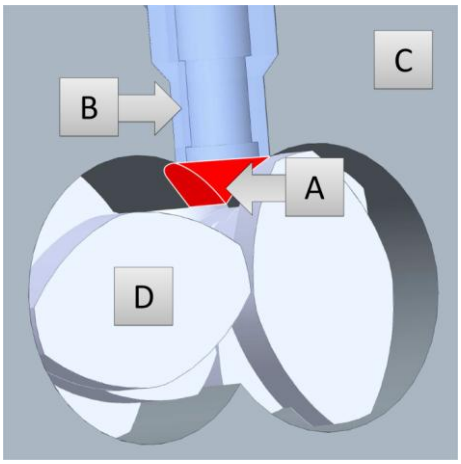

Figure 8: The measurement position directly between the screws. (A) Melt can become trapped in the dead space situated directly in front of the probe. With (B) the Dynisco NIR probe, (C) the extruder barrel and (D) the kneading screws.

nates the resulting sample volume, which indicates a low melt exchange in the measured volume.

From this analysis it is clear that the sample volume is significantly smaller than that collected via thief sampling methods. If the volume is too small compared to the unit dosage form, there might be sub-sampling issues. Sub-sampling can be avoided by choosing a longer integration time or adapting the process to achieve higher velocities of the material. In addition, with a small sample volume only a fraction of the product stream can be monitored. For extrusion purposes, one way to overcome this problem is a smaller inner piping diameter [21], ideally in the order of the penetration depth of the NIR signal. However, there are limitations: the barrel diameter is defined by the extruder specifications and cannot be freely changed.

Special attention must be paid to avoid accumulation of the material in front of the sensor. If accumulation occurs, the sensor signal can be biased strongly and the temporal evolution of material properties cannot be studied correctly. This can be caused due to (1) the probe sapphire window not being in plane with the inner barrel wall for measurements in the 8-0 adapter or (2) an inherent geometrical problem with the sensor design for the measurement position above the screws (Figure 8). The eight-shaped inner barrel wall cannot be reconstructed with the flat probe window. Hence, a dead space is located directly in front of the probe, which will be filled with melt. If

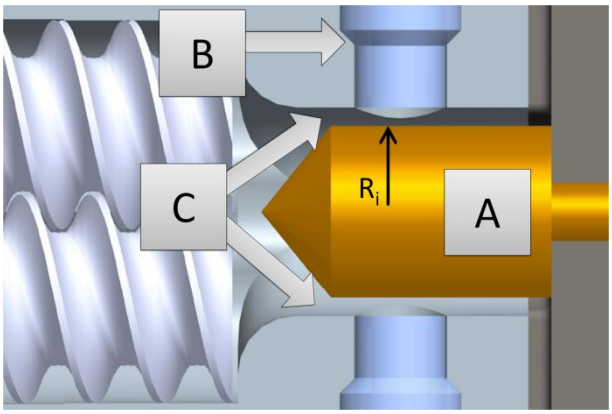

Figure 9: Modifications of the die section and probe: (A) Filling the large melt volume with a tapered metal cylinder ("Apollo" capsule, radius R_i) forming an annular channel at the walls. (B) Turning the 45° face of the probe 1mm to ensure a nearly planar transition between the probe and the barrel wall. (C) This leads to an annular flow of the melt.

the melt viscosity is high, the material exchange within this space will be very slow and the signal does not reflect the actual concentration of the melt.

2.3.1.3 The Modified Measurement Setup

In order to optimize the sampling method, the 8-0 adapter was modified. Inserting a tapered metal cylinder (termed "Apollo" capsule) into the 8-0 adapter created an annular flow pattern at the barrel walls, where the probe was located. To solve the problem of the material accumulation, the NIR probe had to be altered as well. The 45° chamfer of the probe was turned 1 mm to ensure a nearly planar transition between the probe and the barrel wall. Figure 9 shows the sampling region with the modified geometry.

A comparison of the velocity profiles v(r) between the tube flow in the empty die section and the annular flow, as introduced by the "Apollo capsule" with a radius R_i = 7.4 mm, can be seen in Figure 10. The benefit of the annular flow is the increased average velocity due to a smaller cross sectional area and higher shear rates in the vicinity of the probe. According to equation (2) the measured volume nearly doubles to V_{sample} = 6.9 mm^3, caused by the increased velocity at the probe vicinity. The significant advantage of the annular flow is the increased melt exchange, which is around 20 times higher. The disadvantage of the reduced cross section is a higher pressure drop in the

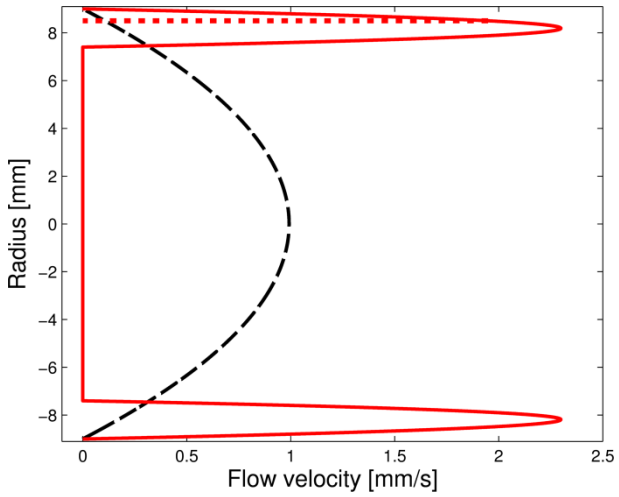

Figure 10: Calculated velocity profiles for circular (black, dashed) and annular (red, solid) flow channel. The measured volume due to melt exchange strongly depends on the penetration depth of the NIR (red, dotted).

region of the "Apollo capsule". However, the cross section of the annular flow (area = 82.4 mm^2) still was 13 times larger compared to the die holes (area = 6.3 mm^2 for eight die holes). Thus the pressure drop was negligible compared to the extrusion die.

From the TOS perspective, this measurement approach requires a circumferentially homogenous melt, since only a segment of the annular flow was measured. However, circumferential fluctuations can be expected to be minor compared to the axial fluctuations due to feeding variations induced by the feeders. The extruder can compensate easily for short term fluctuations, which will result in a good circumferential homogeneity, but is limited in compensation of axial fluctuations with a residence time of about 1-2min. This setup was used for all extrusion runs for model development and API step experiments.

2.3.2 Validation of the NIR Model

The accuracy of the predictions was tested by comparing (1) the predicted API content, (2) the API profile as predefined by the feeder settings and (3) the offline reference measurements with HPLC. Figure 11 shows data for the mixing screw experiment. The predicted API concentration curve is shown in blue and red. The red sections were used later on to calculate the standard deviation (SD) to compare the mix-

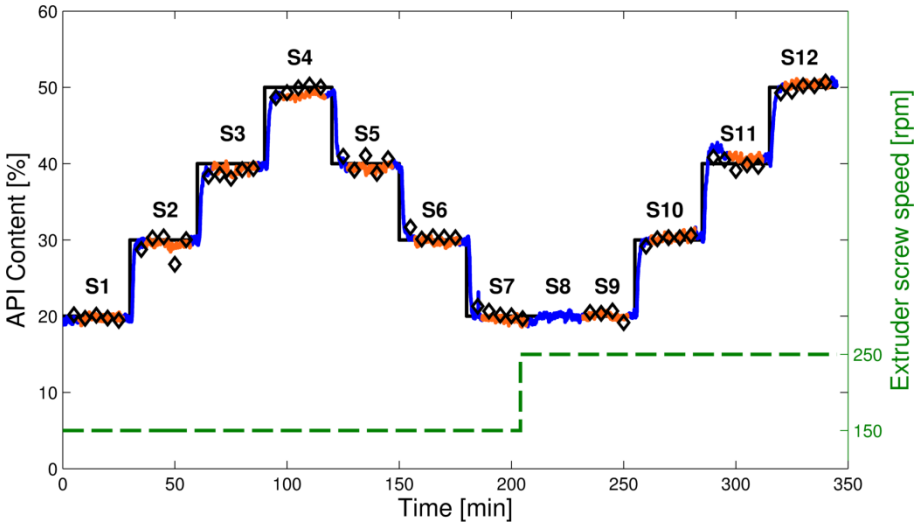

Figure 11: Data for the mixing screw step experiment. Black: preset concentration profile; blue and red: predicted API content; diamonds: offline HPLC measurements; green: screw speed. The predicted drug content was in good agreement with the offline HPLC reference analytics and the preset configuration profile.

ing behaviour. As can be seen there was a very good agreement with the pre-set concentration profile (black). The deviation in the transition from one API content step to the next was due to the residence time in the extruder. Because of the residence time distribution and the mixing behaviour of the extruder, reaching the steady state took about two minutes.

The results of the offline samples are shown with black diamonds. They are in good agreement with the pre-set profile and the NIR prediction. However, one point (out of 55) deviated significantly (10.66%) from the pre-set concentration and can be presumed to be an outlier of the HPLC analysis (which was very sensitive to sampling protocols). The average deviation of all samples was -0.19%, with a SD of 0.87%.

Figure 12 shows data for the conveying screw experiment with the same colour scheme as in Figure 11, except that no offline samples were collected. The API content was predicted with the same model that was used for the mixing screw. The predicted concentration course was in good agreement with the preset concentration. A visual inspection showed only slightly stronger fluctuations of the signal compared to the mixing screw. However, a closer inspection (see below) revealed significant differences.

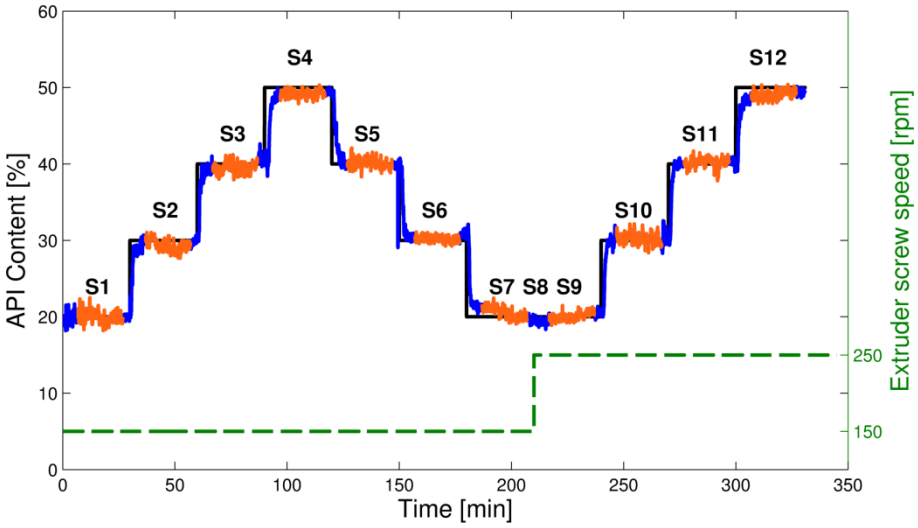

Figure 12: Data for the conveying screw step experiment. Black: preset concentration profile; blue and red: predicted API content; green: screw speed. Note the higher API content fluctuations caused by inferior mixing with the conveying screw.

The NIR signal is influenced not only by the API content, but also by the melt properties, such as moisture, temperature and, possibly, pressure. Evidence of the pressure influence is illustrated in Figure 13. For the mixing screw, during the 20% API content plateau no significant fluctuations were recognizable, whereas the conveying screw showed fluctuations after about 18 min of process time. Here the API content dropped down to around 18%. For the 20% plateau only one feeder was used with a premix. Such fluctuations should not happen unless the premix was not well mixed. Upon examining the collected and archived process data for this event (not shown), a simultaneous pressure peak was detected. Further research needs to be conducted to quantify the influence of the melt properties on the NIR signal. Generally, whenever process parameters are significantly changed, the validity of the model needs to be checked.

2.3.3 *Influential Factors on API Content Uniformity*

The API CU of the extruded strand is critical, since it directly affects the final dosage form. As such, factors that influence the CU must be considered. For the chosen experimental setup the main factors impacting the API CU were: (1) the uniformity of the two premixes, (2) the feeding performance and (3) the mixing behaviour of the

Table 1: Overview of the obtained NIR results.

Screw design	Step	Preset API content [%]	Screw speed [rpm]	Feeding	Average API predicted [%]	Standard deviation [%]
Mixing (Figure 11)	S1	20	150	one feeder	19,8	0,30
	S2	30	150	two feeders	29,5	0,35
	S3	40	150		39,3	0,45
	S4	50	150	one feeder	48,9	0,30
	S5	40	150	two feeders	39,4	0,34
	S6	30	150		29,8	0,33
	S7	20	150	one feeder	19,6	0,31
	S9	20	250		20,0	0,30
	S10	30	250	two feeders	30,4	0,40
	S11	40	250		40,7	0,40
	S12	50	250	one feeder	50,4	0,34
Conveying (Figure 12)	S1	20	150	one feeder	19,9	0,69
	S2	30	150	two feeders	29,3	0,72
	S3	40	150		39,5	0,66
	S4	50	150	one feeder	49,2	0,45
	S5	40	150	two feeders	40,1	0,60
	S6	30	150		30,1	0,39
	S7	20	150	one feeder	20,6	0,70
	S9	20	250		20,1	0,48
	S10	30	250	two feeders	30,2	0,69
	S11	40	250		40,2	0,62
	S12	50	250	one feeder	49,1	0,53

extruder. The uniformity of the premixes was investigated in previous work. Thus the latter two effects were thoroughly examined.

The ability of the two screw designs to achieve CU was compared by analyzing the SD of the concentration signal, which was calculated for the plateaus of each step in API content (red sections in Figure 11 and Figure 12). When the API content significantly deviated for a short time (e.g., due to feeding problems), the data were excluded from

Table 2: Comparing the influence of different process settings on the CU: screw design (mixing, conveying), number of feeders (one, two) and screw speed (150 rpm, 250 rpm). The average SD was calculated based on the aggregation criteria. The ratio of the SD is calculated between high/low settings for each process parameter and screw design.

Screw design	Aggregation criteria	Standard deviation [%]	Ratio
mixing screw	mixing screw	0,345	-
	one feeder	0,310	-
	two feeders	0,375	1,21
	150 rpm	0,338	-
	250 rpm	0,358	1,06
conveying screw	conveying screw	0,593	1,72
	one feeder	0,538	-
	two feeders	0,612	1,14
	150 rpm	0,601	-
	250 rpm	0,578	0,96

the calculation. The average predicted API content and the SD are shown for all feeding levels in Table 1. Note the SD, which is significantly below 1% for all settings. For each plateau the settings of the process parameters, screw design, screw speed and feeder setup, are also given. The results are summarized in Table 2. For better comparison the ratio between high/low settings of each parameter was calculated as follows:

$$\text{ratio} = \frac{SD_{\text{high}}}{SD_{\text{low}}}$$

A ratio > 1 means a higher SD, hence a higher variability in API content, when switching from low settings to high settings (e.g., 150 rpm to 250 rpm for screw speed). The ratio is also calculated between the mixing and the conveying screw.

Based on this analysis, the following conclusions were made:

- The strongest influence on the CU was the screw design: The SD of the conveying screw was 72% higher than that of the mixing screw. Apart from uniformity, the transient time of the extruder also depends on the screw design. The transient time is the delay from changes of the feeder settings until these

changes are detected by the NIR probe in the 8-0 adapter, and is thus an indicator of the residence time. The mixing screw had a longer transient time (Figure 13), which is as expected for additional kneading blocks.

- In addition, the effect of the number of feeders was evident. Compared to a single feeder, split feeding increased the SD by 21% and 14% for the mixing and conveying screws, respectively. This suggests that the more feeders are used, the higher the API content fluctuations are, which can probably be attributed to the superposition of the feeder fluctuations.
- Lastly, although the screw speed also is known to influence the mixing ability of the extruder and thereby the uniformity, no evidence of that was found for the given experimental setup. The SD increased by 6% for the mixing screw, but decreased by 4% for the conveying screw. A change in the screw speed from 150 rpm to 250 rpm had no significant influence on the API CU. Possibly this influence could not be detected, because the melt was already well mixed at low screw speed. The changes in SD might be caused by minor process instabilities.

2.4 Conclusion

This paper presented the development and application of a PAT strategy for quality

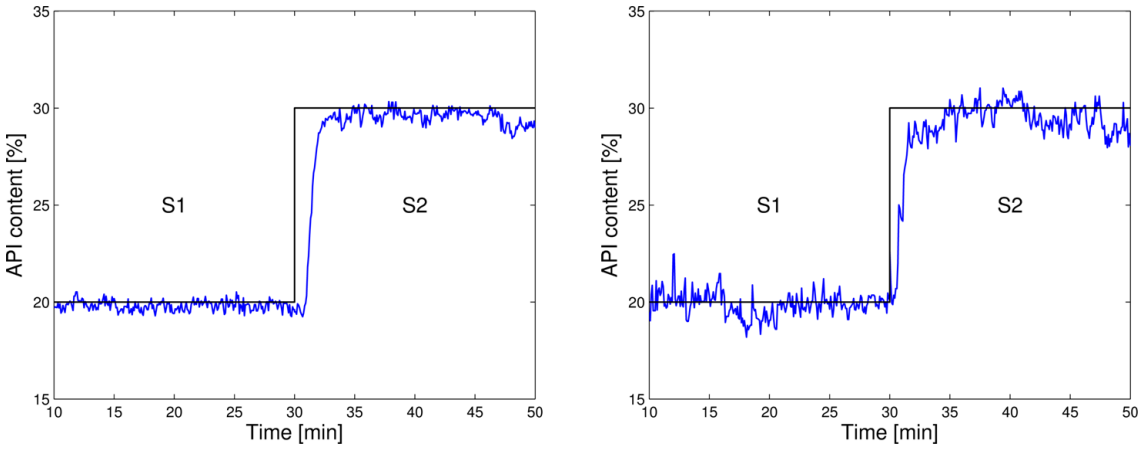

Figure 13: API content (blue) monitored during the step transition from 20% (S1) to 30% (S2) API content. Left: mixing screw; right: conveying screw. Note the differences in the uniformity and the transient time. Black, straight line: preset feed rate.

control of a pharmaceutical hot-melt extrusion process with in-line NIR spectroscopy. Measurements were performed close to the die, in the 8-0 adapter. A chemometric model was developed in a range of 0% to 60% API content. Predictions were in good agreement with the pre-set API content (as determined via feeding rates) and with the offline HPLC reference measurements.

The 8-0 adapter was modified for proper sample preparation. Higher material exchange rates were achieved by introducing a tapered metal cylinder ("Apollo capsule"), which forced the melt into an annular flow with high shear rates in the 8-0 adapter. Due to these modifications, a representative sample presentation was obtained.

Using this setup, experiments with step changes in the API content were performed and the screw speed and design were varied. By analyzing the SD, the most important process parameters for the API CU were identified: the screw design and the number of feeders. The mixing screw was superior to the conveying screw in reducing short-term fluctuations, and employing two feeders simultaneously caused more fluctuations, probably due to the superposition of the feeder fluctuations. For our setup, the change in the screw speed from 150 rpm to 250 rpm did not significantly affect the uniformity.

Our analysis indicates that NIR is a suitable method for monitoring the API content during production and for analyzing the extrusion dynamics. The presented PAT strategy can also be seen as a step towards real-time release of HME-based products.

Future research shall investigate the influence of process parameters as pressure or melt temperature on the measured NIR signal.

Acknowledgements

The authors thank G.L. Pharma GmbH (Lannach, Austria) for supporting this work and providing paracetamol and CaSt. Furthermore, the authors would like to thank the extrusion group at the RCPE GmbH for their great effort.

2.5 References

[1] K. Plumb, "Continuous processing in the pharmaceutical industry," *Chem. Eng. Res. Des.*, vol. 83, no. 6, pp. 730–738, Jun. 2005.

[2] L. Schenck, G. M. Troup, M. Lowinger, L. Li, and C. McKelvey, "Achieving a hot melt extrusion design space for the production of solid solutions," in in *Chemical Engineering in the Pharmaceutical Industry: R&D to Manufacturing*, D. J. am Ende, Ed. John Wiley & Sons, inc., 2011, pp. 819–835.

[3] J. Breitenbach, "Melt extrusion: from process to drug delivery technology.," *Eur. J. Pharm. Biopharm.*, vol. 54, no. 2, pp. 107–17, Sep. 2002.

[4] E. Roblegg, E. Jäger, A. Hodzic, G. Koscher, S. Mohr, A. Zimmer, and J. Khinast, "Development of sustained-release lipophilic calcium stearate pellets via hot melt extrusion.," *Eur. J. Pharm. Biopharm.*, vol. 79, no. 3, pp. 635–645, Nov. 2011.

[5] C. Rauwendaal, *Polymer Extrusion*, 4th ed. Munich: Hanser Publishers, 2001, p. 781.

[6] R. Mudalamane and D. I. Bigio, "Process variations and the transient behavior of extruders," *AIChE J.*, vol. 49, no. 12, pp. 3150–3160, 2003.

[7] T. De Beer, A. Burggraeve, M. Fonteyne, L. Saerens, J. P. Remon, and C. Vervaet, "Near infrared and Raman spectroscopy for the in-process monitoring of pharmaceutical production processes.," *Int. J. Pharm.*, vol. 417, no. 1–2, pp. 32–47, Sep. 2011.

[8] C. Gendrin, Y. Roggo, and C. Collet, "Pharmaceutical applications of vibrational chemical imaging and chemometrics: a review.," *J. Pharm. Biomed. Anal.*, vol. 48, no. 3, pp. 533–53, Nov. 2008.

[9] T. Vankeirsbilck, A. Vercauteren, W. Baeyens, G. Van der Weken, F. Verpoort, G. Vergote, and J. P. Remon, "Applications of Raman spectroscopy in pharmaceutical analysis," *Trends Anal. Chem.*, vol. 21, no. 12, pp. 869–877, 2002.

[10] V. S. Tumuluri, S. Prodduturi, M. M. Crowley, S. P. Stodghill, J. W. McGinity, M. A. Repka, and B. A. Avery, "The use of near-infrared spectroscopy for the quantitation of a drug in hot-melt extruded films.," *Drug Dev. Ind. Pharm.*, vol. 30, no. 5, pp. 505–511, 2004.

[11] L. Saerens, L. Dierickx, T. Quinten, P. Adriaensens, R. Carleer, C. Vervaet, J. P. Remon, and T. De Beer, "In-line NIR spectroscopy for the understanding of polymer-drug interaction during pharmaceutical hot-melt extrusion.," *Eur. J. Pharm. Biopharm.*, vol. 81, no. 1, pp. 237–230, Jan. 2012.

[12] V. S. Tumuluri, M. S. Kemper, I. R. Lewis, S. Prodduturi, S. Majumdar, B. A. Avery, and M. A. Repka, "Off-line and on-line measurements of drug-loaded hot-melt extruded films using Raman spectroscopy.," *Int. J. Pharm.*, vol. 357, no. 1–2, pp. 77–84, Jun. 2008.

[13] L. Saerens, L. Dierickx, B. Lenain, C. Vervaet, J. P. Remon, and T. De Beer, "Raman spectroscopy for the in-line polymer-drug quantification and solid state characterization during a pharmaceutical hot-melt extrusion process.," *Eur. J. Pharm. Biopharm.*, vol. 77, no. 1, pp. 158–63, Jan. 2011.

[14] D. Fischer, T. Bayer, K. J. Eichhorn, and M. Otto, "In-line process monitoring on polymer melts by NIR-spectroscopy," *Fresenius J. Anal. Chem.*, vol. 359, no. 1, pp. 74–77, 1997.

[15] S. E. Barnes, E. C. Brown, M. G. Sibley, H. G. M. Edwards, I. J. Scowen, and P. D. Coates, "Vibrational spectroscopic and ultrasound analysis for in-process characterization of high-density polyethylene/polypropylene blends during melt extrusion.," *Appl. Spectrosc.*, vol. 59, no. 5, pp. 611–619, 2005.

[16] P. D. Coates, S. E. Barnes, M. G. Sibley, E. C. Brown, H. G. M. Edwards, and I. J. Scowen, "In-process vibrational spectroscopy and ultrasound measurements in polymer melt extrusion," *Polymer (Guildf).*, vol. 44, no. 19, pp. 5937–5949, Sep. 2003.

[17] I. Alig, D. Fischer, D. Lellinger, and B. Steinhoff, "Combination of NIR, Raman, ultrasonic and dielectric spectroscopy for in-line monitoring of the extrusion process," *Macromol. Symp.*, vol. 230, no. 1, pp. 51–58, 2005.

[18] U.S. Food and Drug Administration, "Guidance for Industry. PAT - a framework for innovative pharmaceutical development, manufacturing, and quality assurance," US Department of Health, Rockville, MD., 2004.

[19] S. L. Conway, A. Lekhal, J. G. Khinast, and B. J. Glasser, "Granular flow and segregation in a four-bladed mixer," *Chem. Eng. Sci.*, vol. 60, no. 24, pp. 7091–7107, Dec. 2005.

[20] O. Scheibelhofer, N. Balak, P. R. Wahl, D. M. Koller, B. J. Glasser, and J. G. Khinast, "Monitoring Blending of Pharmaceutical Powders with Multipoint NIR Spectroscopy.," *AAPS PharmSciTech*, vol. 14, no. 1, pp. 234–44, Mar. 2013.

[21] K. H. Esbensen and P. Paasch-Mortensen, "Process Sampling: Theory of Sampling - the Missing Link in Process Analytical Technology (PAT)," in in *Process Analytical Technology*, 2nd ed., K. A. Bakeev, Ed. John Wiley & Sons Ltd., 2010, pp. 37–80.

[22] K. Kohlgrüber, *Der gleichläufige Doppelschneckenextruder*. Hanser Publishers, 2007, p. 367.

[23] O. Scheibelhofer, D. M. Koller, P. Kerschhaggl, and J. G. Khinast, "Continuous Powder Flow Monitoring via Near-Infrared Hyperspectral Imaging," *IEEE Int. Instrum. Meas. Technol. Conf. Proc. 2012*, 2012.

Instead of divining the future by studying
anomalies in chicken entrails, chemometricians
attempt to tease meaning out of
various data, spectroscopic and otherwise,
using advanced statistics.

Steven J. Doherty

3. Hot Melt Extrusion as a Continuous Pharmaceutical Manufacturing Process[3]

3.1 Continuous Processing in the Pharmaceutical Industry

In the last years, the interest in continuous manufacturing has increased significantly, albeit for a wide variety of reasons. These include the smaller scale of operations, the lack of scale-up related problems, or the fact that by using a small container-based plant, drugs can be easily manufactured at different locations (which may be a significant issue for the permission to sell drugs in certain countries, such as China). Moreover, the advent of individualized or personalized drugs requires the development of robust and flexible continuous manufacturing methods. From a chemical-engineering point of view, one major advantage of continuous manufacturing is the real-time qual-

[3] This chapter is based on: D. Treffer, P. Wahl, D. Markl, G. Koscher, E. Roblegg, and J.G. Khinast, "Hot Melt Extrusion as a Continuous Pharmaceutical Manufacturing Process," in *Melt Extrusion: Equipment and Pharmaceutical Applications*, M. Repka, Ed. Springer Publishers, 2013, pp. 363–396. The author has solely written the sections 15.4 „PAT Analyzers and Integration" and 15.6.3 „Quantitative Spectral Analysis" and contributed significantly to the other subsections of 15.6 „Continuous Process Analysis".

ity control of the products manufactured, eliminating the need for end-of-pipe testing. Hot-melt extrusion (HME) is an ideal platform for such a manufacturing concept.

The pharmaceutical industry, however, is still manufacturing in batch mode, mostly for historical reasons. Batch quality can be controlled, and thus, accepted or rejected, which is seen as an advantage over continuous manufacturing, especially since regulations are exclusively based on batch concepts. Nevertheless, batch production presents many disadvantages, some of them being:

- Defined batch sizes, thus output is driven by batch size
- Batch-to-batch variability
- Many and long interruptions between process steps
- Numerous transport steps between process steps (e.g., leading to segregation)
- Long throughput times from start to finish
- Large raw material and intermediate inventories required
- Extensive validation and scale-up activities needed
- Quality measured by in-process sampling and end-product testing

In the past, regulatory uncertainty and the perception that the regulatory environment is rigid and opposed to innovation have been cited as the main reasons why pharmaceutical companies have been slow in introducing innovative production technology. This regulatory environment, however, has significantly changed over the last decade. Indeed, the regulatory bodies now actively encourage the development and implementation of innovative pharmaceutical development, manufacturing and quality assurance, among them continuous manufacturing. The advantages are obvious:

- Integration of compliance/quality within the process
- Reduction of systems' footprint, capital costs and operational costs
- Reduction of raw material and intermediate inventories

- Less complex scale-up
- Reduced time to market

Nevertheless, continuous manufacturing poses significant challenges that should not be underestimated, including:

- Continuous operations are not suitable for every process
- Dedicated equipment, facilities and periphery are required
- Process technology is often underdeveloped, especially with regard to secondary manufacturing and at the interface between primary (drug substance, DS) and secondary manufacturing (drug product, DP).
- Advanced and robust process analytical technology (PAT) and control approaches are required
- Many critical sensors simply do not exist (e.g., powder flow rate, impurities, etc.)
- A single failure that can bring down the entire plant
- Definition of a batch is complex, i.e., making recalls more difficult to handle

Continuous systems, depending on the amount of the product made, may run for a few days to a few weeks, before the system is shut down, cleaned and set up for a new campaign with a different product. Thus, continuous manufacturing in the pharmaceutical industry is different from other industries, such as the petrochemical industry, requiring a stronger focus on start-up and shut-down sequences.

3.1.1 Continuous HME

Hot-melt extrusion is generically a continuous process for making a homogeneous material and offers several advantages over traditional processing techniques for pharmaceutical applications. A formulation for hot melt extruded pellets typically comprises a matrix and an active pharmaceutical ingredient (API), as well as other

components, such as plasticizers, anti-tacking agents, pore formers, colorants, stabilizers and others. Carriers that are generally used are (thermoplastic) polymers and waxes or wax-based materials, which control the release (mechanism) of the drug of the final dosage form. The process must be controlled in such way that the softening temperature of the carrier is exceeded, but the degradation temperature of the API is not reached. The development of HME formulations has been described in much detail earlier in the book. Apart from the drug-release aspects, functional additives significantly impact the process [1]. Thus, formulation aspects also impact the processability and robustness of the process, which is a prerequisite for continuous manufacturing. Specifically, the formulation impacts

- the process temperature
- the required screw configuration and screw speed
- the torque
- the transition time
- and the solidification of the strand at the outlet (and possible die swelling)

Thus, a close understanding of the rheological behavior of the material-mixture prior to the experiment and a tight monitoring and control of the above mentioned factors during extrusion are essential for establishing a robust continuous process. Figure 1 shows a schematic of a typical continuous extrusion process, which generally involves (1) the feeding unit, (2) the process unit, (3) a continuous downstream process and (4) the monitoring system. In many new applications it is possible to set (red) and monitor (green) most of the process parameters.

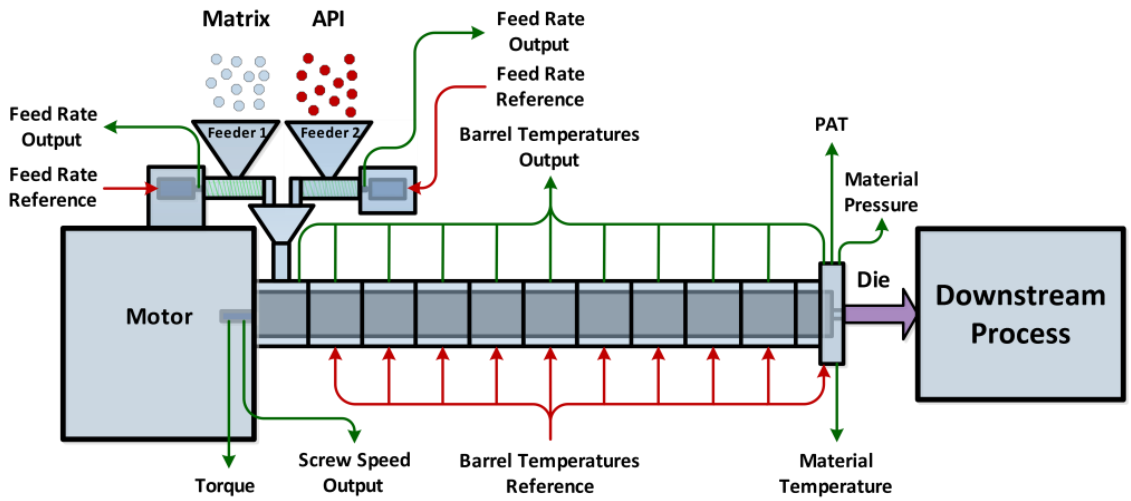

Figure 1: Schematic view of an extruder and periphery.

1.) Feeding: The feeding unit consists of one or more feeders for powders or liquids. If there is one feeder the formulation must be pre-mixed. If multiple feeders are used, the components (or premixes thereof) are fed by a dedicated feeder, resulting in higher design flexibility and eliminating the need for a previous mixing process (and problems related to poor mixing and segregation). Raw materials can be fed volumetrically or gravimetrically (preferred) in the case of powders or pellets. Liquids are typically fed volumetrically or by using a mass flow controller.

Continuous feeding is particularly critical in the development of a continuous process. It is crucial for content uniformity, which is one of the most important requirements that a pharmaceutical product must meet. Each feeding unit experiences fluctuations in the fed material stream, which can be dampened by the extruder which has a certain mixing ability. Extruders can generally dampen high-frequency or short-time fluctuations. Low-frequency fluctuations pass through the extruder almost undamped [2]. Thus, development of optimal feeding strategies (especially for low powder flow rates) is an important prerequisite (and a common problem). The key to the highest product uniformity is selecting an appropriate combination of the feeding equipment and screw. The feeder design is usually chosen based on empirical knowledge, as there is no perfect feeding setup for all powders, due to the wide variety of factors, e.g., particle size distribution, cohesion, electrostatic forces, screw design, etc. As such, the right combination of the raw material and the feeder design is required. A

comprehensive list of factors that impact feeding was provided by Schenk et al. [2]. English and Muzzio [3] suggested a method for characterizing feeding equipment, based on a feeder and a scale with data logging. In their contribution, the feeder feeds the powder to the scale, and the mass increase is measured. Subsequent data analysis delivers statistical information that helps to select the most suitable setup for specific powders.

In our experience, most content uniformity issues are caused by problems in the feeding section. An investigation of the feeding accuracy should be conducted in such cases. Target values are the composition, in case of premixes, and the mass flow rate in case of pure substances. Pure substances with poor flow properties typically cause avalanching at the feeding screw outlet. Premixes can (and often do) show significant segregation in the feeder hopper, usually leading to a concentration drift over time. Another critical issue during continuous feeding is the refilling of hoppers as during this time, the weight signal of the loss-in-weight (LIW) feeders is not available. Special protocols are necessary to ensure constant powder feeding during hopper refilling.

2.) Extrusion: From a process technological point of view the HME process is a continuous manufacturing process that combines multiple batch unit operations in one single process. Different process steps, such as mixing, melting, homogenization and shaping, can be performed sequentially, offering the opportunities for automation of the manufacturing plant to limit material loss, increase the throughput, decrease energy input and yield a product with high quality. Here, areas of research include the design of screw assemblies and extruder dies, mixing in the extruder, long-term operational stability, controlled powder and liquid feeding and the simulation of the flow in unfilled screws. More detail about extruder design and operation is provided in other chapters of this book.

3.) Downstream: Continuous extrusion produces a homogeneous material. Thus, a continuous downstream process is needed to form a final product (pellets, sheets,

powders, etc.) of the extrusion line. An appropriate downstream process is selected based on the targeted dosage form, the material's rheology, the product's purity and the production costs. More detail is given in section 3.2 below.

4.) Monitoring: API-concentration uniformity of the extruded material (in contrast to content uniformity of a final product) can be ensured by several tools. The simplest approach is to monitor closely the actual feed rates of the feeding units (Figure 1). This, however, is only suitable for processes in steady state. Non-steady-state processes and phases, such as start-up, concentration change or simple process disturbances and instabilities, require a process analytical technology (PAT) analyzer at the end of the extruder and a control method to ensure product quality (i.e., the desired concentration uniformity). An overview of the state of the art PAT analyzers is given in section 3.3.

3.2 Downstream Processing

An extruder produces a homogeneous material as an intermediate, in pharmaceutical industry typically in the range of a few kilograms per hour (e.g. 18 mm extruder 1-6 kg/h and 27 mm extruder ~15 kg/h). The downstream process is usually coupled to the extrusion die to form a final product of the extrusion line. The final continuous downstream process is selected based on the target dosage form, the material's rheology, the product's purity and the production costs. It can either be the final dosage form, as in case of injection molding or direct shaping, or an intermediate product, such as sheets, or pellets/granules for capsule filling, tablet compaction or other processes. An overview of common downstream processes is given in Figure 2.

The rheology of the emerging melt is an important factor with regard to the selection. It mainly depends on the product formulation but is also influenced by almost all of the extruder's process parameters and their interactions during a coupled downstream process. Rheological parameters are typically a function of temperature, pressure, shear and in some cases time history [4].

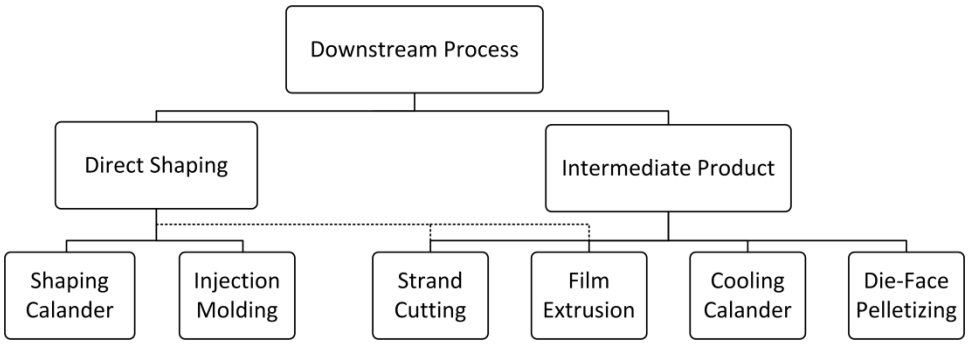

Figure 2: Overview of common downstream processes.

There are no general rules for selecting a downstream process. Rather, it is based on empirical knowledge and trial and error principles. Often, a formulation can be adjusted to be suitable for a desired downstream process. For example in the case of die-face pelletization anti-tacking components have to be added to reduce the stickiness of the material. Various downstream processes are described in more detail below.

3.2.1 Direct Shaping of Final Product

Two continuous processes are established in the pharmaceutical industry for direct shaping, where the extruded molten material is formed into a directly applicable dosage form.

The first process involves a shaping calander (see Figure 3), which consists of two narrow counter-rotating rolls with forming cavities. A homogeneous melt band is fed through a slit die of an extruder. The band passes through the forming calander, where the melt is forced into the cavities to form tablets. A thin film that remains between the tablets can be removed via a subsequent separation process (e.g., using a rotating drum). In some cases the film may be ground and again fed to the extruder. The challenges of this process are the breakage during the operation due to stickiness of the material, as well as product weight uniformity caused by pulsating exit velocity of the melt strand.

Figure 3: Shaping Calander (Picture courtesy of Dr. Collin GmbH)

The second process, which is semi-continuous, involves injection molding. It is one of the primary shaping processes in the plastics industry, during which plastic parts weighing from a gram up to several kilograms are produced in high volume. In comparison, the product weight is low in the pharmaceutical industry: a tablet, for example, typically weighs less than one gram. Implants, however, may weigh several grams.

A conventional injection molding machine, consisting of a two-section mold with cavities, may be coupled to the end of a single screw extruder. The feature of the single screw is the axial movability of the screw, which ensures high pressures during the injection. Generally a single screw extruder has a limited mixing capability compared to a twin screw extruder. Thus, homogeneous materials, such as pellets produced by a preceding twin screw extrusion, are typically used as starting material. Injection molding with a double screw extruder requires more complicated equipment and is therefore an exception to the rule.

Figure 4 illustrates an injection molding process. It is a cyclic process that is divided into five parts:

- **Start plasticizing:** the screw is in the front position and material is molten due internal friction and heat transfer.
- **End plasticizing:** the screw moves backward and the melted material is accumulated in front of the screw.

- **Injection:** the molten material is pushed through the so-called "gate" into the cavity by the forward moving screw.
- **Packing and cooling:** the pressure is retained during the cooling and associated volume shrinkage to supply the cavity with fresh material.
- **Ejection:** the mold opens and the product is ejected.

In injection molding, operating pressures of up to several thousand bars during the filling stage are standard (thus not suitable for all APIs). This pressure is created during the injection either using an axial displacement of the screw or an additional piston. The required pressure depends on the complexity of the mold cavity, which is defined by the dosage form and the quantity per cycle. The production capacity of an injection molding machine depends on the quantity per cycle and the cycle time. The quantity per cycle is limited by the mold area and the shape of the product. In case of a simple tablet, over 100 pieces per cycle are possible. The cycle time depends on the

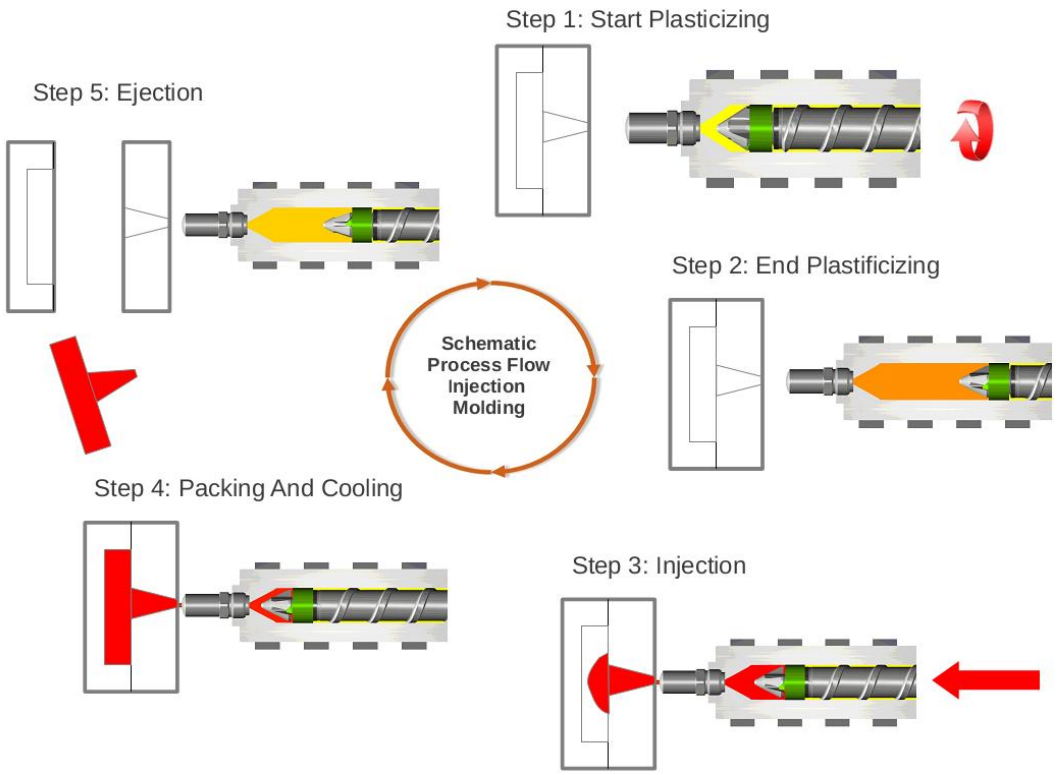

Figure 4: Illustration of an injection molding process (Picture courtesy of Engel Austria GmbH and IPIM, Johannes Kepler University Linz).

formulation and its thermal characteristics and lies in range between 3-10 seconds. In the case of 100 pieces per cycle and a cycle time of a few seconds up to 100,000 tablets can be made per hour.

Injection molding can be applied to the production of various dosage forms, e.g., tablets, capsules, implants, intravaginal inserts and multi-layer devices for controlled release applications. A comprehensive review of pharmaceutical injection molding was given by Zema et al. [5].

3.2.2 Intermediate Products

In many cases an extrusion line produces an intermediate product. Thus, the continuous extrusion process is used as a means for making new materials (solid solutions, solid dispersions, or for embedding nano-particles in a melt, see Khinast et al. [6], [7]). Alternatively, the extrusion process functions similar to a granulation process, i.e., concentration uniformity and flowability of the ground material are achieved and segregation is suppressed. Finally, pellets can be made, which may directly be filled into capsules. Four downstream options for the production of intermediates are commonly used in the pharmaceutical industry and are chosen based on requirement for the next production step and the cuttability above the softening point.

The first method (Figure 5) is strand cutting, which is used for sticky materials. Here, the extruder produces cylindrical strands. A conveyer belt with air knifes cools the strand, leading to solidification, and transports the material to the strand cutter, which consists of a cutting rotor, a bed knife and two feeding rolls. The strands pass between the feeding rolls and are subsequently cut by the cutting rotor. The obtained pellets are small cylinders with a relatively narrow size distribution. Typically, the throughput is not rate-limiting, but must match closely the extrusion flow rate. Thus, control of the strand cutter speed (both feeding and cutting) is critical for obtaining a stable continuous process for making uniform pellets. The pellet size uniformity depends strongly on constant operating conditions of the extrusion system and on the brittleness of the material. Many amorphous dispersions are brittle glasses and can cause fracturing of the pellets during the cutting process. In rare cases, strand cutting

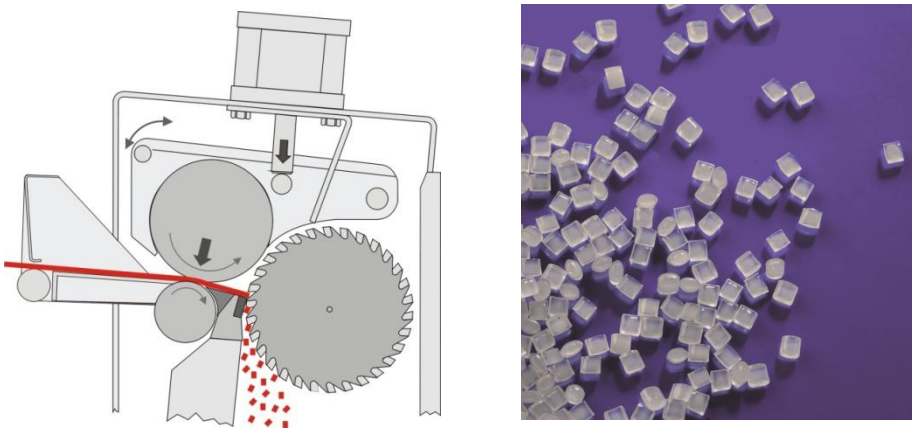

Figure 5: Strand cutting (Picture courtesy of Automatik Plastics Machinery GmbH)

is used to form final products like flat-faced plain tablets [8]. The diameter of the tablet is equal with the stand diameter. However, the optical appearance still is inferior to conventional tablet production.

The second method is film extrusion, which is used, for example, for the production of transdermal, transmucosal or transungual films [9]. In this process, the extruder is equipped with a sheet die. An extrudate is formed into a thin film of molten material. The film is cooled between counter-rotating chill rolls and subsequently coiled. These coils are the base material for the final production step, such as cutting or attaching to a patch.

The third method is hot die-face cutting (Figure 6). A hot die-face cutter is directly connected to the extrusion die. An extruder generates cylindrical strands, and a cutting rotor cuts the emerging strands directly at the die plate into pellets. The pellets are transported pneumatically into a product container. Several authors obtained almost spherical pellets via hot die face cutting [10], [11]. The spherical shape is due to surface tension and viscoelastic behavior of the material and results in a better flowability of the pellets, which may eliminate a subsequent spheronization process. The challenge is the cutting above the softening point of the formulation. The formulation must have a suitable rheology for the hot cutting, otherwise the product smears up knifes and die plate, which leads to lumps and sometimes to burnt material as well. The cooling of the emerging material has strong impact on the rheology and therewith on the cuttability [12]. The material is usually cooled with compressed air.

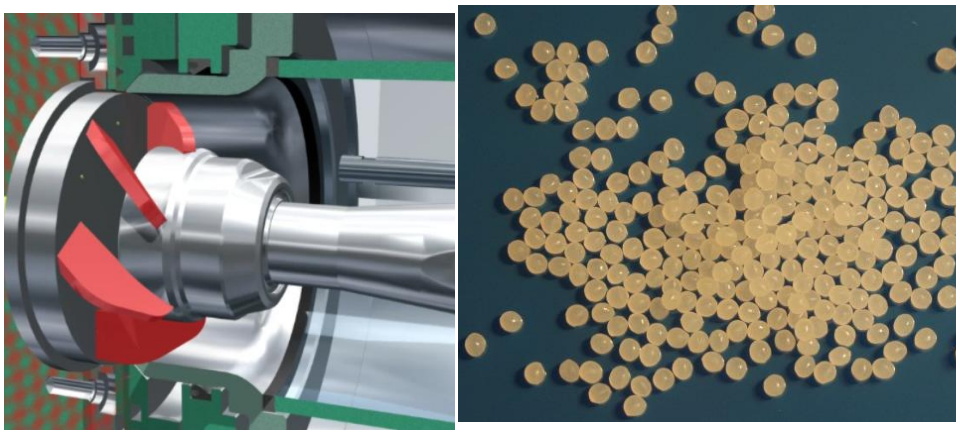

Figure 7: Hot die face cutting (Picture courtesy of Automatik Plastics Machinery GmbH)

The plastics industry uses water to achieve high cooling rates. However, water is in most cases not suitable for pharmaceuticals due to solubility of API's and products purity requirements. Thus, the design and control of the cooling air flow is critical for achieving a robust process.

The third method involves a cooling calander, also termed a drum cooler or chill roller (Figure 7). In this process, the extrudate is formed into a thin sheet by passing between a cooling drum and a counter rotating in-feed roll. A belt presses and redirects the sheet to the cooling drum. The sheet solidifies on the cooling drum and detaches from the belt. During the detachment it breaks, and a subsequent crusher reduces the fragments into small particles. Although the particle size is not uniform, the material may milled again and may be used for direct compaction.

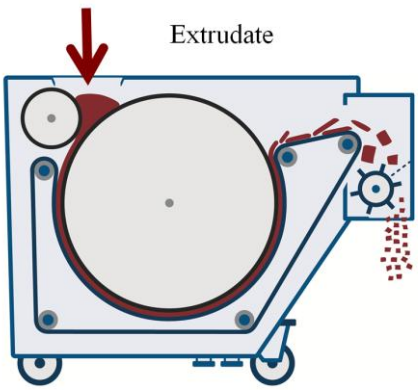

Figure 6: Cooling calander principle (Picture courtesy of BBA Innova AG)

3.3 PAT Analyzers and Integration

Powder/liquid feeding, hot melt extrusion and most of the downstream processes can be utilized in a continuous production line. However, these processes must be constantly monitored to ensure the design quality of the final product. Disturbances in the input parameters (e.g., during hopper recharging or due to segregation of a premix) or the process parameters (e.g., pressure build up), even only for a few seconds, can lead to significant output fluctuations [2]. Therefore, an adequate control strategy of the entire process is necessary to ensure the appropriate product quality. The toolbox provided by process analytical technology (PAT) can provide the necessary link between monitoring and control. This link is of importance, especially since the U.S. Food and Drug Administration (FDA) increasingly requires in-line monitoring and process control of manufacturing processes, as prescribed by the PAT initiative [13] and the subsequent ICH guidelines [14]. This includes:

- **Monitoring:** Collecting and aggregating real-time, in-line data of all kinds of analyzers.
- **Supervision:** Extracting information from the data regarding the state of the system. The analysis is based on the process knowledge obtained from previous runs. This knowledge is applied to statistical models, ideally combined with mechanistic models.
- **Diagnosis:** Check for possible deviations from the desired state of the system. This must include automatic root cause identification.
- **Control:** Decide which process settings must be manipulated to eliminate the root cause of the deviation and move back to the desired state of the system.

The next sections focus on commercially available PAT tools, their integration into the extrusion process and into modern IT infrastructure.

3.3.1 Overview of Available PAT Analyzers

Most of the available PAT analyzers for extrusion originate from the plastics or chemical industry. Some of the tools are well known in the pharmaceutical industry, e.g., near-infrared spectroscopy for monitoring moisture, drug content and uniformity, and Raman for polymorph detection, as reviewed in literature [15][16][17]. Some applications are used for validated systems, i.e., [18]. However, the requirements for an extrusion PAT sensor are higher than for other purposes. High pressure, high temperature and possibly abrasive materials require robust sensor design and materials. For optical interfaces quartz glass is the standard choice. Moreover, the location of the sensing device is critical for obtaining accurate information of the process status (see chapter 3.3.2).

Below is an overview of commercially available PAT tools for in-line monitoring of the extrusion process. The overview focuses on NIR and Raman spectroscopy and particle size measurements since these PAT analyzers have significant potential for standard production monitoring. A recent review of available sensors and their applications can be found in [19]. For additional reading, see chapter PAT and QbD applications in melt extrusion.

3.3.1.1 Near-Infrared Spectroscopy

Near-Infrared (NIR) spectroscopy is based on the attenuation of light by absorption. To avoid complicated sample preparation, diffused reflected light is often used. The sample is irradiated with light in the wavelength range of about 1000 nm – 2500 nm, depending on the spectrometer system. The light photons can be absorbed by the sample's molecules, and the energy of the photons is used to excite higher vibrational states. Because the wavelengths of the incident light that excite such vibrational states are absorbed, less intensity at this wavelength is reflected back to the detector. Only molecular vibrations, which result in a change of dipole moment, can be excited [20]. Therefore, polar bonds show stronger absorption of NIR radiation. Additionally, bonds with a pronounced difference in atomic mass have stronger NIR absorption and the most prominent bands belong to -CH, -OH and -NH functional groups [21].

Within the NIR region mainly overtones and combination vibrations of these functional groups are present. The spectral pattern is also influenced by further physical rules, i.e., Fermi resonance [21][22].

With regard to extrusion, this means that the spectrum changes along with the varying melt composition, temperatures (or pressure) and with everything that influences these parameters, i.e., the screw speed and the screw filling ratio. As such, the spectrum provides a lot of information, but it is harder to interpret without knowing other process parameters.

In pharmaceutical extrusion NIR has been used for studying the API content [2] (no accuracy stated) and the polymer-API interactions directly in the die [23] (accuracy of 1.5% API, determined by error of prediction) and the API content in film extrusion [24] (accuracy of 3.5% API, determined by HPLC reference).

3.3.1.2 Raman Spectroscopy

Raman spectroscopy is based on frequency shifts in reflected light vs. incident monochromatic laser light. These shifts are caused by inelastic scattering of photons on a molecule, with induced transitions between vibrational states of the irradiated molecules. The incident laser light is in the VIS to NIR region, but most commonly 785nm diodes or 1064nm Nd:YAG lasers are used.

Radiation excites molecules to a virtual state, which does not correspond to electronic or vibrational levels. The virtual state is not stable, hence the molecules relax quickly. When relaxing, they may return to an excited vibrational state, whereby a part of the incident energy is converted and the scattered light shifts to lower frequencies (so-called Stokes radiation). At room temperature it is the most commonly observed effect in Raman spectroscopy [21]. At higher temperatures a certain fraction of molecules is already in an excited vibrational state, according to the Boltzmann distribution [25]. Therefore, they can relax back to the ground state whereby the rotational energy is converted and the reflected light shifts to higher frequencies (Anti-Stokes radiation). The transition from Stokes to Anti-Stokes radiation is a temperature effect and thus, the spectrum will be affected by temperature changes. Another possible

influence is a pressure change, e.g., by undesired process effects like a pulsating melt stream through the die or plugging of the die. These effects might cause a model to be valid only in a small process parameter range.

A molecule is Raman active, if the polarizability changes with the inter-atomic distance of a bond [26]. Polarizability a is the proportionality constant between an external electric field E, such as the irradiating laser light, and the induced dipole moment P.

$$P_{Induced} = aE$$

High polarizability implies high mobility of the electrons. Thus, Raman is well suited to measure non-polar bonds, i.e., C-C, C=C, S-S, N=N [20], like carbon chains and aromatic rings. The spectra are not affected by the presence of water, which is highly polar. In contrast to Raman the NIR signal is strong for polar bonds and the two spectroscopic techniques can be used complimentary. Especially for symmetric molecules a vibration can be seen either in Raman or NIR. This is caused by different selection rules for the visibility of a vibration in the spectrum [20].

3.3.1.3 Chemical Imaging

For chemical imaging primarily Raman and NIR sensors are used to obtain spatially resolved (2D) information of the chemical structure, i.e., the API distribution on the tablet surface. The 2D image cannot be taken in one shot, but rather via several techniques: (1) Filter techniques: 2D images are taken by a detector chip using optical band-pass filters for different wavelengths. Although this method is inexpensive and fast, it involves only a limited number of wavelengths. (2) Push broom principle: A 1D line is projected onto a detector chip. The second dimension of the chip is used for wavelength separation, which is achieved by reflecting the light at a grating. If the sample is moving in relation to the detector, the surface can be mapped as a function of time. The “surface” can also refer to the time evolution of the process. For this technique NIR camera systems are used. (3) Rasterizing the surface: The surface is scanned point by point (0D) in x and y direction, resulting in a 2D image. Because the sample should not move during rasterizing, this method is impractical for in-line

measurements. Moreover, measurements can be time consuming: using Raman to map a tablet with a 100x100 pixel image 10,000 single point measurements are necessary, which can easily last overnight. One major advantage of such systems is the high resolution, which is superior to the push broom principle. Both, Raman and NIR systems exist.

Depending on the complexity of the system either filter or push broom techniques are the method of choice in a manufacturing environment. For rather simple tasks, if few wavelengths are sufficient, i.e. moisture detection, filter techniques are used. For complex formulations and also during development push broom is necessary. It can be used for film extrusion, for studying the drug content uniformity over time and the die cross section followed by a shaping calander or for testing the final product after injection molding.

3.3.1.4 Particle Size Analysis

There are many techniques for particle size analysis. Typically, these methods provide information regarding particle size distribution (PSD) and the particle's parameters, such as sphericity, i.e., Feret-Min and Feret-Max. In a continuous extrusion process, PSD and sphericity can be important for quality control of downstream processes. Typical examples are die-face pelletizing or strand cutting. The following techniques have been used on- or in-line to study particulate matter:

- **Image analysis:** Images of dispersed individual particles or of the product stream are analyzed by advanced computational algorithms. Image analysis has the distinct advantage of delivering information about the particle shape and can measure in very dense systems (i.e. powder streams). Novel systems use special lighting (i.e., Eyecon by Innopharma Labs uses red, green and blue LEDs from different angles) for better particle-edge detection.
- **Focused beam reflectance measurement:** A focused laser beam, rotating at high frequency, illuminates the product stream. If the laser beam hits a particle, the light is scattered back to the detector. Thereby, the chord length can be calculated, which is related to the mean particle diameter.

- **Laser diffraction:** A broad laser beam is diffracted from the particles, and the angle of diffraction is detected. Large particles exhibit a small diffraction angle, as opposed to small particles. From the diffraction pattern the volume equivalent sphere diameter is calculated. An assumption of the Mie theory, which is used to analyze the diffraction pattern, is the existence of spherical particles. Therefore, non-spherical particles, like needles or flakes, will result in incorrect measurements.
- **Spatial filter velocimetry:** A laser beam is focuses on a detector, consisting of a fiber-optical array. If a particle passes the beam, it casts a shadow on the detector. Results are the chord length and notably the particle velocity at the probe position, which is not accessible with other techniques.

3.3.2 Integration in the Extruder

Selecting an appropriate measurement position to integrate the analyzer probes into the extruder is critical for obtaining accurate results and for developing a reliable control strategy. Therefore, possible measurement positions must be evaluated, according to the theory of sampling. Temperature and pressure probes for melt characterization have been used for many decades. Still, achieving repeatable and accurate results remains a challenge. Melt pressure probes usually detect pressure differences, thus require a pressure calibration at the beginning of each operation to set the pressure baseline correctly. Appropriate conditions during the calibration procedure are essential, as otherwise an incorrect absolute pressure, i.e., a baseline offset between different extrusion runs can occur. The calibration procedure has to be defined in the manual and usually clean probes and steady temperature conditions are required. The probes can be very sensitive to inexact calibration conditions, for example during contact with small amounts of material and temperature gradients due to incomplete heating of the machine.

During temperature measurement, the measured melt temperature is strongly influenced by the barrel temperature, more so for low throughput extrusions due to direct

contact with the barrel. Thus, the melt temperature measured is always some value between a local barrel and the actual melt temperature.

In addition, there are challenges associated with spectroscopic measurements of the API concentration in the melt. In-line measurements of melt composition with spectroscopic sensors during extrusion are discussed in detail below.

3.3.2.1 General Considerations Regarding the Theory of Sampling

Sampling is critical for correct measurements. This applies to classical thief sampling with off-line analysis as well as to in-line PAT sensors. There are practical rules regarding correct sampling defined by the theory of sampling (TOS) [27] that need to be applied to evaluate different measurement positions for the extrusion process. For this purpose the material stream in an 8-0 plate (i.e., the plate between the 8-shaped extruder barrel and the circular, 0-shaped die, see Figure 9) shall be approximated as a pressure-driven flow through a pipe.

Modeling the die section as a cylinder with a laminar flow of a Newtonian liquid, the steady-state velocity profile u(r) is described by the Hagen–Poiseuille equation

$$u(r) = -\frac{1}{4\eta}\frac{\Delta P}{\Delta x}(R^2 - r^2)$$

where u depends on the viscosity η, the pressure drop ΔP, the length of the cylinder Δx Δx, the cylinder radius R and the radius r where the flow velocity shall be calculated. Figure 8 compares the velocity profiles of a perfect plug flow (red) and a Newtonian fluid (black) in a tube in the steady state, without slip. A perfect plug has the same velocity u_{av} at every point in the tube, whereas the Newtonian profile exhibits a parabolic shape with the maximum velocity u_{max} in the center. For non-Newtonian flows, as typically seen in extrusion, the inhomogeneity may be even more pronounced. However, the velocity profile of a shear thinning non-Newtonian liquid is somewhere between the ideal plug flow and the Hagen Poiseuille profile. The shape of the real profile in the die section of the extruder depends on the rheology [28][29], the temperature field and the pulsation of the inlet stream.

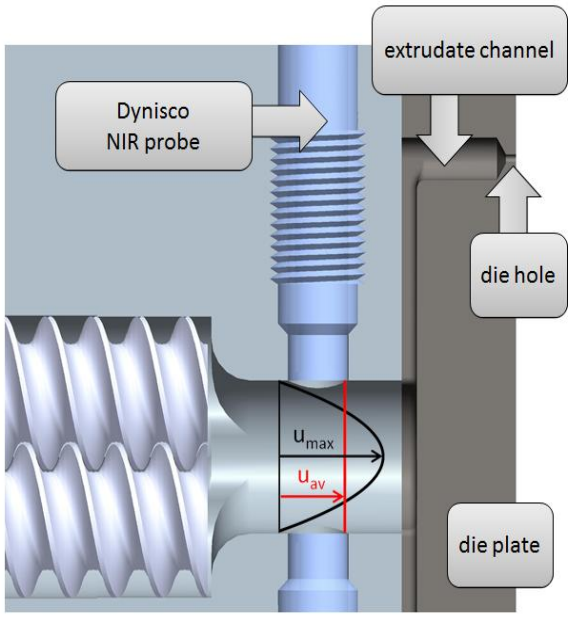

Figure 8: A section of the extruder where the NIR probe is situated. The figure shows the velocity profile of (red) a perfect plug with constant velocity u_{av} and (black) a Newtonian melt with a parabolic shape and the maximum velocity u_{max} in the center.

As can be seen from Figure 8, the material exchange close to the barrel wall (i.e., the region sampled by a spectrometer with a small penetration depth) is small compared to the core region. Therefore, a sample taken close to the barrel wall does not necessarily represent the overall concentration, but rather the local concentration in the vicinity of the barrel wall. If for some reason fluctuations in the API concentrations occur, sampling of the wall region does not provide an accurate representation of the products quality.

3.3.2.2 Application to Extrusion

The TOS rules for thief sampling can be applied to in-line PAT measurements. For in-line spectroscopic sensors the sample amount depends on several factors: (1) the irradiated volume, as defined by the spot size of the sensor and the penetration depth in the material, (2) the integration time per spectrum and (3) the velocity of the material in the irradiated volume [30].

The sample volume is often significantly smaller, compared to thief sampling methods. If the volume is too small compared to the unit dosage form, there might be sub-

sampling issues. Sub-sampling can be avoided by choosing a longer integration time or adapting the process, to achieve higher velocities of the material. In addition, with a small spot size only a fraction of the product stream can be monitored. For extrusion purposes, one way to overcome these problems is using a smaller inner piping diameter [27], ideally in the order of the irradiated volume. However, there is one more issue: the barrel diameter is defined by the extruder specifications and cannot be freely changed. As such, another approach must be taken.

Special care must be taken to avoid accumulation of the material in front of the sensor, in which case the sensor signal can be biased, preventing a correct measurement of temporal evolution of the material's properties. This could happen, for example, if the probe's sapphire window is not in plane with the inner barrel wall for measurements in an 8-0 plate. Two measurement positions will be presented below, which fulfill the above criteria for measuring the actual melt composition.

Modified 8-0 Plate: The 8-0 plate may be modified to perform measurements directly in the plate. The necessary modifications depend on the actual design of the extruder. The example below involves a Coperion ZSK 18 connected to a novel die-face pelletizer developed by Automatik Plastics Machinery GmbH.

The original pipe flow was changed to an annular flow by placing a tapered metal cylinder (we termed it "Apollo" capsule) in the 8-0 plate. The capsule forced the melt in an annular flow close to the barrel walls, where the probe was located. Figure 9 shows the sampling region with the modified geometry. The benefit of the annular flow is the increased average velocity due to a smaller cross-sectional area and higher shear rates in the vicinity of the probe. Thus, the material exchange in the volume sampled by the spectrometer is much increased and more representative of the total mass flow. The disadvantage of the reduced cross-section is a higher pressure drop and increased shear. However, in the case under consideration these effects are negligible compared to the condition in the extrusion die (annular gap dimension: inner diameter is 15.8mm, outer diameter is 18mm and length 19mm; die plate configuration: 2 holes with diameter 1mm and length of 1mm).

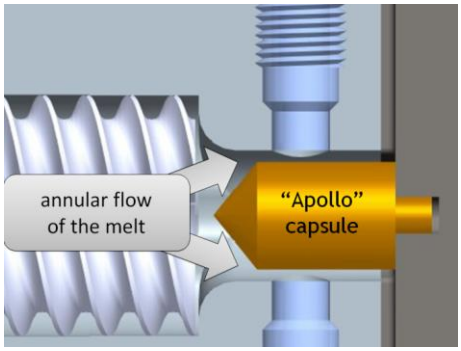

Figure 9: Modification of a die section by inserting a tapered metal cylinder, thus creating an annular channel.

Custom-Made Die or Bypass: In several studies a custom made slit-die [19][31], a flow cell directly attached to the die [32] (both in-line) or a bypass for at-line measurement [33][34] were used. The advantages included good interface possibilities and a good exchange of the material in front of the sensor. These setups allow a fast and easy comparison of different measurement techniques (i.e., spectrometers) to select the most suitable one [19]. However, it cannot be used in conjunction with downstream processes like die face pelletizing or direct shaping methods. Still, if the extrudate is milled to powder for further downstream processing, a custom-made slit die might be the method of choice.

3.4 Process Integration into Computerized Systems

Process understanding requires the identification and explanation of all critical sources of variability, thus offering an accurate and reliable prediction of the product quality [35]. Ideally, it should be based on a mechanistic understanding of formulations and process factors, which in turn comprises (1) the identification of key parameters and effects, (2) real-time and continuous measurement of selected key parameters and (3) a control strategy based on selected uni- and multivariate real-time measurements [36].

Clearly, these tasks require for an IT infrastructure that can aggregate real-time process data from multiple unit operations, raw material data, PAT data and equipment status [2], which may also be used for process control. Moreover, the pharmaceutical industry intends to move away from paper and towards electronic systems, again requiring computerized systems.

3.4.1 Introduction to Computerized Systems

In response to the growing industry requirements, the regulatory authorities developed guidelines and regulations for computerized systems, including:

- EU GMP Annex 11 Computerized Systems [37]
- EU GMP Chapter 4 Documentation [38]
- 21 CFR (Code of Federal Regulations) Part 11 [39].

Moreover, the Good Automated Manufacturing Practices (GAMP5) Guidelines [40] of the International Society for Pharmaceutical Engineering (ISPE) present a suitable approach for validation of computerized systems. GAMP has become a state-of-the art guideline for computer validation throughout the pharmaceutical industry [41].

Requirements for all forms of computerized systems (needed for an automated continuous manufacturing setup) are:

- Computerized systems should not result in a decreased product quality or process control.
- The overall risk of the process should not be increased.

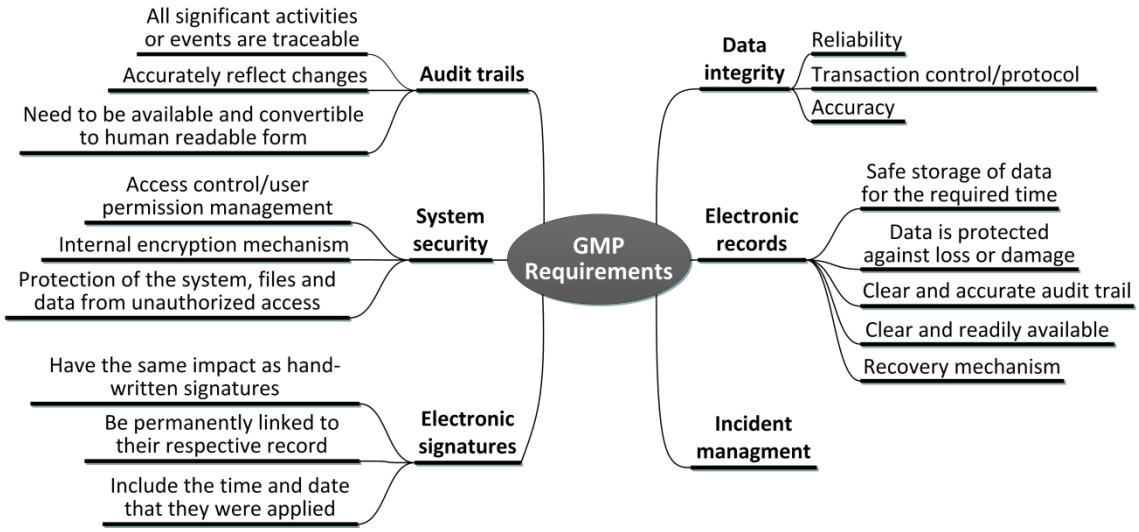

Figure 10: GMP requirements for a computerized system that focus on data acquisition and process control systems. For more details on GMP requirements see publications of the regulatory authorities.

In the context of continuous manufacturing, a subcategory of computerized systems, namely data acquisition and process control systems, are important. Moreover, data acquisition and process control systems are a prerequisite for successful continuous process applications. Specifically, for the implementation of real-time quality control as well as process control, a certain IT infrastructure is essential. With respect to the above stated requirements the developer of the IT infrastructure has to consider the GMP requirements:

- **Data integrity**: A data acquisition and process control system must have built-in checks for the correct and secure data entry and processing. Data integrity and system security (e.g., access authorization for the operator) must be considered during the design stage of the system [37].
- **Electronic records**: Electronic records must be readable, accurate and accessible throughout the retention period [42].
- **Electronic signatures**: Many situations in our paper-based world legally require a signature or initials. One of the main reasons to promote and establish computerized systems in the pharmaceutical industry is avoiding a vast amount of archived paper. Thus, electronic signatures must be equivalent to handwritten signatures, initials, etc., required under the regulations. Depend-

ing on the country-specific legislation, electronic signatures may need to be linked to their respective records and include the time and date when they were entered [43], [44].

- **Audit trails**: A record of all GMP-relevant data and changes to the configuration data (e.g., creation, change and cancellation of access authorizations) must be documented. Thus, audit trails need to accurately reflect the changes and must be convertible to a human readable form[45]–[47].
- **System security**
- **Incident management**

This basic implementation guideline is summarized in Figure 10. For further information regarding the implementation and validation of computerized systems from a regulatory perspective refer to publications and guidelines of the regulatory agencies, such as GAMP 5.

3.4.2 Architecture of Supervisory Control Systems

The basic implementation of the data acquisition and process control system for a continuous HME system contains the following hardware and software units in order to assure the functionality and to meet the GMP requirements:

- Processes units
- Interfaces
- Data processing unit
- Databases
- Audit trail unit

A basic architecture of a supervisory control system is shown in Figure 11. In the following the basic units (cf. gray blocks in Figure 11) are discussed in more detail:

Processes: Several processes (e.g., HME, pelletizer, etc.), each equipped with univariate (e.g., temperature) and multivariate (e.g., spectrometers) sensors and actuators from different manufacturers, must be monitored and controlled.

Interfaces: The interface from the sensors and actuators to the computerized system has to be selected carefully with the consideration of the GMP requirements. Especially data integrity has to be guaranteed. An easy integration of the sensor systems and actuators into the software can be accomplished via standardized interfaces. This increases the flexibility and ease of use of the sensor systems, actuators and software. A common interface in the automation industry is OPC (Object Linking and Embedding for Process Control) technology.

OPC technology is used to distribute data from different univariate sensors to OPC clients and from OPC clients to actuators. An OPC server determines the interface between the sensors/actuators and several different software packages that implement an OPC client. Thus, each OPC client can access the data provided by the OPC server simultaneously. In continuous manufacturing several OPC servers (e.g., one OPC server per process or sensor system) have to be merged. In the context of OPC, different

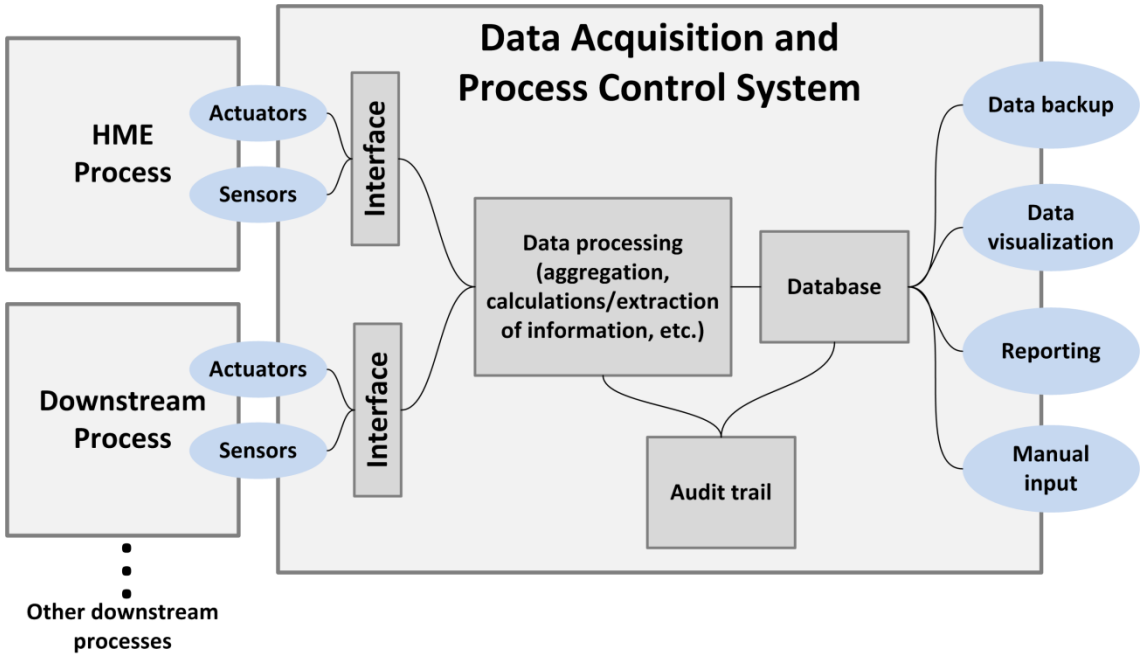

Figure 11: Schematic of a basic data acquisition and process control system for a continuous manufacturing line consisting of several processes (i.e., feeding, extrusion, downstream, etc.).

interface types are available. For example, OPC Data Access (OPC DA) specifications define communication protocols for real-time communications between sensors/actuators and computerized systems. As such, OPC DA deals only with real-time and not with historical data. However, the next generation of software automation solutions belongs to the concept of OPC Unified Architecture (UA). It overcomes a drawback of OPC DA, i.e., the communication is based on COM (Component Object Model) and DCOM (Distributed Component Object Model) and thus tightly depends on Windows operating systems. COM and DCOM are standards introduced by Microsoft that allow the communication between different applications on the same machine (COM) as well as the communication across network boundaries (DCOM). Specifically in continuous manufacturing the data exchange between different machines and one central unit has to be reliable, secure and fast. Thus, OPC UA offers an enhanced interoperability with other platforms and guarantees data reliability and security. OPC UA has the additional advantage of allowing the exchange of higher level structured data, e.g. PAT data.

To integrate PAT tools (e.g., NIR spectrometer) into a computerized system, a large amount of data must be collected, analyzed, visualized, transferred, processed and stored within a short timeframe. Many manufacturers of PAT tools provide an OPC DA server. This entails the limitations as discussed above. OPC UA would provide a reliable, efficient way to transfer higher level structured data, but this will take some time until it is established in the industry.

Data processing unit: One of the most important tasks of the data processing unit is the aggregation of sensor data from several different interfaces. Each sensor system has its own sampling rate, which is a trade-off between noise reduction, relevance to the dynamics and restrictions from a computational performance perspective. However, the data processing unit has to timely-align the data from several sensor systems in an appropriate way in order to allow real-time process analysis. Additionally the integration of multi-variate (MVDA) models and basic calculations in the system should be realized by the data processing unit.

Database: Data from several processes and sensors, independent of their interfaces to the computerized system, must be time-aligned stored in a database. The operator should have access to the data from the database for off-line analysis via a graphical user interface.

Audit trail: As discussed in the previous section, all significant activities and events must be traceable, with a certain service responsible for an accurate audit trail.

Moreover, the system should provide some basic functionality, such as data visualization and the capability to export reports and to backup data frequently. Additionally, the system needs an interface for the operator to enable electronic signatures and set inputs manually.

3.4.3 Monitoring the Hot Melt Extrusion Process via SIMATIC SIPAT

In response to the growing interest in PAT, Siemens among other companies developed a PAT software solution, SIMATIC SIPAT (Siemens AG, Brussels, Belgium), that was designed to meet the basic GMP requirements discussed in the previous section (i.e., data integrity, electronic records, incident management, electronic signatures, system security, audit trail).

SIPAT collects data in real-time from various monitoring sources and performs an aggregation function to guarantee time alignment [48]. Observations, including measurements, manipulated variables (MVs) and PAT data (spectra, images, etc.) are available in real-time. SIPAT supports external calculation engines to transform process data into information that can further be used to detect abnormalities in the process. For example, in our work external calculation engines used are MATLAB (Mathworks, Inc., USA) and SIMCA-Q (Umetrics, Sweden). The real-time prediction engine SIMCA-Q facilitated the integration of models developed in SIMCA-P+ (Umetrics, Sweden), from which multivariate data analysis (MVDA) models (e.g., PCA,

PLS) were developed. MATLAB is a programming environment for algorithm development, data analysis and numerical computation, and integrating MATLAB functions extended SIPAT's capability to perform complex calculations (e.g., multivariate calculus).

In order to monitor and control a continuous process, appropriate uni- and multivariate sensors and actuators must be introduced in SIPAT. On the one hand, SIPAT offers common communication interfaces (i.e., OPC technology), making it possible to use sensors from different manufacturers. On the other hand, it allows the developer to import PAT tools (e.g., spectrometer) by providing customized communication interfaces.

In the context of SIPAT, a base station, collector stations, clients and central database exist. A collector station is responsible for acquiring data of a certain sensor system, which means that each spectrometer and univariate sensor (e.g., temperatures, feed rates, etc.) provided by the extruder represents a collector station. A base station unifies several collector stations belonging to one or several unit operations, e.g., extrusion, blending, tableting, etc. [48], [49]. A central database is mandatory for the SIPAT system, where all of the system's configuration information and historical and real-time data are stored.

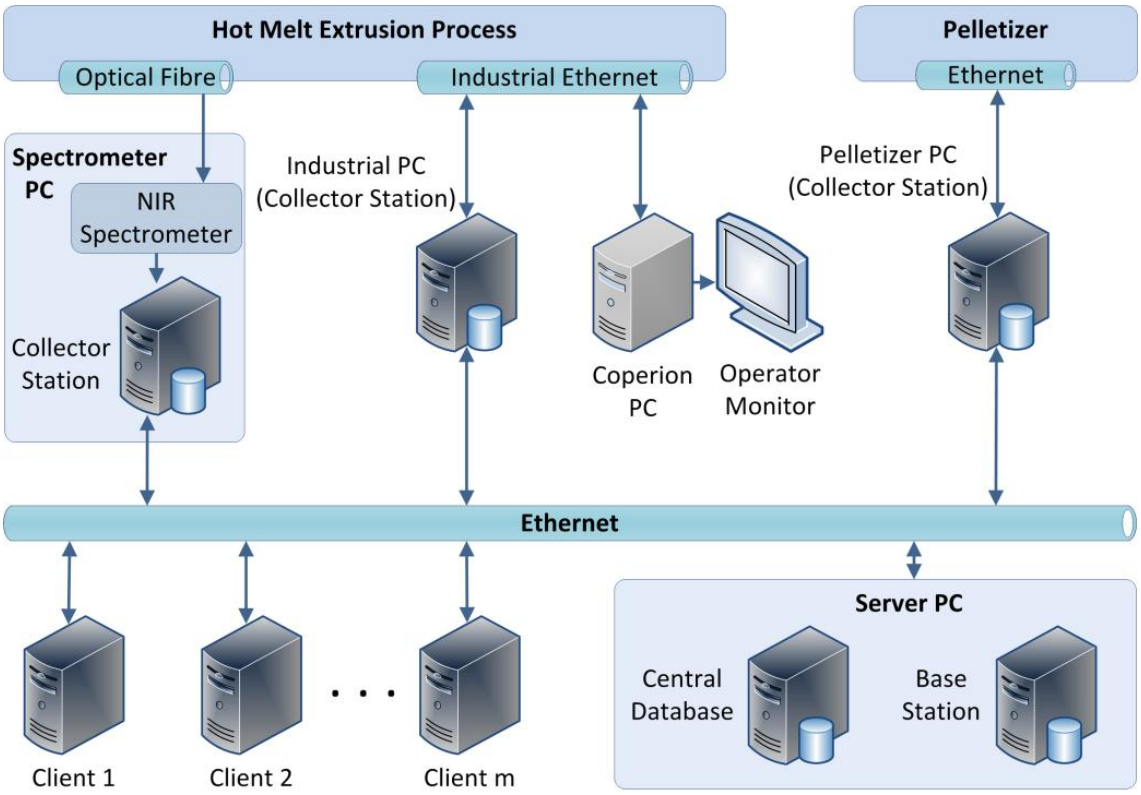

Figure 12: Network architecture of the hot melt extruder and the pelletizer.

A certain network architecture (Figure 12) based on the software design of SIPAT and the given hardware was required. The main components were (1) a spectrometer PC as a collector station, (2) an industrial PC as a collector station for all extrusion data, (3) a Coperion PC with an operator monitor (independent from the SIPAT system), (4) a HME process, (5) a server PC with a central database and a base station and (6) a number of clients. Communications between the SIPAT components was based on Ethernet technology.

The HME system had two collector stations: (1) the spectrometer was integrated into SIPAT via its own collector interface. Sentronic provides a driver that integrates the SentroPAT FO spectrometer into SIPAT. The configuration of the spectrometer (e.g., definition of the integration time, the number of spectra that were averaged, etc.) was predefined by an in-house software from Sentronic and loaded from the SIPAT collector interface. (2) based on OPC technology, an OPC server and the SIPAT collector station (acting as an OPC client) were installed on an industrial PC. Furthermore, the Coperion PC and the operator monitor were used to display SIMATIC WinCC. Win-

dows Control Center (WinCC) served as supervisory control, a data acquisition system and a human machine interface (HMI). This allowed the operator to monitor the process via either WinCC or SIPAT, the latter processing the spectra in real time.

Figure 13 shows interactions between SIPAT, SIMCA-Q, MATLAB and the process itself. A predefined input sequence (e.g., reference feed rate) was generated off-line in MATLAB. After acquiring a new set point of the reference feed rate, SIPAT distributed the scalar to the extruder via OPC technology. The extruder forwarded the value to the feeder that modified the feed rate.

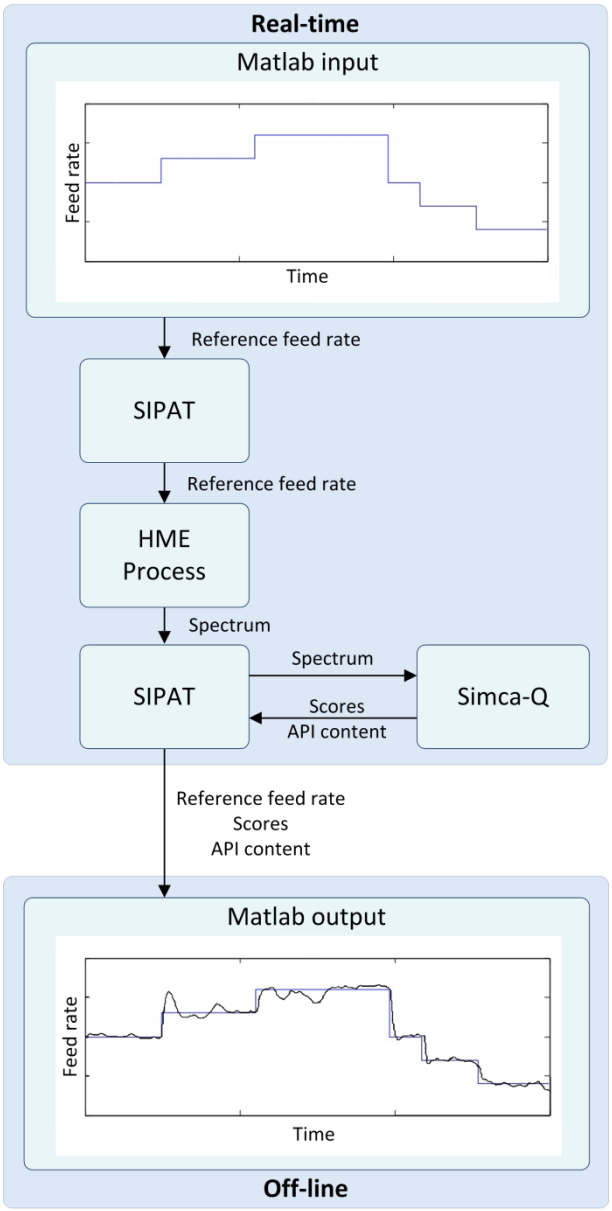

Figure 13: Manipulation of the reference feed rate and observation of the spectrum that can be analyzed in real-time using SIMCA-Q. Input and output data can be analyzed off-line, i.e., in MATLAB.

In order to investigate the influence of input parameters on the product quality, the observed spectrum was interpreted in real time using SIMCA-Q by projecting the data onto a reduced dimensional space. After the experiment, the observed data were analyzed directly in SIPAT or exported in a standard file format. A similar procedure was applied to gather the required data for the development of MVDA models, which will be discussed in the next section.

3.5 Continuous Process Analysis

Process analysis is important throughout the whole life cycle of a drug, from process development to production monitoring and continuous improvement. In all phases rational decisions depend on good data. Especially during continuous manufacturing, the state of the process needs to be known. For example during extrusion, if the melt temperature increases, the rheological behavior changes, impacting the processability by downstream operations, i.e., die face pelletizing. Temperature can also influence the polymorphic forms of the API, or if the API dissolves in the matrix or remains crystalline. Thus, temperature needs to be tightly controlled. However, by displaying all measured process parameters, e.g., all temperature readings along the barrel, it is hard to grasp important information, as raw data may overwhelm operators. Additionally, computerized fault detection also needs to summarize multiple process parameters. Therefore, methods for condensing information are critically needed and are generally described as *process analysis.* Process analysis helps providing the necessary understanding of the inter-dependencies of various factors.

In this section, examples of process analysis approaches are presented, including:

- **Monitoring of process parameters:** Here data are collected, to develop and optimize a process and to avoid all kinds of process upsets (i.e., pressure build up). This facilitates the development of a knowledge space, in which the process is yielding consistent results.
- **Qualitative analysis**: An important utility to summarize the information contained in the large amount of process parameters or spectra is qualitative analysis, i.e., principal component analysis (PCA). Additionally it can be useful for detection of deviations from the desired state during continuous extrusion.
- **Quantitative analysis**: Often critical quality attributes (CQAs) cannot be measured directly by a sensor. Therefore, the impact of the process state on the CQAs has to be predicted. Exemplarily, the API content prediction with a PLS model is presented.

In the following examples, a co-rotating twin screw extruder (ZSK 18, Coperion GmbH, Germany) was used, and the raw material was fed with two twin screw loss-in weight feeders (K-PH-CL-24-KT20 & K-CL-KT20, K-Tron, Switzerland) at the first barrel. The pellets were obtained by a novel pelletizer, developed by Automatik Plastics Machinery GmbH. For spectral acquisition a diode array-based near-infrared spectrometer, SentroPAT FO (Sentronic GmbH, Germany), with a fiber-optic Dynisco NIR probe was used. The Dynisco probe is a special probe for 1/2'' UNF thread, as used for extruders. The spectrometer covers the wavelength range of 1100nm-2200nm with a resolution of 2nm. NIR spectra were collected in the 8-0 plate as described above. 120 spectra were averaged and an integration time of 0.014s per spectrum was used. SIPAT (Siemens AG, Belgium) was applied as data acquisition software to collect, timely-align and store the process and spectral data.

3.5.1 Monitoring of Process Parameters

The main driving force behind process analysis, as part of the QbD development, is to develop a routine process, which produces a consistently high product quality. This requires process parameter settings which provide a stable process. A stable process means that constant input variables (such as temperature profile, knife speed, etc.) lead to constant output variables (product quality), for example die pressure, material temperature. A theoretical steady-state process is defined by constant process parameters over the entire process time. In reality, however, measurement accuracy or process fluctuations lead to varying output variables within a process window. As long as all variables stay within a defined range, the process is assumed to be stable. However, first this stable process needs to be developed on the basis of an analysis of process parameters that have a strong impact on the CQAs. Evaluation and validation of the root causes of a stable or an unstable process yields important information about the relation between the process parameter and the stability of a process.

Figure 14 shows data of an early development stage of the extrusion line coupled with a hot die face cutter. Here, process monitoring was used to investigate the interaction between extruder and die-face cutter. For illustrative reasons only three variables (over 50 variables are recorded), cutter speed, material pressure and temperature were chosen for a simple analysis. The material temperature and pressure showed significant dependence of the cutter. Each start of the die face cutter (A, B, C in Figure 15) caused an increase of the material pressure. The reason for the increase was a cooling of the die by the air stream of the cutter, which was used to quench the hot-melt strand and the cut pellets. Subsequently, the melt temperature was reduced and the viscosity was increased, resulting in a higher pressure drop. The first two starts (A & B) of the hot die face cutter caused such a high increase (100 bars) that the emergency shutdown of the extruder was triggered. After the second shutdown the energy balance at the extrusion die was changed by lowering the cooling air flow rate and the third start (C) was running for a longer period. Such information can be used to develop a better understanding of the interaction between the individual process parameters. Thus, optimal process settings can be easier defined or the insight triggers a modification of the experimental setup. In this example a better thermal decoupling of the melt temperature in the die zone and the hot die face cutter was enough to achieve an improved process.

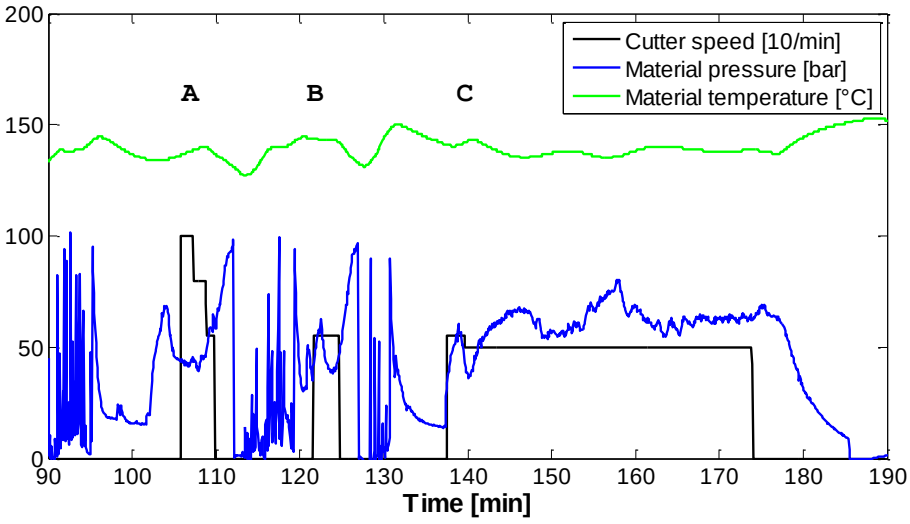

Figure 14: Qualitative Analysis: instable process (early stage of process development).

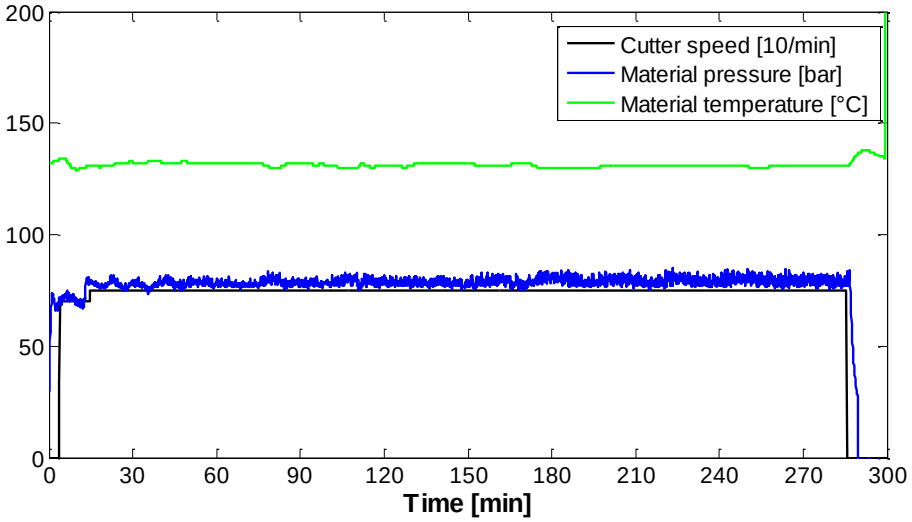

Figure 15: Stable process performance over 5 hours (stable process).

Figure 15 shows data of the same extrusion line but for an optimized process. As can be seen the fluctuations of the process variables are within a small range around a steady mean value. The data of such a stable process may provide the basis for the development of an advanced PAT strategy. In the next sections the development of PAT models for qualitative and quantitative analysis based on a stable process is shown.

3.5.2 Qualitative Process Analysis

The online monitoring of chemical (e.g., assay, morphology) and physical parameters (e.g. the moisture content, particle size or temperature of an intermediate material) is even more important in continuous manufacturing, as processes are connected with each other. For example, our downstream process requires an intermediate product (i.e., the hot strand) with consistent physical parameters (temperature, viscosity) in order to process the material properly.

In general, a large number of process variables can be monitored and are available for off-line and real-time analysis. Specifically in continuous manufacturing, where several processes are combined to a production line (i.e., feeding, extrusion and pelletization), the number of variables is even larger. Thus, it is hard to evaluate trends based on these data. Moreover, many process parameters are highly correlat-

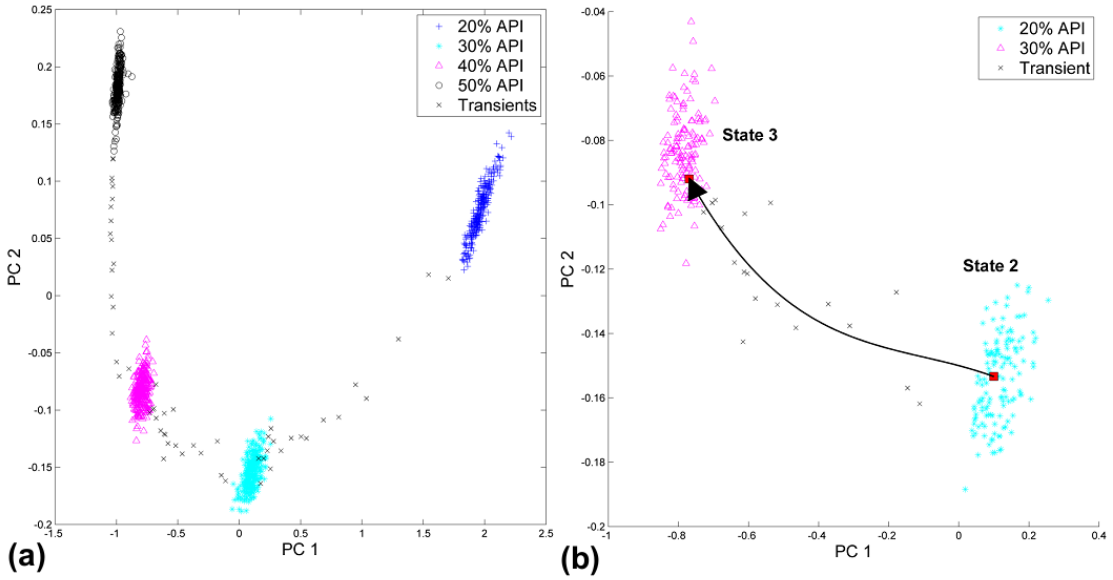

Figure 16: (a) Different API concentrations (20%, 30%, 40% and 50%) result in the clustering of samples in the score plot (PC 1 versus PC 2). (b) The trajectory from state 2 (30% API concentration) to state 3 (40% API concentration) was monitored in real-time via SIPAT. The mean settling time from one process condition to the next stable state was approximately 100 seconds.

ed (e.g., neighboring barrel temperatures of the extruder), and therefore a much lower number of independent variables can be used to monitor the process status.

Principal component analysis (PCA) is an excellent method to extract the essential information of large data sets (process parameters or spectral data). Here, PCA was employed for analysis of NIR spectra, collected while adjusting the feed rates to obtain different API concentrations. The projection of the spectra to a reduced space (i.e., the principal components) was applied to determine trends and variations of the physical and chemical parameters of the intermediate product and to identify process upsets in real-time. Figure 16 (a) illustrates the score plot of the principal components 1 versus 2. Adjusting the feed rates of the feeders resulted in different API concentrations in the melt, which appear in the score plot as clusters of observations. Applying PCA to the data could thus be seen as classification of the main events affecting the process. The four clusters represented 20% (blue), 30% (cyan), 40% (magenta) and 50% (black) API content in the melt in the die section (the observations in grey related to transitions between stable process conditions). A closer inspection of the trajectory from state 2 (30% API concentration) to state 3 (40% API concentra-

tion) allowed real-time monitoring of the process stages, as illustrated in Figure 16 (b).

3.5.3 Quantitative Spectral Analysis

As mentioned above, a quantitative method is useful to predict a CQA, for example, the API content. This can be done (amongst other methods) by analyzing the NIR spectrum. Unlike qualitative analysis, the prediction of the CQA with quantitative methods should be independent of changes in physical properties (i.e., melt temperature, material pressure). It should be a soft sensor for this specific attribute. The development of such models is only feasibly for a robust process, with no major process upsets.

For API content analysis the method chosen was partial least squares regression (PLS-R), which is also known as projection to latent structures [50]. To develop a PLS model, spectra of samples with known API content are taken. The PLS algorithm analyzes the spectrum, and latent variables are statistically computed, which provide the best achievable linear relationship to the known API content. Thereby, the information contained in the spectrum, which commonly consists of > 500 variables (wavelength), is projected to only a few latent variables. Quality measures of the model are R^2 and Q^2, which account for the explained variance within the model data (R^2) and for validation (Q^2). $R^2 = 1$ means, that the model can accurately predict the API content of spectra that are included in the model. But this could also imply that the model fitted noise. This is called overfitting and results in an unstable model. Therefore, a cross validation technique is commonly used. If there is a large difference, greater than 0.2 between R^2 and Q^2 the model is unstable. A model with high Q^2, close to 1, suggests a robust model. Using the PLS method, the API content was predicted from the measured NIR spectrum.

3.5.3.1 Development and Validation of a PLS Model to Determine the API Content

For model building a premix of each API concentration was prepared, ranging from 0% to 60% API with 10% increments. These premixes were extruded and the accord-

ing spectra recorded. Based upon this data a PLS model was established. The PLS model consisted of the first four latent variables, with R^2 = 0.999, Q^2 = 0.974 and RMSEP = 0.53% (root mean square error of prediction). This suggested an accurate model. The validation was determined by excluding a premix from the model, i.e., 10% API, and predicting the excluded premix.

The resulting model is presented in Figure 17, in which the model data are shown in black and the validation data in blue. The validation data for 0% API, with a predicted API content of around -9% was notably off the correct value. When including 0% API in the model, the predictions were accurate. The main reason was found in the optical properties of the melt. At the extrusion process temperatures, the pure matrix was more translucent compared to a matrix with embedded drug crystals. By adding 10% crystalline API the melt became significantly more opaque. As such, in the case of a solid dispersion with a translucent matrix in the low API regime the NIR signal was very sensitive to concentration changes. This feature could be exploited to detect low dosage APIs, which is useful, for example, for high-potential APIs.

The model was validated in subsequent continuous extrusion runs. Samples were taken directly at the die, analyzed with HPLC and compared with the NIR determined drug content value. The results are presented in Figure 18, with the NIR determined API content shown in red. The results of the offline samples are represented by black

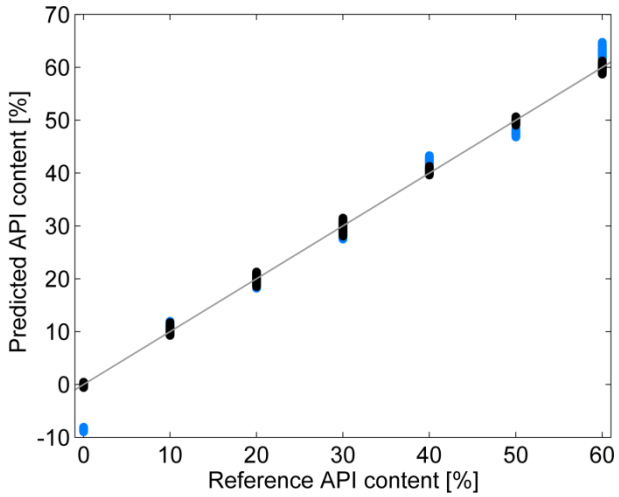

Figure 17: The chemometric model with 0% to 60% API content in the melt with R^2 = 0.999 (black), Q^2 = 0.974 (blue), RMSEP = 0.53% and four latent variables. Due to the translucent matrix, cross validation (blue) of the 0% group failed with a predicted API content of about -9%. Yet, the predictive capability of the model, including 0%, is high.

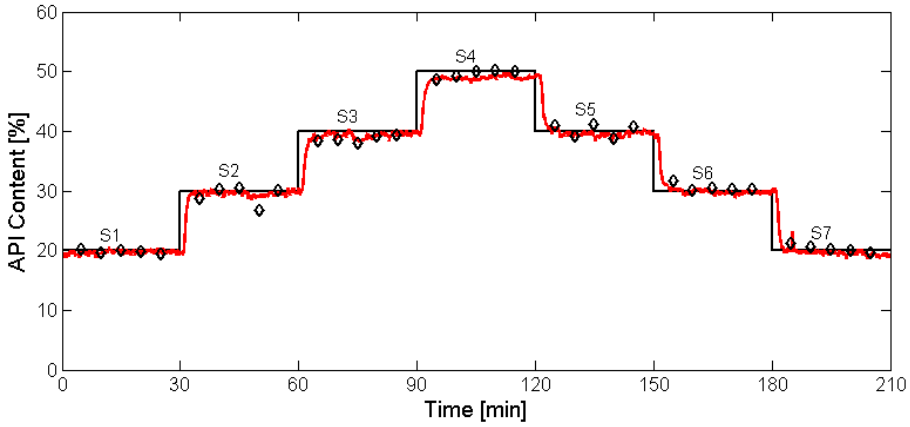

Figure 18: Data of one continuous extrusion run with seven steps in API content, 20% to 50%. Black: pre-set concentration profile, red: NIR determined API content, diamonds: offline HPLC measurements.

diamonds. The points showed a good agreement with the pre-set profile and the NIR predictions. One point out of thirty-five strongly deviated (10.66%) from the pre-set concentration and was presumed an outlier. The reason for this point being an outlier is probably due to the sample preparation for HPLC analysis. The average deviation of all samples was -0.47% and without the outlier -0.16%. Therefore, the model can be used for drug content monitoring during production and for studying the influences upon it.

3.5.3.2 Comparing Different Screw Designs

One of the major factors that influence uniformity of the drug content is the screw design, which can change the mixing capabilities of an extruder (mixing is the ability to compensate for feeder dosing fluctuations, i.e., pulsating streams). Figure 19 compares two screw designs: one with three kneading zones and the other only with conveying elements. The differences in the drug content uniformity between the screws can be easily assessed by visual inspection. As can be seen the kneading screw produces a much more homogenous API concentration. Obviously, strong high-frequency fluctuations of the feeder exist, which are transported through the extruder, if no kneading elements are present. Thus, kneading elements are critical for obtaining a robust continuous process.

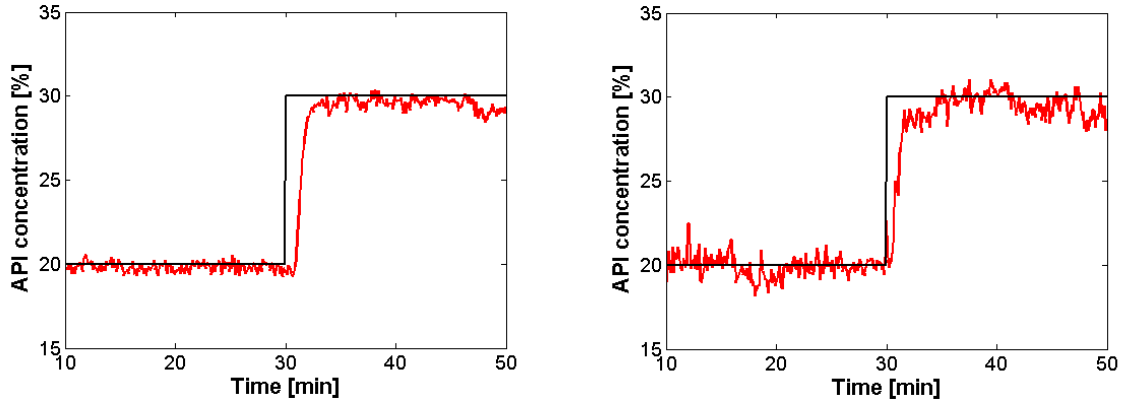

Figure 19: Comparison of different screw designs. Left: screw with three kneading zones. Right: screw with conveying elements only. Note the differences in the drug content fluctuations. The kneading screw produces a more homogenous melt.

Deviations of NIR determined API content and feeder settings in the transition region between subsequent steady states were due to the residence time in and the mixing behavior of the extruder. Thus, these curves can be used to obtain a good understanding of the mixing and the residence time distribution (RTD) in the extruder. Mixing can be assessed by analyzing the standard deviation (SD) during the steady state between step changes. A low SD indicates a more homogenous melt. The RTD can be calculated by the first derivative of the response by the NIR determined API content to a change of feeder settings. The mean residence time in the extruder is approximated by the delay between the step change of feeder settings and the corresponding concentration increase by half of the step height. The difference in delay times confirm a longer residence time for the kneading screw (Figure 19, left), compared to the conveying screw (right). The average residence time in the extruder is in the order of one to three minutes.

For the purpose of controlling the feeder, only low frequency fluctuations can be handled. The measurement setup in the 8-0 plate does not allow controlling (i.e., mitigating) high-frequency fluctuations, since the material has already passed the extruder. Therefore, for high frequency fluctuations this setup cannot be used as quality control, while long-term feeder deviations can be controlled.

3.6 Conclusion

Continuous manufacturing is not yet widely used in the pharmaceutical industry. However, there is significant interest. The unit operations of a continuous manufacturing line are similar to other industries. However, the requirements concerning purity, choice of materials and GMP documentation for pharmaceutical production are typically more stringent. In this chapter the requirements and challenges for continuous manufacturing and process monitoring have been discussed. The key results of our work can be summarized as follows:

Continuous extrusion

- Development of a stable process is a prerequisite for continuous manufacturing
- Feeding, extrusion (screw design, etc.) and downstream processes need to be tailored to fit a specific formulation
- Strong relationships between feeding performance and content uniformity

Downstream

- Numerous products and shapes can be manufactured
- There is a strong coupling between upstream and downstream processes (i.e. material temperature at the extrusion die due to an altered energy balance)
- Control strategies for process disturbances are needed

PAT analyzers

- Suitable sensor positions need to be determined
- In-line monitoring systems need to be adapted to the process and carefully tuned
- Robust in-line API content determination is required to ensure quality

Computerized systems

- GMP requirements for computerized systems need to be met
- Integration of unit operations and PAT analyzers into a central system is beneficial (e.g., via SIPAT or other software)
- Data acquisition and real-time monitoring of process parameters is mandatory

3.7 References

[1] M. M. Crowley, F. Zhang, M. A. Repka, S. Thumma, S. B. Upadhye, S. K. Battu, J. W. McGinity, and C. Martin, "Pharmaceutical applications of hot-melt extrusion: part I.," *Drug Dev. Ind. Pharm.*, vol. 33, no. 9, pp. 909–26, Sep. 2007.

[2] L. Schenck, G. M. Troup, M. Lowinger, L. Li, and C. McKelvey, "Achieving a Hot melt extrusion design space for the production of solid solutions," in *Chemical Engineering in the Pharmaceutical Industry: R&D to Manufacturing*, D. J. am Ende, Ed. John Wiley & Sons Ltd., 2011, pp. 819–836.

[3] W. E. Engisch and F. J. Muzzio, "Method for characterization of loss-in-weight feeder equipment," *Powder Technol.*, vol. 228, pp. 395–403, Sep. 2012.

[4] T. Mezger, *The Rheology Handbook*, 3rd Revise. Vincentz Network, 2011, p. 432.

[5] L. Zema, G. Loreti, A. Melocchi, A. Maroni, and A. Gazzaniga, "Injection Molding and its application to drug delivery.," *J. Control. Release*, vol. 159, no. 3, pp. 324–31, May 2012.

[6] J. G. Khinast, R. Baumgartner, G. Koscher, and E. Roblegg, "R1142GB: System for producing a solid preparation from a suspension," 2012.

[7] J. G. Khinast, R. Baumgartner, and E. Roblegg, "Nano-extrusion: a One-Step Process for Manufacturing of Solid Nanoparticle Formulations Directly from the Liquid Phase.," *AAPS PharmSciTech*, 2013.

[8] T. Kipping and H. Rein, "A new method for the continuous production of single dosed controlled release matrix systems based on hot-melt extruded starch: analysis of relevant process parameters and implementation of an in-process control.," *Eur. J. Pharm. Biopharm.*, vol. 84, no. 1, pp. 156–71, May 2013.

[9] M. A. Repka, S. Majumdar, S. K. Battu, R. Srirangam, and S. B. Upadhye, "Applications of hot-melt extrusion for drug delivery," *Expert Opin. Drug Deliv.*, vol. 5, no. 12, pp. 1357–1376, 2008.

[10] S. Bialleck and H. Rein, "Preparation of starch-based pellets by hot-melt extrusion.," *Eur. J. Pharm. Biopharm.*, vol. 79, no. 2, pp. 440–448, Oct. 2011.

[11] E. Roblegg, E. Jäger, A. Hodzic, G. Koscher, S. Mohr, A. Zimmer, and J. Khinast, "Development of sustained-release lipophilic calcium stearate pellets via hot melt extrusion.," *Eur. J. Pharm. Biopharm.*, vol. 79, no. 3, pp. 635–645, Nov. 2011.

[12] R.-K. Mürb, "Kunststoff granulieren und/oder pelletieren?," *Chemie Ing. Tech.*, vol. 84, no. 11, pp. 1885–1893, Nov. 2012.

[13] *Guidance for Industry. PAT - A Framework for Innovative Pharmaceutical Development, Manufacturing, and Quality Assurance*, no. September. Rockville, MD.: FDA, US Department of Health, 2004.

[14] I. C. on Harmonisation of Technical Requirements for Registration of pharmaceuticals for Human Use, "ICH Harmonised Tripartite Guidline: Pharmaceitical Development Q8(R2)." 2009.

[15] Y. Roggo, P. Chalus, L. Maurer, C. Lema-Martinez, A. Edmond, and N. Jent, "A review of near infrared spectroscopy and chemometrics in pharmaceutical technologies.," *J. Pharm. Biomed. Anal.*, vol. 44, no. 3, pp. 683–700, Jul. 2007.

[16] T. De Beer, A. Burggraeve, M. Fonteyne, L. Saerens, J. P. Remon, and C. Vervaet, "Near infrared and Raman spectroscopy for the in-process monitoring of pharmaceutical production processes.," *Int. J. Pharm.*, vol. 417, no. 1–2, pp. 32–47, Sep. 2011.

[17] T. Vankeirsbilck, A. Vercauteren, W. Baeyens, G. Van der Weken, F. Verpoort, G. Vergote, and J. P. Remon, "Applications of Raman spectroscopy in pharmaceutical analysis," *Trends Anal. Chem.*, vol. 21, no. 12, pp. 869–877, 2002.

[18] A. Peinado, J. Hammond, and A. Scott, "Development, validation and transfer of a near infrared method to determine in-line the end point of a fluidised drying process for commercial production batches of an approved oral solid dose pharmaceutical product.," *J. Pharm. Biomed. Anal.*, vol. 54, no. 1, pp. 13–20, Jan. 2011.

[19] I. Alig, B. Steinhoff, and D. Lellinger, "Monitoring of polymer melt processing," *Meas. Sci. Technol.*, vol. 21, no. 6, Jun. 2010.

[20] M. Reichenbächer and J. Popp, "Schwingungsspektroskopie," in *Strukturanalytik organischer und anorganischer Verbindungen*, Teubner, 2007, pp. 61–118.

[21] H. W. Siesler, "Basic principles of near-infrared spectroscopy," in *Handbook of Near-Infrared Analysis*, 3rd ed., D. A. Burns and E. W. Ciurczak, Eds. CRC Press, 2007, pp. 7–20.

[22] H. W. Siesler, Y. Ozaki, S. Kawata, and H. . Heise, Eds., *Near-Infrared Spectroscopy: Principles, Instruments, Applications*. Weinheim: Wiley-VCH, 2002.

[23] L. Saerens, L. Dierickx, T. Quinten, P. Adriaensens, R. Carleer, C. Vervaet, J. P. Remon, and T. De Beer, "In-line NIR spectroscopy for the understanding of polymer-drug interaction during pharmaceutical hot-melt extrusion.," *Eur. J. Pharm. Biopharm.*, vol. 81, no. 1, pp. 237–230, Jan. 2012.

[24] V. S. Tumuluri, S. Prodduturi, M. M. Crowley, S. P. Stodghill, J. W. McGinity, M. A. Repka, and B. A. Avery, "The use of near-infrared spectroscopy for the quantitation of a drug in hot-melt extruded films.," *Drug Dev. Ind. Pharm.*, vol. 30, no. 5, pp. 505–511, 2004.

[25] I. V. Hertel and C.-P. Schulz, "Zweiatomige Moleküle," in *Atome, Moleküle und optische Physik 2*, Heidelberg, 2010, pp. 1–88.

[26] I. V. Hertel and C.-P. Schulz, "Molekülspektroskopie," in *Atome, Moleküle und optische Physik 2*, Heidelberg, 2010, pp. 247–327.

[27] K. H. Esbensen and P. Paasch-Mortensen, "Process Sampling: Theory of Sampling - the Missing Link in Process Analytical Technology (PAT)," in *Process Analytical Technology*, 2nd ed., K. A. Bakeev, Ed. John Wiley & Sons Ltd., 2010, pp. 37–80.

[28] C. Rauwendaal, *Polymer Extrusion*, 4th ed. Munich: Hanser Publishers, 2001, p. 781.

[29] K. Kohlgrüber, *Co-Rotating Twin-Screw Extruder*. Carl Hanser Verlag GmbH & CO. KG, 2007, p. 369.

[30] O. Scheibelhofer, D. M. Koller, P. Kerschhaggl, and J. G. Khinast, "Continuous Powder Flow Monitoring via Near-Infrared Hyperspectral Imaging," *Instrum. Meas. Technol. Conf. (I2MTC), 2012 IEEE Int.*, pp. 748–753, 2012.

[31] I. Alig, D. Fischer, D. Lellinger, and B. Steinhoff, "Combination of NIR, Raman, ultrasonic and dielectric spectroscopy for in-line monitoring of the extrusion process," *Macromol. Symp.*, vol. 230, no. 1, pp. 51–58, 2005.

[32] D. Fischer, T. Bayer, K. J. Eichhorn, and M. Otto, "In-line process monitoring on polymer melts by NIR-spectroscopy," *Fresenius J. Anal. Chem.*, vol. 359, no. 1, pp. 74–77, 1997.

[33] P. D. Coates, S. E. Barnes, M. G. Sibley, E. C. Brown, H. G. M. Edwards, and I. J. Scowen, "In-process vibrational spectroscopy and ultrasound measurements in polymer melt extrusion," *Polymer (Guildf).*, vol. 44, no. 19, pp. 5937–5949, Sep. 2003.

[34] D. Fischer, J. Müller, S. Kummer, and B. Kretzschmar, "Real time monitoring of morphologic and mechanical properties of polymer nanocomposites during

extrusion by near infrared and ultrasonic spectroscopy," *Macromol. Symp.*, vol. 305, no. 1, pp. 10–17, Jul. 2011.

[35] K. Bakeev, *Process Analytical Technology: Spectroscopic Tools and Implementation Strategies for the Chemical and Pharmaceutical Industries*. John Wiley & Sons, 2010.

[36] D. M. Koller, A. Posch, G. Hörl, C. Voura, S. Radl, N. Urbanetz, S. D. Fraser, W. Tritthart, F. Reiter, and M. Schlingmann, "Continuous quantitative monitoring of powder mixing dynamics by near-infrared spectroscopys," *Powder Technol.*, vol. 205, no. 1–3, pp. 87–96, Jan. 2011.

[37] European Commission, "Annex 11: Computerized Systems," *Good Manuf. Pract. Med. Prod. Hum. Vet. Use*, vol. Volume 4, p. 5, 2011.

[38] European Commission, "Chapter 4: Documentation," *Good Manuf. Pract. Med. Prod. Hum. Vet. Use*, vol. Volume 4, p. 9, 2011.

[39] U.S. Food and Drug Administration, "Guidance for Industry. 21 CFR Part 11; electronic records; electronic signatures, glossary of terms," vol. Volume 1, 2011.

[40] ISPE Headquarters, "GAMP® 5: A Risk-Based Approach to Compliant GxP Computerized Systems," p. 352, 2008.

[41] T. Linz and S. Seeger, "21 CFR Part 11 Revesited," in *Encyclopedia of Pharmaceutical Technology*, Third., J. Swarbick, Ed. New York: Informer Healthcare USA, Inc., 2006, p. 4370.

[42] M. Roemer, "Computervalidierung," in *GMP-Berater*, Maas und Peither AG - GMP-Verlag, 2011.

[43] T. Linz and S. Seeger, "21 CFR Part 11 Revesited," in *Encyclopedia of Pharmaceutical Technology*, Third., J. Swarbick, Ed. New York: Informer Healthcare USA, Inc., 2006, p. 4370.

[44] "Annex 11: Computerized Systems," in *Good Manufacturing Practices for Medicinal Products for Human and Veterinary Use*, vol. 4, Brussels: European Commission, 2011.

[45] M. Roemer, "Computervalidierung," in *GMP-Berater*, Maas und Peither AG - GMP-Verlag, 2011.

[46] S. O'Neill, B. Grout, B. Diehl, E. Garsthein, S. Hammond, M. Moshgbar, S. Maris, J. Timmermans, K. Redl, and J. O'Sullivan, "Prozessanalytische Technologien," in *GMP-Berater*, Maas und Peither AG - GMP-Verlag, 2011.

[47] M. Hiob, "Dokumentation," in *GMP-Berater*, Maas und Peither AG - GMP-Verlag, 2011.

[48] F. De Frenne, "User Manual; Simatic SIPAT Version 3.1.1," *History*. Siemens AG, p. 230, 2011.

[49] P. De Tandt, "Exception Handling; SIMATIC SIPAT Version 3.1.1," Siemens AG, p. 21, 2011.

[50] S. Wold, M. Sjöström, and L. Eriksson, "PLS-regression : a basic tool of chemometrics," *Chemom. Intell. Lab. Syst.*, vol. 58, pp. 109–130, 2001.

Nature is relentless and unchangeable,
and it is indifferent
as to whether its hidden reasons and actions
are understandable to man or not.
Galileo Galilei

4. In-line Implementation of an Image-based Particle Size Measurement Tool to Monitor Hot-Melt Extruded Pellets[4]

4.1 Introduction

Hot-melt extrusion is a continuous manufacturing process with increasing importance for the pharmaceutical industry. It offers a robust manufacturing alternative for solid solutions and solid dispersions, which are used to increase the bioavailability of poorly soluble drugs [1], [2] or to achieve sustained-release behavior [3]–[5], respectively.

An extruder processes a formulation comprising of powders, pellets or liquids to form homogeneous strands of molten material. The molten material can be formed into various shapes, such as pellets, tablets or implants. In this work the strands are in-

[4] This chapter is based on: D. Treffer, P.R. Wahl, T. Hörmann, D. Markl, S. Schrank, I. Jones, P. Cruise, R.-K. Mürb, G. Koscher, E. Roblegg and J.G. Khinast, "In-line Implementation of an Image-based Particle Size Measurement Tool to Monitor Hot-Melt Extruded Pellets.," Int. J. Pharm., accepted, 2014. This paper is a co-publication of D. Treffer and the author of this thesis. Both authors have contributed significantly.

tended to be shaped into spherical pellets, which are used as intermediates for capsule filling [6],[7], tablet compaction [8],[9] or other processing steps. A typical way of achieving spherical pellets is extrusion-spheronization [10]–[12]. Here, after extrusion, the pellets are irreguly shaped (e.g., strands or cylinders) and need to be spheronized in an extra spheronization step. During spheronization the material is heated up to soften it and rounded by collisions with each other and the equipment walls. Highly uniform and spherical pellets are desired as this increases dosing precision (e.g., in pellet-dosing processes) and improves flowability.

However, this additional downstream process can be avoided by using hot-die face pelletizing that combines pelletizing and spheronization in one processing step. Figure 1 illustrates the described process. Hot-die face pelletizing is a method where cutting of the extrudate strands takes place above the softening point of the material. Thus, surface tension acts on the viscous pellets after cutting as a driving force for spheronization. Several authors found that the pellet morphology depends on formulation and process parameters and reported the production of nearly-spherical pellets by hot die-face pelletizing [13], [14]. The obtained sphericity with an aspect ratio of 1 to 1.1 is superior to typical spheronization results. Additionally, the particle size distribution (PSD) can be much narrower. An extensive overview of the available pelletizing methods can be found in [15].

The downstream processes after pelletizing require constant pellet quality to obtain a robust process with high dosing accuracy. In order to ensure a certain quality a suitable monitoring approach needs to be applied.

The pellet quality can be monitored with two main approaches [16]. First, in off-line monitoring [17] the samples are taken from the product stream at regular intervals and analyzed in the laboratory. Second, in/on-line monitoring [18]: for on-line monitoring a small bypass stream of the product stream is lead through the measurement device and analyzed in real time. In contrast in-line analyzers are situated in the main product stream. The distinct advantage of in/on-line approaches is real-time information. In case of out-of-spec products the operator or an automated process control

system can react immediately, so that only small amounts of waste arise from a single process disturbance and the whole batch does not have to be disposed or reworked.

Several techniques are available for in-line particle size measurement, of which focused beam reflectance (FBRM), spatial filter velocimetry, laser diffraction and various image analysis methods are common [16]. In the pharmaceutical context they are mainly used for fluid bed granulation, crystallization and spheronization.

In this work an image-analysis-based method has been chosen to acquire visual information of shape and surface morphology besides pellet dimensions. Specifically, we focus on the implementation of a novel in-line photometric stereo image analyzer for production of nearly-spherical pellets. The analyzer uses photometric stereo techniques to derive 3D information based on 2D images to accurately measure particles size and shape. By monitoring a production of pellets by hot-melt extrusion and hot-die face pelletizing (Sphero-THA, Automatik Plastics Machinery GmbH) the capabilities of manufacturing nearly-spherical pellets by this downstream method will be presented.

4.2 Materials and Methods

4.2.1 Materials

The model matrix carrier for the hot-melt extrusion was calcium stearate CaSt (Werba-Chem GmbH, Austria; mean particle size 16.62 µm). The use of CaSt as a carrier matrix was recently introduced by Roblegg et al. [14]. The model active pharmaceutical ingredient (API) was paracetamol, donated by GL Pharma GmbH, Austria (mean particle size 139.2 µm). Glycerol-mono-stearate (GMS) was used as a plasticizer to lower the viscosity, and thus, the required process temperature. All CaSt-based experiments were performed with a formulation consisting of 75% CaSt, 20% Paracetamol and 5% GMS.

In addition, two different types of pellets, based on pure ethylene vinyl acetate EVA Ateva®1807EG (Celanese, USA) and based on a formulation consisting of 40%

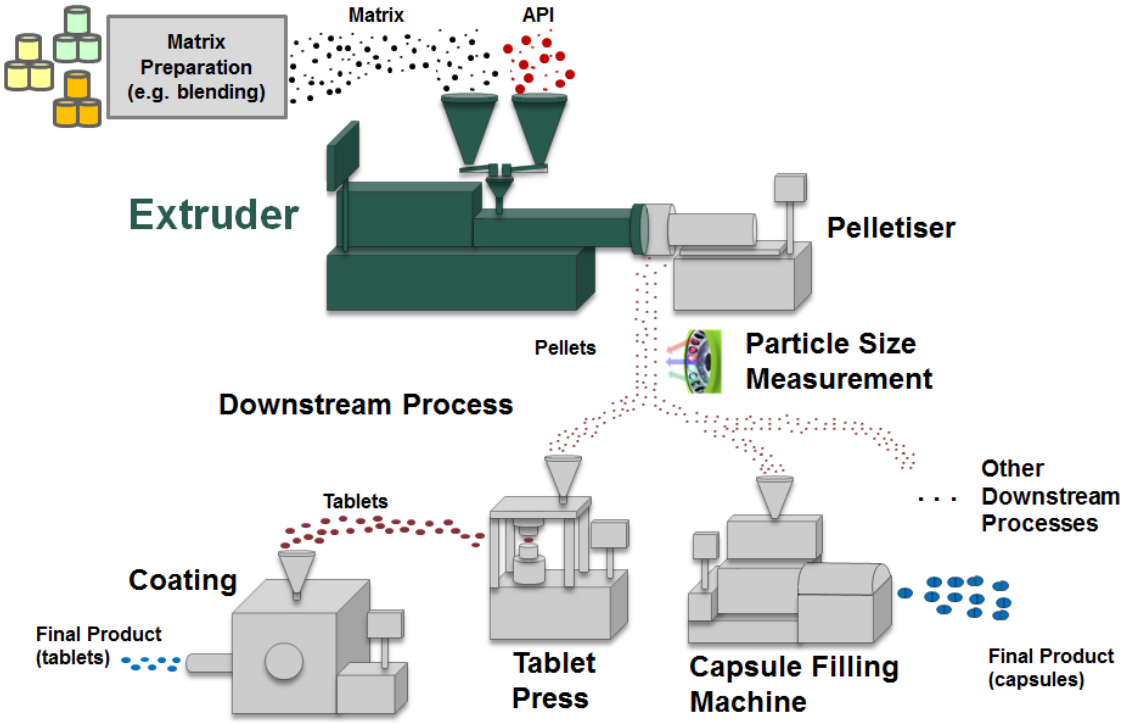

Figure 1: Process options in combination with a die-face pelletizing step.

Eudragit RS, 40% Eudragit PO (Evonik Industries, Germany) and 20% Talcum (donated by GL Pharma GmbH, Austria) were used in the experiments.

4.2.2 Methods

4.2.2.1 Hot Melt Extrusion

Figure 1 shows a schematic of the extrusion line. It combines a co-rotating twin screw extruder ZSK 18 (Coperion GmbH, Germany) and a novel hot-die-face pelletizer Sphero®-THA (Automatik Plastics Machinery GmbH, Germany). Both systems are implemented into a SIPAT system (Siemens AG, Belgium) for process control and monitoring. The extrusion line is also capable of monitoring the API content of the produced melt as described in [19], [20].

Figure 2 shows a photograph of pelletizing equipment and provides a detailed view of the cutting chamber. It is based on a rotor knife, which cuts the strands to form pellets of a predefined size, i.e., the emerging strands are cut into pellets directly at the

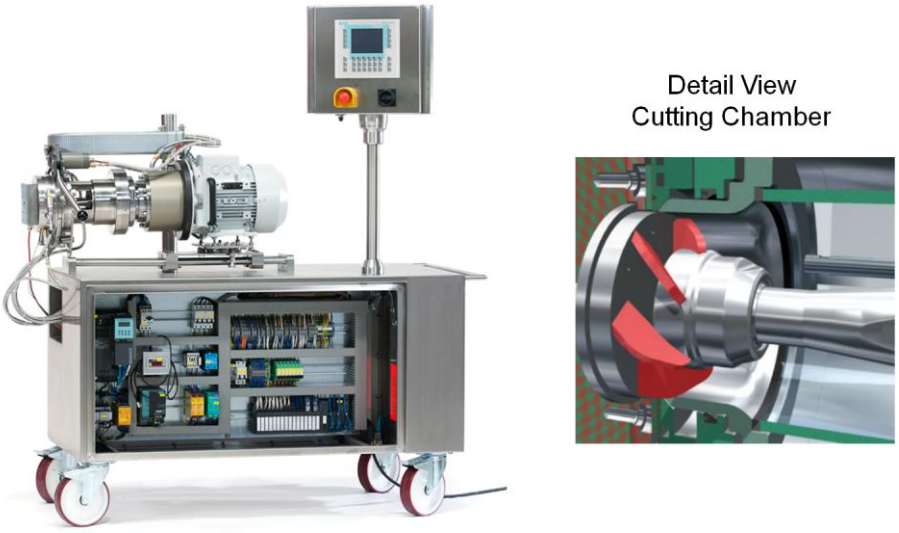

Figure 2: Picture of the Sphero®-THA and a detailed 3D illustration of the cutting chamber (Picture courtesy: Automatik Plastics Machinery GmbH).

hot-die face. A previous study showed that almost spherical pellets can be obtained via hot die face pelletizing [14].

4.2.2.2 In-line Monitoring of Pellet Size Properties

The pellet monitoring method is based on image analysis. The Eyecon™ particle characterizer technology uses concepts from 3-D machine vision. It enables capturing both the size and shape of particles between 50 and 3000 microns. A CCD camera is used to capture a continuous image sequence of the particles every 600 ms, using pulses of direct illumination with a length of between one and five microseconds. This brief pulse avoids motion blurring of particles, which may be moving at speeds of up to ten meters per second. The illumination is arranged according to the principle of photometric stereo for capturing the 3D features of the particles in addition to a regular 2D image (Figure 3, A)

The particle size is estimated from the images using the 2-D and 3-D information, applying novel image analysis methods and direct geometrical measurement [21][22]. The color information improves the edge detection. In case of overlapping or touching particles, the particles can be distinguished by color change, while conventional methods have problems with this situation and often overestimate the particle di-

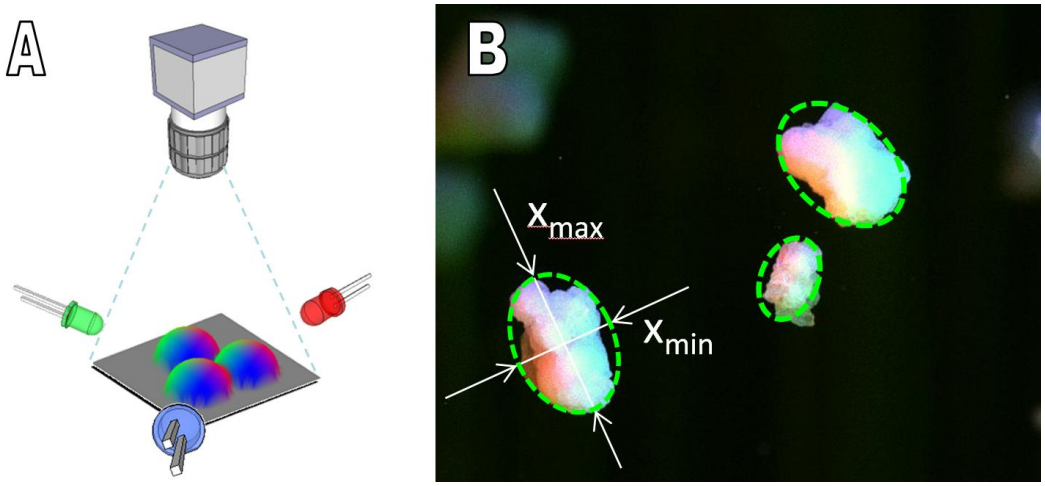

Figure 3: A: photometric stereo illumination arrangement (3 RGB LEDS); B: ellipses fitted to detected particles (Picture courtesy: Innopharma Labs Ltd.).

mensions, as two particles are counted as one. Only fully captured particles are analyzed by the system. Partially captured particles, occurring at the image boundaries and in case of overlapping by overlying particles, are not analyzed. Each particle detected within an image is first identified, and then described in terms of a best-fit ellipse (Figure 3, B). The maximum and minimum diameters of this ellipse are used to calculate the volume of the particle. By combining all of the measured particle volumes the x_{10}, x_{50} and x_{90} values for the analyzed sample can be computed. The sample size can be adjusted from a single image to multiple images (e.g., to determine a x_{50} time course) up to the entire sampling period to obtain representative information for all particles.

As the technology is based on direct measurement instead of indirect, such as laser diffraction, there is no need for material-based calibration. In addition, the method is a non-contact methodology and uses RGB LEDs to illuminate the field of view (9x6.5mm), so that no specific background is necessary. Thus, it can be applied externally to a process, e.g., through a glass window. However, there are some restrictions: the principle is based on diffuse reflected light, thus it cannot correctly detect black, strongly reflecting or transparent particles. Examples for the two later cases are shown in the results section. Applicability must be tested case by case, yet can be done off-line.

The data are processed in real-time and the time evolution of the characteristic diameters are displayed, e.g. x_{10}, x_{50}, x_{90}. In addition the data are stored as a number-based density distribution (q0). This information can be used to derive the more common cumulative volume-based particle size distribution (Q3) by applying basic conversion rules [23][24].

4.2.2.3 Area Fraction Calculation

The area fraction is used for a quantitative evaluation of the applied implementation approaches. It is an indication of the amount of particles within the optical sampling volume. The calculation of the area fraction is performed with the open source software ImageJ (National Institutes of Health (NIH), USA) [23]. The images are processed in the following sequence. First the color images are converted into 8-bit grayscale images. Subsequently, the grayscale is inverted and the pellets are separated with a suitable threshold. The area fraction is obtained by averaging 20 images. To prevent distortion of the result, e.g. caused by dust on the measurement window, only particles greater than 1000 pixel^2 are included in the calculation. This pixel area corresponds to an actual area of ~0.04 mm^2 or ~0.11 mm diameter of a circle of equal projection area (EQPC).

4.2.3 Reference Particle Analysis

For reference particle analysis an off-line image analysis tool (QICPIC, Sympatec GmbH, Germany) is used. The high-speed imaging tool is based on shadow projection. The sample is dispersed in a controlled way by means of a RODOS dry disperser and a VIBRI vibrational conveyor. At this configuration the system is capable of capturing particles in the range of 1 µm to 6 mm. The particle size is determined by EQPC. Analysis using this method is carried out with at least 50,000 particles. Measurements were always done in triplets.

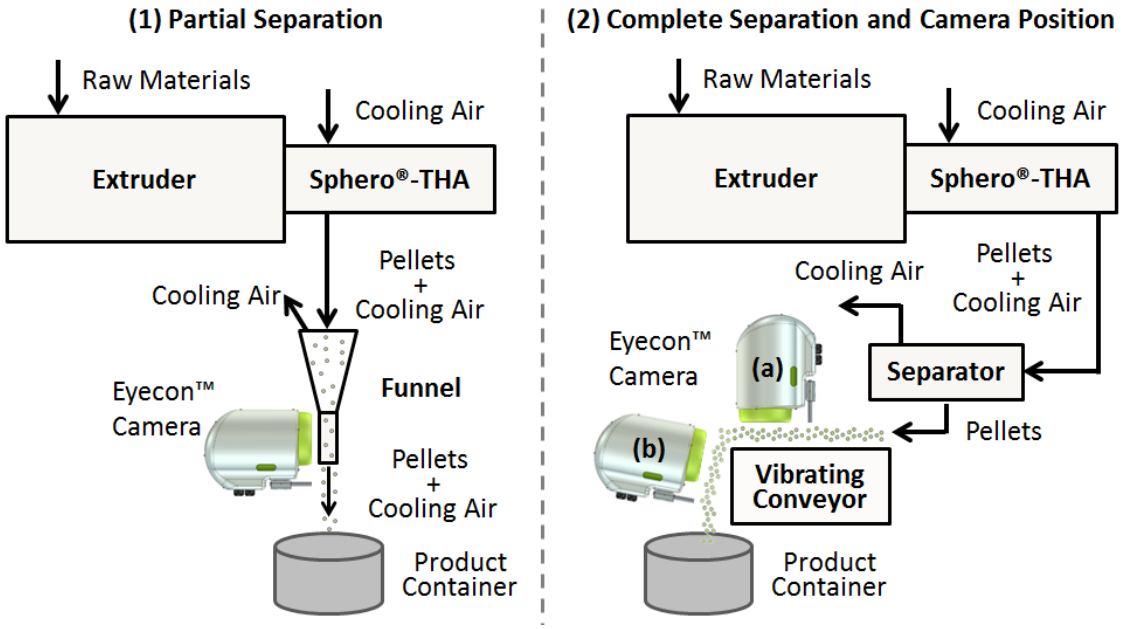

Figure 4: Implementation approaches

4.2.4 Implementation

The in-line measurement tool has a field of view of 9x6.5 mm and depth of focus of 1.4 mm. The rather small optical sampling volume required some effort during the implementation to the pelletizer because of two reasons: First, the mean particle size in general is in the range of 1 mm, which is in the range of the depth of focus. Thus, for ideal recognition the pellets should pass the sampling volume in a monolayer arrangement. Second, the particles are conveyed by a cooling air stream at low volume concentrations.

A low volume concentration with a large particle diameter gives a very low particle amount. When assuming a pellet diameter of 1 mm and an air volume stream of 500 l/min, this results in 63 pellets per liter cooling air. The optical sample volume is approximately 0.23 ml, which would lead to a 593-fold exchange of the sample volume per second by direct implementation into the pelletizing system. Therefore, different implementation approaches with partial and full separation of the cooling air were developed and compared. The extruder was operated at constant throughput of 0.8 kg/h. The analysis was carried out with regard to the particle count per image,

particle orientation and area fraction (a/a) of the analyzed particles. The values of area fraction and particle count per image have been analyzed for 20 consecutive images of each implementation approach.

In general, the main criterion for particle measurement by image analysis is to have focused images and a sufficient number of particles in each image. Apart from pellets, dust may be generated during cutting and transportation of the pellets which may influence the measurement. In this section two different implementation approaches regarding separation of the pellets and dust from the conveying air are described (Figure 4). Corresponding experimental results and their evaluation are discussed in detail in the section 4.3.2.

4.2.4.1 Partial Separation of the Transportation Gas

The pellet outlet of the Sphero®-THA is a cylindrical pipe with 44.3 mm in diameter. The exit velocity depends on the cooling air stream that is required to render the pellets non-sticky and has typical values between 2.7 – 10.8 m/s for air flow rates of 250-1000 l/min. Figure 4.1 shows the investigated direct implementation approach.

The maximum velocity of the pellets is assumed to be the average outlet velocity of the exiting air flow. Furthermore, the pellets have velocity components in all directions due to turbulent eddy flow. Therefore, the outlet stream is guided into a funnel made of transparent glass and Plexiglas. The camera is located behind the glass plate, due to better optical properties compared to Plexiglas. Furthermore, the glass plate protects the lenses against dust. The major part of the gas flow is separated and exists at the top funnel inlet. The particles collide with the wall and fall subsequently through the funnel. The in-line measurement captures the particles at the rectangular funnel outlet which has the dimensions of 8 x 6 x 20 mm. The narrow gap is designed to transport a sufficient amount of particles into the measurement area.

4.2.4.2 Complete Pellet Separation and Camera Position

The pellets are first completely separated from the air stream. Two different types of separation units are investigated. First, a centrifugal separator, a so called cyclone

and second an impact separator with a subsequent classifier. The cyclone separates the solid particles from the air including dust that arises during cutting or transportation from the air stream.

Contrarily, the impact separator offers the option of separating dust and air stream from the pellets. This is performed by gravity separation against the air stream in a vertical pipe with an appropriate diameter. In both cases, the separated pellets drop on a chute of a vibrating conveyor. Two different measurement positions are investigated. First, the camera is located above the chute and captures the vibrating pellets during transportation (Figure 4.2a). Second, the camera is placed in front of the vibrating conveyor and captures the pellets immediately after dropping off the edge of the vibrating chute (Figure 4.2b).

4.3 Results and Discussion

All presented snapshots show the entire field of view (9x6.5 mm) of the in-line measurement tool. They are taken in-line and are representative of the described configuration except for where otherwise specified.

4.3.1 Applicability to Pellet Analysis

First, the applicability to the investigated material was tested by off-line analysis. The stereo photometric system was operated in an off-line bench-top mode and the pellets were located on a moveable stage. Figure 5, A shows an image of CaSt pellets. The opaque white pellets reflected the light uniformly (diffuse) and all three RGB colors can be identified on the image. The pellets were placed as a monolayer with some overlying particles. However, the measurement system cannot handle every type of material, as shown in Figure 5, B-D. Figure 5, B shows the pellets composed of EVA, which is a transparent material. The transparency is apparent by looking at the upper layer pellets: the borders of the hidden particles can be seen through them. One of the boarders is highlighted with a dashed white line as an example and a detail view of the white solid box is shown in Figure 5, C. The light can pass through the transparent

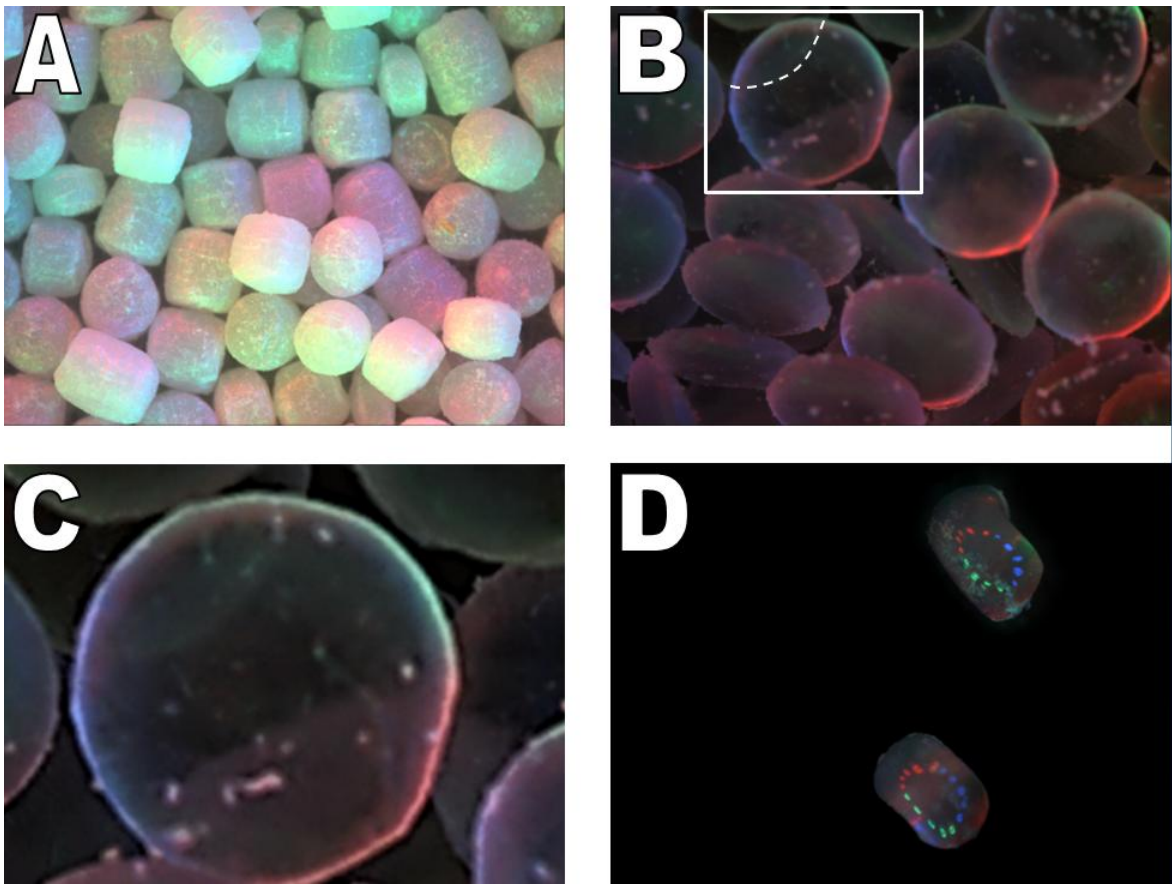

Figure 5: Snapshots of pellets with different optical properties. A: diffuse reflecting CaSt pellets; B: transparent EVA pellets (note the RGB light sources); C: detail view of the highlighted region in Image B; D: reflecting EVA pellets (in-line).

material and is partially scattered at the surface. In addition, the particle edges are brighter on the images. This situation cannot be handled by the implemented detection algorithm. Thus, measurements were not possible. Figure 5, D shows free-falling EVA pellets. Here, the light is to some extent specularly reflected by the particles. One can see the reflections of the individual LEDs which are circularly arranged around the lens. This is due to either over-illumination or due to a change of optical properties caused by the elevated material temperatures as the measurement was performed in-line and the pellets were not at room temperature.

In summary, it has been shown that the system is applicable to CaSt pellets due good diffuse reflection. However, the system is not applicable to transparent EVA pellets.

4.3.2 Implementation Evaluation

The number of analyzed particles impacts the reliability of the PSD. In this section the implementations are evaluated through a comparison of the quantity of captured particles and their orientation. The particle volume concentration at the pelletizer exit has been calculated with the following assumptions: air volume stream = 500 l/min; particle mass stream = 1 kg/h, density = 1 kg/dm^3, resulting in a very low particle volume concentration of c=0.0033% (v/v). Thus, an increase in concentration is necessary to enable the measurements.

4.3.2.1 Partial Separation of the Transportation Gas

Figure 6 shows two typical snapshots from the partial air separation implementation. The particle orientation in the optical sampling volume is random due to the freely falling pellets. As can be seen, a very low particle count is observed. On average only 1.5 particles were captured per image, which corresponds to an area fraction of 3.5 % (a/a). This is even more problematic as only fully captured particles are analyzed. Particles which cross the image border are not evaluated. Moreover, small dust particles settle on the funnel walls and disturb the image capturiyng process. This effect can be compensated by the evaluation algorithm by defining a particle detection range so that small dust particles are not evaluated, e.g., a minimum detection range of 300 µm.

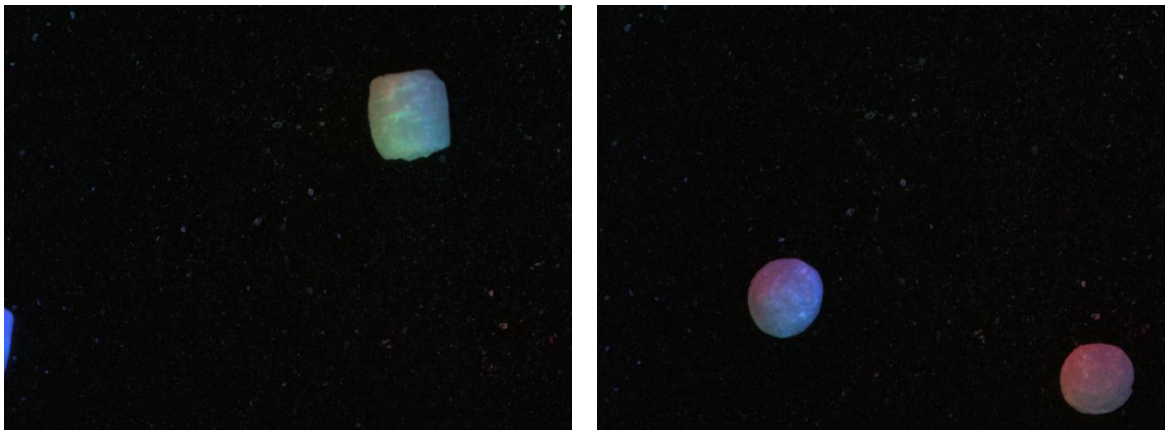

Figure 6: Snapshots of the partial separation implementation.

In summary, this implementation is prone to errors if used in relation to non-stationary production (e.g., start up, shut down, disturbances) and the production of larger particles. Such particles could easily block the funnel and would need to be removed manually.

4.3.2.2 Complete Air Separation and Camera in Top View Position

In this case the evaluation of the particle concentration was performed by image analysis and area fraction and the calculation of the area fraction (a/a) only.

In the experiments, the cutting frequency of the hot-die pelletizer was varied from low to middle to high, resulting in three different types of pellets. Figure 7 shows snapshots of each operating point. The shape of the pellets was cylindrical with different length to diameter (L/D) ratios: first, at the low cutting frequency an L/D ratio of approximately 1.5 (left snapshot), at the middle cutting frequency an L/D ratio of close to one and at the high cutting frequency an L/D ratio of approximately 0.5 were obtained, i.e., in the last case pellets resembled disks.

The use of a vibrating chute results in a preferred orientation of particles. The pellet rotation axis for an L/D ratio greater than one is parallel to the chute surface, while for L/D ratios smaller to one it is normal to the chute surface, leading to an overestimation of the pellet volume. This is significant drawback for this implementation approach. For L/D close to one the vibration energy is sufficient to establish a random representation of the pellets.

The evaluation of the area fraction resulted in values from 87% for the left and middle pellet dimensions and 90% for thin plates: the number of particles was depending

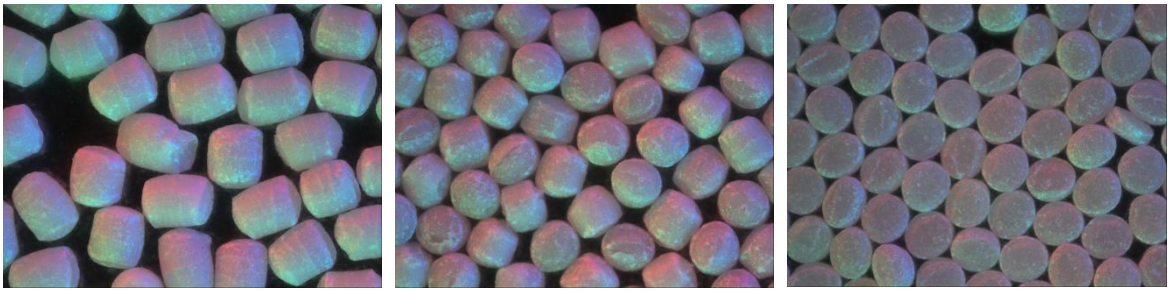

Figure 7: Snapshots of pellet obtained with complete air separation and camera position above the vibrating conveyor (cutting frequency; left-low; center-middle; right-high).

on the actual size between 15-30 particles per image. For this implementation multi-sampling of the same pellet was possible, which could distort the results. The residence time within the optical sampling volume and thus the chance of multi-sampling depends on the particle properties like weight and shape.

4.3.2.3 Complete Pellet Separation and Lateral Camera Position

The pellets were separated from the air stream using the same method as described above. However, the camera was located right after the edge of the chute. The pellets were captured while dropping into the storage bin following a parabolic trajectory. Therefore, the camera was tilted by a few degrees to maximize the optical sampling volume, as indicated in Figure 4.2b. The area fraction was used to describe the quantity of particles captured by the camera. The average particle count was 4.5 particles per image and the area fraction was 7.2% (a/a) on average.

Figure 8 shows two representative snapshots for this implementation. The left image shows four pellets which are located farther away, while the right image shows pellets closer to the camera. If pellets are too close the size may be overestimated and vice versa, if pellets are too far way an underestimation may occur or pellets may become invisible. This source of error has a minor impact, as the depth of focus is narrow and particles far outside the focus are not illuminated via the LED flash, and thus are not visible. Therefore, accurate alignment of the sampling volume is important for measurement reliability.

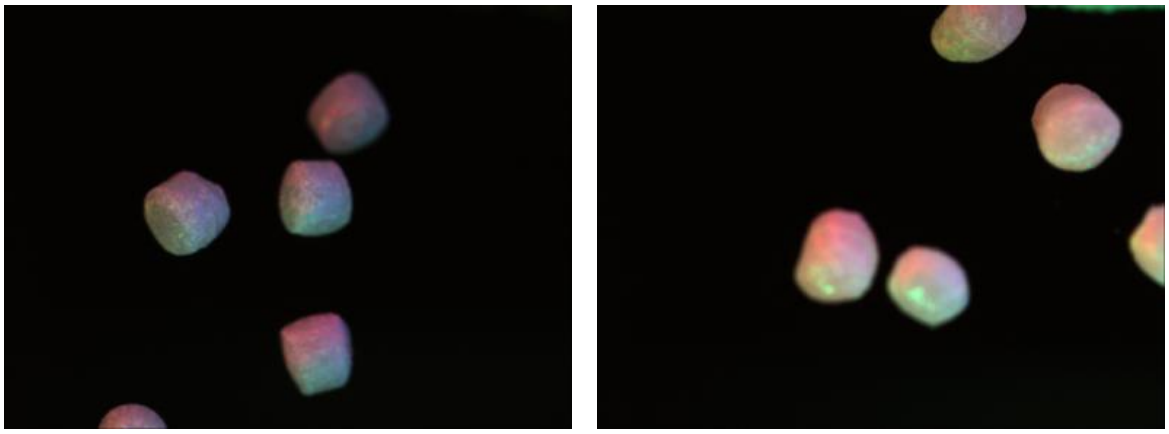

Figure 8: Snapshots of the implementation with complete pellet separation and lateral camera position.

Table 1: Overview of the image-analysis relevant results for the three setups.

Setup	Area Fraction (a/a)	Volume Fraction (v/v)	Number of Particles per Image [-]	Particle Orientation [-]
Partial Separation	3	0.0033%	1.5	Random
Complete Separation & Above Camera Position	88	-	30	Oriented
Complete Separation & Lateral Camera Position	7.2	-	4.5	Random

4.3.2.4 Comparison of the Implementation Approaches

In this section the results for the three different setups are compared and a recommendation for the most suitable approach is given. In Table 1 the results of the three setups are summarized. The first approach with partial separation has an advantage in terms of random particle orientation. However, the risk of blockage and a low number of particles for a reliable determination of the PSD are reasons for excluding this approach. The second setup approach has been developed to increase the number of analyzed particles. The area fraction was approximately increased by a factor of 30. However, the particle orientation was not random, effectively presenting the largest area in the image plane. This fact biased the PSD dramatically. Thus, this approach was also not deemed accurate enough for a quality control of pellets.

The aim of the last approach was to combine the advantages of the previous implementation while minimizing its drawbacks. The resulting statistics lie between the first two approaches. However, the clear advantages of this implementation are the statistically random pellet representation, the background-free images (no dust) and the single capturing. The number of particles is 4.5 which is still at the lower limit for an efficient quality analysis; however in a production environment higher throughputs are normal and would lead to a higher number of pellets per image. As a result, a clear recommendation for the last implementation can be given. This setup was fur-

ther tested by in-line monitoring of an actual manufacturing process of pellets. The results are shown in section 4.3.3.

4.3.3 Application to In-line Process Monitoring

The final setup of the analysis system was applied to in-line monitor the pellet size distributions during an extrusion process with subsequent hot-die face pelletizing. The objective was to show a comparison between in-line PSD data and the reference method. First, an experimental design to obtain pellets at different sizes was chosen. The material throughput of 0.8 kg/h was kept constant and the cutter speed was changed from 2000 rpm to 3600 rpm in 400 rpm steps, resulting in different length to diameter ratios of the pellets (Figure 9). Thus, five settings were investigated. The cutter setup consisted of two die holes and two knifes. Thus, cutting frequencies of 133 to 240 pellets per second were achieved. A sampling period of 10 minutes was chosen. The in-line PSD data have been extracted for the investigated sampling period and averaged. The off-line analysis has been applied to all produced pellets for each investigated set of parameters, which corresponds to sample sizes between 80 and 140 thousand pellets.

Figure 10 shows the PSD data obtained from the experiment, both from the in-line measurement system and the reference measurements. The in-line data are shown as solid lines and the reference data as dashed. Clearly, a decreasing pellet sizes with increasing cutting frequency can be seen, as the curves are shifted from right to left. The results have also been verified against size ratio estimation for average pellets obtained from the highest (3600 rpm) and lowest (2000 rpm) cutting frequencies. Clearly, the ratio of cutting frequencies of 1.8 should be identical to the volume ratio of ideal spherical pellets, resulting in a theoretical ratio of the diameters of 1.21. The measured ratio of 1.24 between the x_{50}=1480 µm at 2000 rpm and x_{50}=1198 µm at 3600 rpm corresponds well with the theoretical diameter ratio for ideal spherical pellets. The small deviation was probably caused by the non-spherical shape of the pellets.

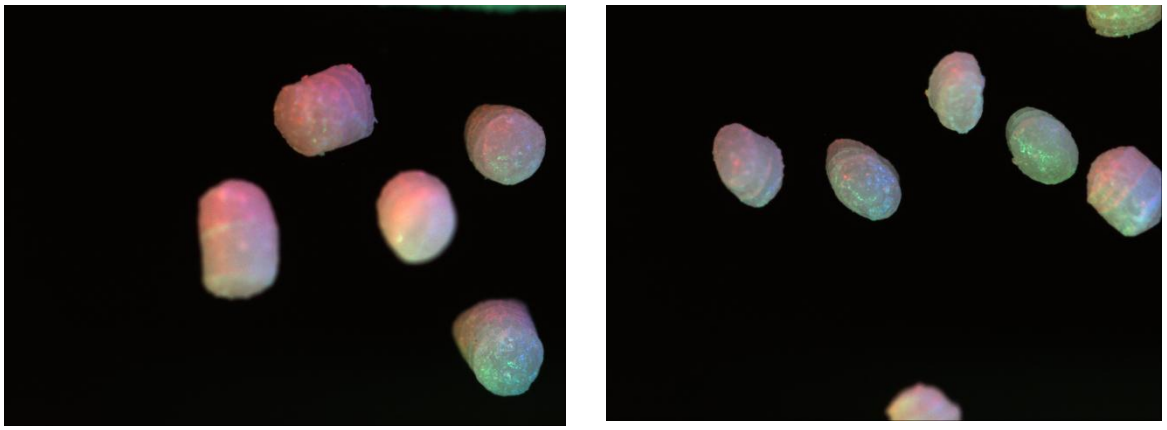

Figure 9: Snapshots of 2000 rpm (left) and 3600 rpm (right). Note the different length to diameter ratio of the pellets.

The comparison between the off-line and in-line approach showed - in general - a good agreement (compare Figure 10 and Table 2). The x_{50} and x_{90} values were almost identical (deviations < 5%) and the shape of the curve was quite similar. Differences, as observed for x_{10}, might be explained by the different measurement approach of 3D diffuse reflected light vs. 2D shadow projection and the small number of pellets analyzed by the in-line measurement in this setup. The system analyzed approximately 50 pellets per minute, whereas the reference method analyzed the entire bulk produced during the 10 minutes sampling time. Thus, the in-line analysis considered on-

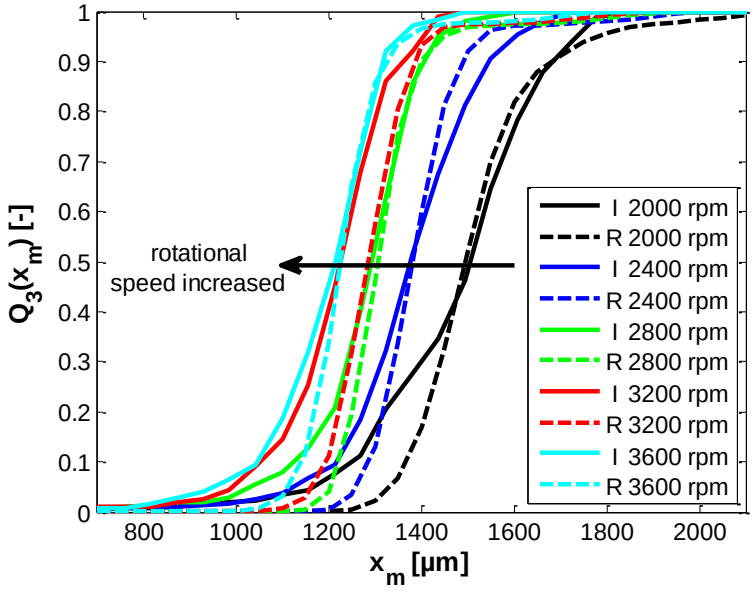

Figure 10: Comparison of the in-line PSD data to the reference method (I: In-line; R: Reference).

Table 2: Comparison of important PSD measures of Figure 14 (I: In-line; R: Reference).

	x_{10} [µm]			x_{50} [µm]			x_{90} [µm]			x_{90}/x_{10} [-]		x_{90}-x_{10} [µm]	
RPM	**I**	**R**	**Dev.**	**I**	**R**	**Dev.**	**I**	**R**	**Dev.**	**I**	**R**	**I**	**R**
2000	1250	1366	9%	1506	1494	-1%	1685	1682	0%	1.35	1.23	435	316
2400	1217	1284	6%	1378	1381	0%	1548	1490	-4%	1.27	1.16	331	206
2800	1124	1219	8%	1294	1306	1%	1408	1399	-1%	1.25	1.15	283	180
3200	1052	1192	13%	1225	1286	5%	1362	1388	2%	1.29	1.16	310	195
3600	1047	1141	9%	1214	1226	1%	1320	1327	1%	1.26	1.16	273	186

ly 0.3 to 0.6% of the total number of pellets to calculate the PSD. Despite the low particle count the comparison suggested that the results were quite accurate, with some deviations towards smaller particle sizes.

In general, the more narrow a distribution the fewer particles are required for a reliable PSD analysis [24]. A simple approach to describe the width of a distribution is to calculate the x_{90} to x_{10} ratio, i.e., the span of the distribution. At normal operating conditions the pellets produced by die face cutting show a ratio well below 1.5, which corresponds to a narrow PSD according to the classification shown in Table 3 [24]. By comparing the PSD width (x_{90}-x_{10}, Table 2) one can see that the width became narrower with increasing cutting frequency (Figure 10), with a slight minimum at 2800 rpm. The reason for a narrower PSD was identified by analyzing the particle shape measures in Table 4. Both in-line and reference analytics show lowest aspect ratios (a_{50}), thus the roundest pellets, for rotational speeds of 2800 rpm and 3200 rpm. These pellets also showed the lowest span of the aspect ratio distribution (a_{90}/a_{10}). At lower cutting frequencies the pellets became more elongated with a higher length to diameter ratio. This resulted, due to the random orien-

Table 3: PSD width classification [24]

	x_{90}/x_{10} [-]
Monosized	<1.02
Ultra narrow	1.02-1.05
Narrow	1.05-1.5
Medium	1.5-4
Broad	4-10
Very Broad	>10

Table 4: Comparison of particle shape measures of Figure 14 (I: In-line; R: Reference).

	a_{50} [-]			a_{90}/a_{10} [-]
RPM	**I**	**R**	**Dev.**	**R**
2000	1.27	1.35	6%	1.30
2400	1.21	1.25	3%	1.19
2800	1.20	1.20	0%	1.16
3200	1.20	1.19	-1%	1.17
3600	1.24	1.23	0%	1.27

tation of the pellets in the observation window, in a broadened PSD, as well as larger aspect ratios and a broadened distribution of the aspect ratios. Thus, the broadening did not necessarily correspond to physical deviations between the pellets. In that sense, the same non-spherical particle multiple times captured in a random orientation would result in a particle size distribution and different aspect ratios due to the 2D analysis method. This fact has to be taken into account when regularly shaped particles are analyzed. Thus, additional parameters, such as shape factors, are important to be considered.

In most in-line applications, the monitoring of the entire PSD over time leads to an unmanageable amount of information. Therefore, only a single parameter of the PSD can be extracted and monitored together with the real time snapshots. An example is shown in Figure 11.

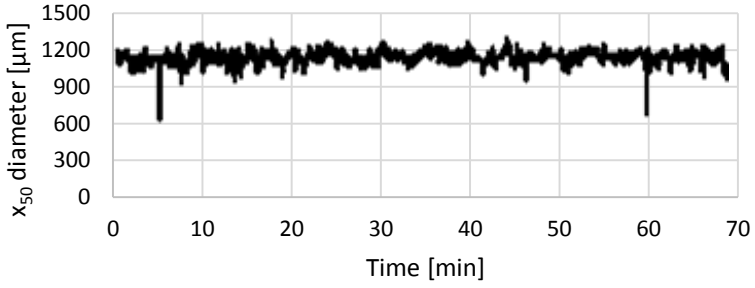

Figure 11: x_{50} time curve in-line monitoring (10 seconds averaging window).

4.3.4 Application in Process Development

In general, pelletizing is performed as the last step of a hot-melt extrusion process, with formulations comprising a carrier matrix, an API and possible functional additives. The material properties (rheology, heat capacity, heat conductivity...) of such mixtures are difficult to measure. In some cases the properties are also time dependent, i.e., they depend on the processing history in the extruder as well. Thus, the prediction of a process window is difficult due to the complex interactions. A common approach is to start with known parameters, e.g., for a similar formulation or pure components and to stepwise adjust the process towards an optimum setup with satisfactory product quality criteria. This approach can be sped up by providing real-time information.

Figure 12 shows four examples of visual real-time information. The Eudragit pellets (A) were acorn-shaped. This shape was probably obtained by a predominant elastic behavior. The pellets were teed off like a golf ball by momentum transfer of the impacting knife during cutting. Thereby, the material in the die plate section was expanded and contracted until it ruptured. The CaSt pellets (B) show occasional voids or shrinking holes in the pellets, which occurred when gas was entrapped in the melt passing the die section or volume contraction during cooling. Here, information about the surface texture can be obtained, which can exhibit various forms for complex systems, e.g., CaSt with liquid crystal meso-phases. Image (C) shows elongated pellets, which are sometimes termed longs, elbows or sausages. Furthermore, it shows another surface texture of CaSt, namely a glossy appearance. Image (D) shows almost spherical pellets after adjustment of the process parameters.

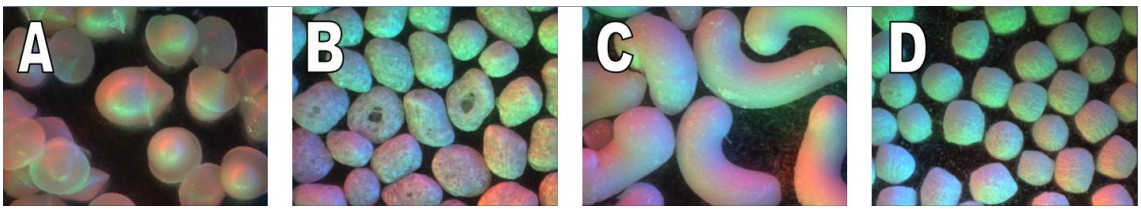

Figure 12: Off-line snapshots of pellets consisting of (A) Eudragit, (B) CaSt with rough surface and shrinking holes, (C) CaSt with glossy surface texture and (D) almost spherical CaSt pellets.

These examples demonstrate that an imaging method based on diffusive light can provide, besides the PSD, important visual properties, such as surface texture, void detection and information about shape. However, the qualitative visual information is not further processed by the applied in-line measurement system. Thus, additional analysis tools are required to transform this visual information into quantitative measures for quality assessment.

Finally, it is recommended to implement a separation mechanism to separate the product into acceptable or inacceptable quality, e.g., by using a switch for the product stream. In this case, a suitable residence time between the image analysis and the switch must be chosen.

4.4 Conclusion

It has been shown that photometric stereo image analysis is a suitable tool to monitor the particle size distribution and shape of pellets produced by hot melt extrusion with hot die-face pelletizing. Challenges concerning the limitations of a very low volume fraction of particles in the transportation air had to be overcome. Additionally, a random orientation of the particles was necessary, in order to obtain statistically valid data. The selected measurement setup included an impact separator to split pellets from the transportation gas and measurement of the pellets directly after a vibratory chute in a lateral position. After optimization the amount of measured pellets was still only about 500 for 10 min sample time, compared to around 10^5 pellets for off-line analysis.

The reduction in the x_{50} of the pellets by increasing the pelletizer rotational speed could be accurately monitored and was were verified off-line by reference measurements. Despite the small amount of pellets measured in-line, good agreement in x_{50} between both methods was found. Image shape information was found to be a significant advantage of the diffusive light methodology. It allowed capturing of in-line information about surface texture and shape. This is of particular importance for development purposes, when for example, the interactions of a process parameter with a specific product property or set of properties is subject to research.

Based on the results, photometric stereo image analysis appears to be a suitable tool for in-line measurement of particle size and shape. A drawback of the current image analysis algorithm is the restriction to diffusive-reflective materials.

Acknowledgements

This work has been funded by the Austrian COMET Program by the Austrian Federal Ministry of Transport, Innovation and Technology (bmvit), the Austrian Federal Ministry of Economy, Family and Youth (bmwfj) and by the State of Styria (Styrian Funding Agency SFG). We thank our colleagues from the extrusion group at the Research Center Pharmaceutical Engineering for making this work possible.

4.5 Literature

[1] J. Breitenbach, "Melt extrusion: from process to drug delivery technology.," *Eur. J. Pharm. Biopharm.*, vol. 54, no. 2, pp. 107–17, Sep. 2002.

[2] D. A. Miller, J. T. McConville, W. Yang, R. O. Williams, and J. W. McGinity, "Hot-melt extrusion for enhanced delivery of drug particles.," *J. Pharm. Sci.*, vol. 96, no. 2, pp. 361–76, Feb. 2007.

[3] N. Follonier, E. Doelker, and E. T. Cole, "Various ways of modulating the release of diltiazem hydrochloride from hot-melt extruded sustained release pellets prepared using polymeric materials," *J. Control. Release*, vol. 36, no. 3, pp. 243–250, Oct. 1995.

[4] F. Zhang and J. W. McGinity, "Properties of sustained-release tablets prepared by hot-melt extrusion.," *Pharm. Dev. Technol.*, vol. 4, no. 2, pp. 241–50, May 1999.

[5] C. De Brabander, C. Vervaet, and J. . Remon, "Development and evaluation of sustained release mini-matrices prepared via hot melt extrusion," *J. Control. Release*, vol. 89, no. 2, pp. 235–247, Apr. 2003.

[6] F. Podczeck, "Dry filling of hard capsules," in *Pharmaceutical Capsules*, 2nd ed., F. Podczeck and B. E. Jones, Eds. Pharmaceutical Press, 2004.

[7] R. Chopra, F. Podczeck, J. M. Newton, and G. Alderborn, "The influence of pellet shape and film coating on the filling of pellets into hard shell capsules," *Eur. J. Pharm. Biopharm.*, vol. 53, no. 3, pp. 327–333, May 2002.

[8] S. Abdul, A. V Chandewar, and S. B. Jaiswal, "A flexible technology for modified-release drugs: multiple-unit pellet system (MUPS).," *J. Control. Release*, vol. 147, no. 1, pp. 2–16, Oct. 2010.

[9] D. Ghanam and P. Kleinebudde, "Suitability of κ-carrageenan pellets for the formulation of multiparticulate tablets with modified release.," *Int. J. Pharm.*, vol. 409, no. 1–2, pp. 9–18, May 2011.

[10] C. Vervaet, L. Baert, and J. P. Remon, "Extrusion-spheronisation A literature review," *Int. J. Pharm.*, vol. 116, no. 2, pp. 131–146, Mar. 1995.

[11] C. Lustig-Gustafsson, H. Kaur Johal, F. Podczeck, and J. . Newton, "The influence of water content and drug solubility on the formulation of pellets by extrusion and spheronisation," *Eur. J. Pharm. Sci.*, vol. 8, no. 2, pp. 147–152, May 1999.

[12] C. R. Young, J. J. Koleng, and J. W. McGinity, "Production of spherical pellets by a hot-melt extrusion and spheronization process.," *Int. J. Pharm.*, vol. 242, no. 1–2, pp. 87–92, Aug. 2002.

[13] S. Bialleck and H. Rein, "Preparation of starch-based pellets by hot-melt extrusion.," *Eur. J. Pharm. Biopharm.*, vol. 79, no. 2, pp. 440–448, Oct. 2011.

[14] E. Roblegg, E. Jäger, A. Hodzic, G. Koscher, S. Mohr, A. Zimmer, and J. Khinast, "Development of sustained-release lipophilic calcium stearate pellets via hot melt extrusion.," *Eur. J. Pharm. Biopharm.*, vol. 79, no. 3, pp. 635–645, Nov. 2011.

[15] R.-K. Mürb, "Kunststoff granulieren und/oder pelletieren?," *Chemie Ing. Tech.*, vol. 84, no. 11, pp. 1885–1893, Nov. 2012.

[16] A. F. T. Silva, A. Burggraeve, Q. Denon, P. Van der Meeren, N. Sandler, T. Van Den Kerkhof, M. Hellings, C. Vervaet, J. P. Remon, J. A. Lopes, and T. De Beer, "Particle sizing measurements in pharmaceutical applications: comparison of in-process methods versus offline methods.," *Eur. J. Pharm. Biopharm.*, Apr. 2013.

[17] K. Lövgren and P. J. Lundberg, "Determination of Sphericity of Pellets Prepared by Extrusion/Spheronization and the Impact of Some Process Parameters," *Drug Dev. Ind. Pharm.*, vol. 15, no. 14–16, pp. 2375–2392, Jan. 1989.

[18] A. Burggraeve, N. Sandler, J. Heinämäki, H. Räikkönen, J. P. Remon, C. Vervaet, T. De Beer, and J. Yliruusi, "Real-time image-based investigation of spheronization and drying phenomena using different pellet formulations.," *Eur. J. Pharm. Sci.*, vol. 44, no. 5, pp. 635–42, Dec. 2011.

[19] P. R. Wahl, D. Treffer, S. Mohr, E. Roblegg, G. Koscher, and J. G. Khinast, "Inline monitoring and a PAT strategy for pharmaceutical hot melt extrusion.," *Int. J. Pharm.*, Jul. 2013.

[20] D. Treffer, P. Wahl, D. Markl, G. Koscher, E. Roblegg, and J. Khinast, "Hot Melt Extrusion as a Continuous Pharmaceutical Manufacturing Process," in *Melt Extrusion: Equipment and Pharmaceutical Applications*, M. Repka, Ed. Springer Publishers, 2013.

[21] R. J. Woodham, "Photometric method for determining surface orientation from multiple images," *Opt. Eng.*, vol. 19, no. 1, pp. 139–144, 1980.

[22] P. Hansson and Fransson, "Color and Shape Measurement with a Three-Color Photometric Stereo System," *Appl. Opt.*, vol. 43, no. 20, pp. 3971–3977, 2004.

[23] W. S. Rasband, "ImageJ," *Image Processing and Analysis in Java*. [Online]. Available: http://rsb.info.nih.gov/ij/index.html.

[24] H. G. Merkus, *Particle Size Measurements*. Springer Science+Business Media B.V., 2009.

Unfortunately, in reality,
the gap between
theory and reality
is larger than in theory.

Otto Scheibelhofer

5. PAT for Tableting: Inline Monitoring of API and Excipients via NIR Spectroscopy[5]

5.1 Introduction

Starting in 2004 the FDA [1] and ICH (Q8 to Q11) [2] have released a series of guidelines regarding Quality by Design (QbD) and Process Analytical Technology (PAT). The QbD framework has led to an important paradigm change by giving pharmaceutical companies the freedom to develop well-controlled and consistently optimized manufacturing processes. However, documenting a science-based understanding of the process variability and the critical process parameters (CPPs) is required. Here computer simulation can be beneficial to provide a deeper understanding [3]. No additional approval is necessary for changes within a well-documented range of CPPs (i.e., the design space) that satisfies the quality requirements of the product (i.e., the critical quality attributes, CQAs).

[5] This chapter is based on: P.R. Wahl, G. Fruhmann, S. Sacher, G. Straka, S. Sowinski, and J.G. Khinast, "PAT for Tableting: Inline Monitoring of API and Excipients via NIR Spectroscopy.," Eur. J. Pharm. Biopharm., submitted

The Process Analytical Technology (PAT) is key for the analysis and control of manufacturing processes. Especially, continuous production concepts rely on real-time inline measurements of the product quality and on respective control strategies. PAT can also be utilized in batch processes, even after their initial design and approval, to optimize the existing processes. The most common PAT analyzer in the manufacturing of solid dosage forms is near-infrared spectroscopy (NIRS) and has been extensively described in the literature [4]–[7]. This paper addresses the use of NIRS for tablet manufacturing.

NIR was used to monitor the content uniformity of intact tablets [8], also in combination with physical properties, such as hardness [9]–[13]. Further publications focused on the subsequent coating process, where the thickness of the coating layer was determined [14] and its impact on the release profile was investigated [15]. In these publications, tablets were primarily analyzed manually, resulting in limited sampling capabilities during routine manufacturing. For real-time information about the process, inline methods are preferable. In the field of coating inline systems have been reported for a pan coater [16] and a fluid bed coater [17], [18]. In order to study content uniformity, NIR was used inline during ejection of tablets [19], at 6000 tablets per hour. Clearly, higher inspection rates are needed for a 100% control. NIR Chemical Imaging (NIR-CI) allows much higher throughputs, as multiple tablets can be scanned simultaneously. Another approach that does not limit the amount of tablets per hour (and is not limited to scanning only the tablet's surface) involves mounting a NIR sensor on the feed frame [20], i.e., to monitor the powder mixture similar to inline monitoring of powder blenders [21]–[25]. However, difficulties concerning sample presentation in the feed frame arise, which are associated with the paddle wheel moving the powder.

NIRS also allows analysis of the crystalline state of the API in tablets. Reflectance NIR was used to study the polymorphic state of pharmaceutical materials, with similar prediction accuracy as transmission Raman [26]. Differentiation between different polymorphic states, i.e., form A and B of Irbesatan, was achieved using NIR measurements [27]. Final tablets were analyzed via NIR-CI techniques to determine the dis-

tribution of API and excipients. For API quantification an augmented multivariate curve resolution-alternating least squares (MCR-ALS) method was applied [28], [29]. After calculating the distribution map, further multivariate image analysis (MIA) methods were applied to detect API clusters in the tablets [29]. NIR-CI was also used in the coating distribution analysis [30].

An industrial application of PAT requires appropriate monitoring techniques and an accurate and robust model, i.e., a model that can handle differences in sample presentation between lab and manufacturing, and calibration transfer strategies for dealing with differences between spectrometers and different sample presentation. The simplest way to address spectral differences between laboratory-scale implementations and real process analyzers was proposed by Blanco et al. [31]. Adding process spectra with observed deviations to the model spectra resulted in a more robust PLS model. In order to guarantee that process deviations are included in the model, a method of monitoring the validity of calibration over time is needed. Cogdill et al. suggested to monitor spectral features, i.e., Hotelling's T^2 and the residuals Q [32]. More advanced mathematical approaches for separating noise induced by the process (clutter) were proposed, e.g., Noise Augmentation (NA) of the calibration spectra with the spectral shapes from the clutter followed by net analyte pre-processing (NAP) [33]. A comparison between different methods of including pure component spectra and removing clutter were presented in [34], including NAP, Improved Direct Calibration (IDC), Science Based Calibration (SBC) and Augmented Classical Least Squares Calibration (CLS).

Several transfer methods for handling differences between spectrometers or differing environmental conditions were described and evaluated in the literature, including direct standardization (DS), piecewise direct standardization (PDS), artificial neural networks (ANN), wavelets, orthogonal signal correction (OSC), reverse standardization (RS), slope and bias correction, model updating (MU) and local centering (LC) [35]–[37]. The suggested methods for calibration transfer, if transfer samples are available on both systems, are PDS [35], RS [36] or LC [37]. LC was preferred by Bergman *et al.* as the smallest number of transfer samples was needed and transfer

was simple to perform [37]. If no transfer samples are available, MU was suggested [36].

In this work we present the use of inline NIR spectroscopy for monitoring the content uniformity of tablets compacted in an industrial setting. The NIR probe was mounted on the feed frame of the tablet press. The spectra for the PLS model were collected in the lab using premixes on a rotating plate. To enable predictions during manufacturing, the model was transferred via LC. We report here the use of a calculated transfer sample, consisting of the nominal mixture measured in the laboratory and an average of all process spectra during manufacturing. For validation, the NIR results were compared with the offline UV-Vis analysis of selected tablets. Both methods confirm segregation at the end of the process. Finally quality improvement opportunities by inline measurements are discussed and questions are raised concerning a new definition of the USP 905 "Uniformity of Dosage Units" for inline measurements.

5.2 Materials and Methods

5.2.1 Materials

The tablet formulation consisted of a drug (API) load of about 30% and two main excipients (EX1 and EX2), which in total accounted for about 65%. The other excipients had a total fraction of less than 5%. The composition of powder was simultaneously monitored for API, EX1 and EX2 via NIR spectroscopy

5.2.2 Tablet Press

The compaction of tablets was carried out using a Kilian Synthesis 500 (Kilian GmbH & Co. KG, Germany) rotary tablet press. For routine manufacturing, the speed was set to 300,000 double concave tablets per hour. The level sensor in the powder inlet chute halts the production once the lower acceptable level is reached. For research purposes, it was continued until the feed frame was empty and no more tablets could be pressed.

5.2.3 NIR Spectroscopy

NIR spectra were collected in diffuse reflection mode via the process spectrometer SentroPAT FO (Sentronic GmbH, Germany), which is a diode array spectrometer with a spectral range of 1100 nm - 2200 nm and a resolution of 2 nm. To monitor the composition of the powder, a SentroProbe DR LS with a large spot size of 6mm was used. The probe had an internal light source and a unique internal micro-mechanical white reference directly behind the sample window, which allowed measuring the internal reference spectrum whenever required, even during the process. Once the internal reference standard was measured, any changes in the signal path, including probe optics and glass fiber transmission, were calculated and used to correct the sample's further measurements. Drifts may be caused by changes in the environmental conditions, such as temperature variations and vibration, or aging of the light source and the resulting intensity loss. Correcting for the drifts can significantly improve the long-term stability of the acquired spectra in routine operation during manufacturing.

The software SentroSuite was used to control the spectrometer. The integration time was set to 0.02s and an averaging window of 150 spectra. The total acquisition time was 3s per spectrum. An internal drift correction was performed every 3 minutes, with an integration time of 0.01s, averaged over 100 spectra, to correct for heating of the probe head.

5.2.4 Probe Position in Feed Frame

Collection of the powder spectra was performed in the feed frame of the tablet press. One inspection window was replaced by an adapter for mounting of the NIR probe directly above the paddle wheel, where the powder was distributed into the tablet dies. To ensure proper sample presentation, with the least variations and without window fouling, the probe had to be positioned at the appropriate distance to the paddle wheel to monitor the powder composition just before compaction.

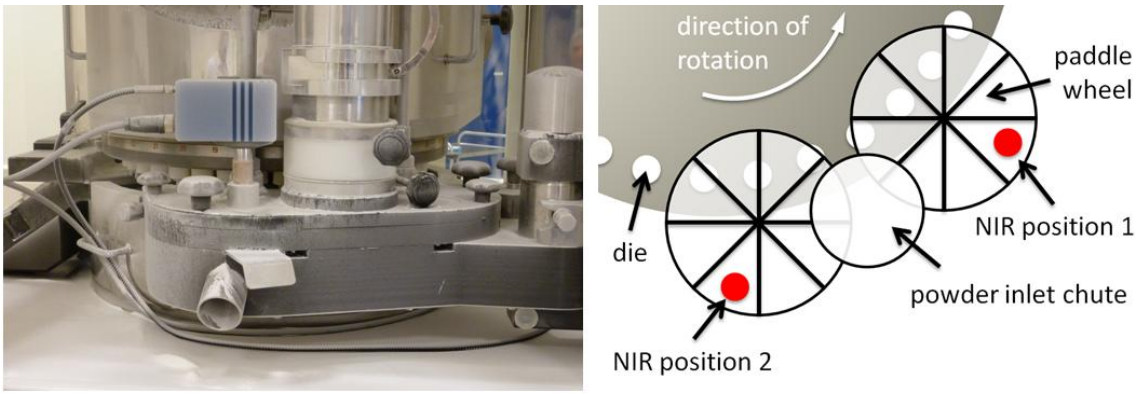

Figure 1. Left: NIR probe mounted to observation window of feed frame. Right: Schematic drawing of feed frame and rotating dies with two NIR measurement positions, above right and left paddle wheel.

5.2.5 UV-Vis Reference Analytics

Reference measurements of the API content were conducted using the Perkin Elmer LAMBDA 950 UV-Vis spectrometer. The tablets were weighed prior to UV-Vis analysis to correct for weight variations. After pre-filtering through a 0.2 µm cellulose nitrate filter (Sartorius, Germany), the tablets were dissolved in 20ml EtOH and diluted 1:50 with purified water (MicroPure, TKA, Germany). Quantification was performed using a five-point calibration curve in the range of 25-100 µg/ml with R^2=0.9998.

5.2.6 Chemometric Model and Mixture Design

In order to correctly predict the composition of the powder, a Design of Experiments (DoE) approach was chosen to select the mixtures that were used in the NIR model. The API, EX1 and EX2 were varied ± 20% relative to their nominal value (e.g., 15% to 23% for a nominal value of 19%). The ternary mixtures were selected according to a D-Optimal solution via eight experiments (numbers 1-7 in Figure 2), covering all corners and the center point of the mixture space. At the center point, all constituents in the mixture had the nominal values. The remaining excipients (e.g., lubricants) were kept constant throughout all mixtures. To achieve nearly equidistant steps in mass

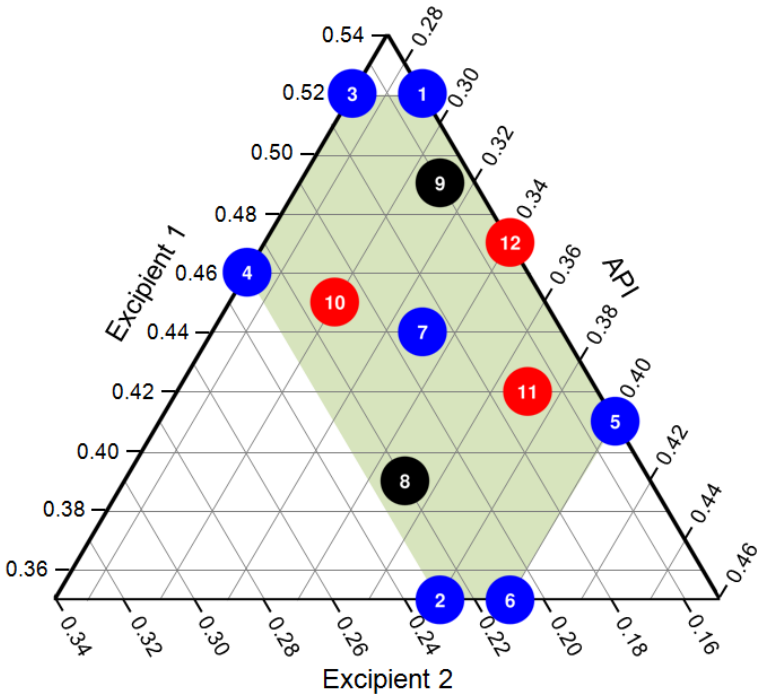

Figure 2. Ternary mixture design for NIR calibration measurements. Points 1 to 7 (blue) are according to a D-Optimal design; points 8 and 9 (black) are chosen to achieve nearly equidistant steps in content for each component; points 10 to 12 (red) are for validation purposes.

fraction for calibration, two further experiments were conducted (numbers 8 and 9). Three additional mixtures were chosen to validate the model (numbers 10-12).

Mixtures of 15g each were prepared and mixed in a Turbula T2F tumbler blender (Maschinenfabrik Willy A. Bachofen AG, Switzerland) for 5 min at 60Hz, followed by adding the lubricant and mixing for additional 2 min. To avoid segregation after mixing, the powder was carefully distributed on a rotary plate rotating at a speed of around 30rpm (i.e., 2s per revolution). Further details of the procedure can be found in Scheibelhofer et al. [23] .

With the collected spectra a chemometric model was built with Simca 13 (Umetrics, Sweden). The spectra were pretreated with SNV (1200nm – 2160nm), followed by first-order derivate with Savitzky-Golay smoothing (second-order polynomial, kernel: 23 points) in the same wavelength region (see Figure 3). A PLS model (1214nm – 2146nm, four latent variables) was applied, with a predictive capability of R^2= 0.97, Q^2=0.95. The RMSEP and RMSECV values, of prediction and cross-validation, respectively, were calculated as relative error in relation to the nominal formulation. The

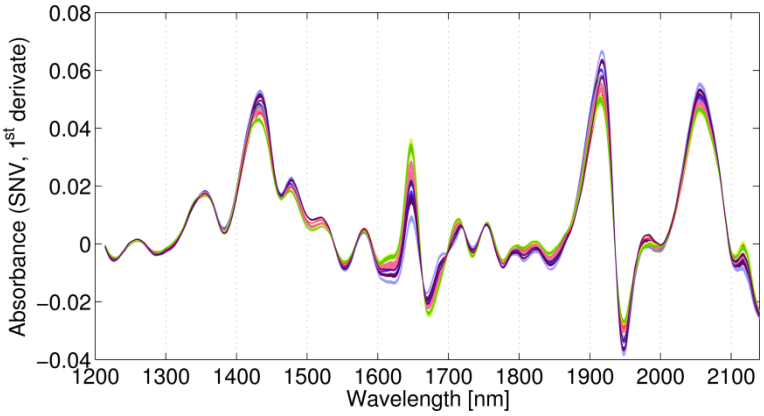

Figure 3. Model spectra after pretreatment with SNV and first order derivative. Colored according to mixtures (1-9) of the DoE.

calculated values of RMSEP (RMSECV) were 2.7% (4.4%) for API, 1.7% (2.4%) for EX1 and 2.6% (4.5%) for EX2.

Validation experiments (Figure 2, numbers 10-12) exhibited relative RMSEP values for API: 2.0%, EX1: 0.69% and EX2: 2.3%, respectively, indicating a robust model.

To use the model for the monitoring of a real tableting process, further effects had to be considered. The paddle wheel of the tablet press, which distributes the powder into the dies, passes directly under the probe, causing agitation of the powder and possibly affecting the spectrum. A LC transformation, necessary to correct for these effects, was based on assuming a correct overall composition of the powder for tableting, which was reasonable for an industrial process. The transfer sample for LC was calculated instead of measured. The average spectrum of the process $\bar{A}_{\text{process}}$ was calculated, with all major deviations excluded (e.g., start, end, stop). This averaged spectrum of the process had to be identical to the average spectrum of the center point $\bar{A}_{\text{center point}}$ of the mixture DoE, which had the same composition as the formulation.

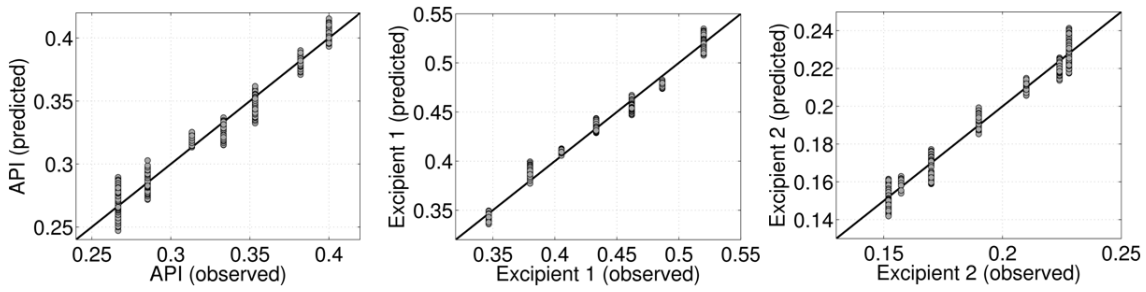

Figure 4: Observed vs. predicted plots for PLS model for API, EX1 and EX2.

After normalizing the minimum and maximum absorbance values of the spectra between zero and one (zero-to-one normalization, 1200nm – 2160nm), the centering was performed using the equation:

$$A_{i,\,\text{centered}} = A_{i,\,\text{process}} - \bar{A}_{\text{process}} + \bar{A}_{\text{center point}}$$

where $A_{i,\,\text{process}}$ is a spectrum taken in the feed frame and $A_{i,\,\text{centered}}$ is the centered spectrum. The PLS model was applied to these corrected spectra to accurately predict the powder composition in the feed frame.

5.3 Results and Discussion

5.3.1 PCA Analysis to Detect Process Irregularities

An industrial tableting process with a batch process time of around 13 hours was monitored via NIR in the feed frame, as described above. Throughout the process, a PCA of the original spectra was performed to check for any major deviations. The first principle component (98% explained variance) captured the baseline shift of the spectra towards the process end. Towards the end of the process, when the feed frame emptied, the distance between the probe head and the powder surface increased, resulting in less reflected light. The PC1 versus PC2 for the entire 13-hour

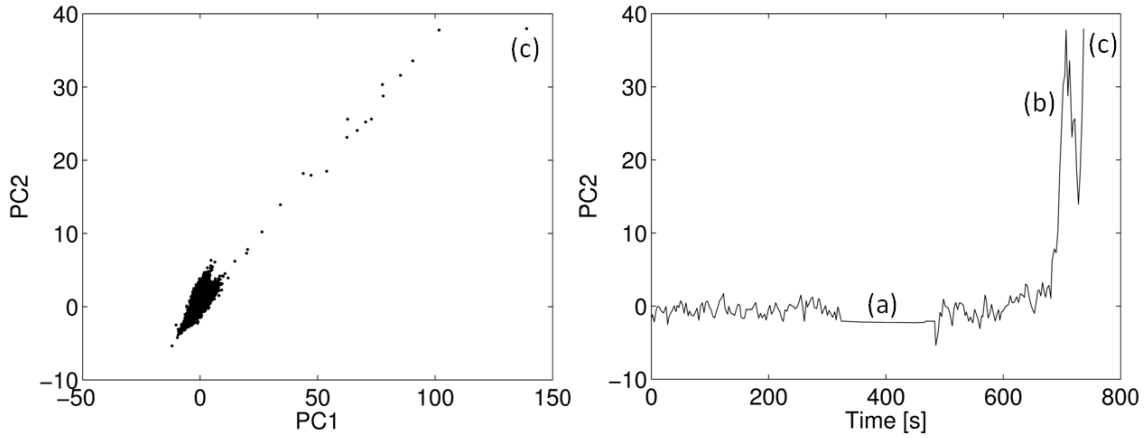

Figure 5. Left: PC1 vs. PC2 of the entire production process. Only a small number of measurements deviate strongly. Right: Recognizable process events during the last ten minutes of the process: (a) process stop, (b) possibly too much API and (c) powder emptying. The spectra (b) and (c) correspond to the observed deviations on the left side.

process are plotted in Figure 5, left. While comparably minor deviations were observed during the process, strong outliers became apparent towards the process end. In Figure 5, right, the second principle component is shown (2% explained variance), which correlated best with the API content according to the loadings. The loadings of PC2 showed no "noise," despite the low explained variance. The process stopped at around 400 sec (Figure 5, (a)), which was triggered by the level sensor in the powder inlet chute between the hopper and the feed frame. Shortly thereafter the tablet press was restarted and continued until no more powder was left in the feed frame (Figure 5, (c)). Just before the end of the process, pronounced deviations in PC2 were observed (Figure 5, (b)), indicating an excess API content in the mixture. Since this could have led to overly potent tablets, further investigations were performed.

5.3.2 Confirmation of Deviations with UV-Vis

To confirm the findings of the PCA analysis, the tablets were sampled and analyzed by means of UV-Vis spectroscopy. At two points during the process (after around 4h and 9h), samples consisting of 5 tablets were taken and analyzed for inter-tablet fluctuations. The relative standard deviation (RSD) was found to be RSD_{sample} = 3%. Additionally, 13 samples were drawn throughout the process at intervals of about 1h (Figure 6). For the process, a $RSD_{process}$ = 5.4% was determined, which was only 80% higher than a single sample and which suggested a stable process with minor, well-controlled variations over time. A discussion of the API content tolerances with regard to the inline monitoring is presented below.

In order to resolve the end of the process, regular samples were taken in 30-s intervals starting at the point of time where the process was re-started. The UV-Vis analysis of samples from three batches confirmed the PCA findings (Figure 6). Variations in the API content of 12% (Figure 7, left) to 30% (Figure 7, right) of the label claim were identified, which are likely due to (stochastic) segregation effects in hopper feeding powder to the feed frame. Many parameters influence the segregation tendency during discharge of a hopper, including particle diameter ratio and fines mass fraction, the hopper cross-sectional shape and hopper angle [38]. The volume mean particle

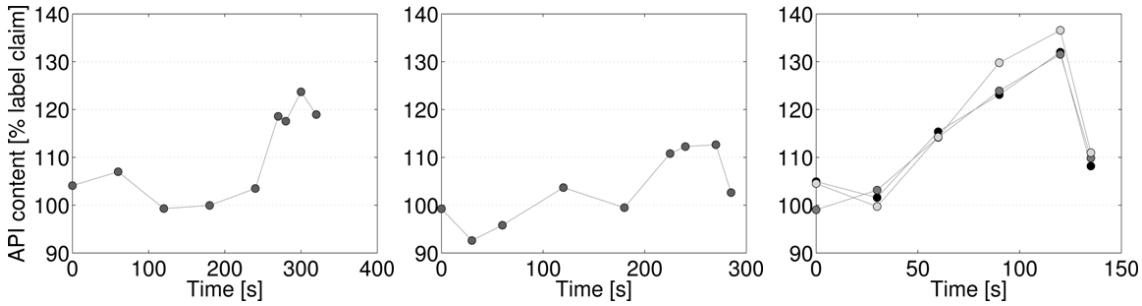

Figure 6. Significant deviations in API content (up until +30% of label claim) for three batches towards the end of the process.

size of the API was 140µm, which was significantly larger compared to the non-granulated excipients. Size segregation during discharge of the hopper, leading to an accumulation of large API crystals towards the process end [39], could have occurred. The vibrations of the tablet press might have induced further segregation [40], [41]. To confirm reproducibility, the batch with the most pronounced deviations was analyzed in triplicate (Figure 7, right).

5.3.3 Inline Monitoring of the Powder Composition

Based on the confirmed variations, a PLS model to predict the API and two main excipients was developed and used to analyze several production runs, one of which is discussed below. Pre-tests were performed to select the best measurement position above the left or right paddle wheel (see Figure 1). Finally, all measurements were performed above the left paddle wheel for two reasons: First, the time interval between taking spectra and tableting is shorter and subsequent (de-)mixing effects are minimized. Second, since the sample presentation was better, with less (long-term) variations in the captured spectra (not shown) the left position was selected. These variations may be due to the way the powder is filled into the die holes: the left paddle transported the powder to the turret and into the die holes, while the right paddle mainly removes and recycles the superfluous powder, which is later transported back to the left paddle and re-distributed into the die holes. Since the powder at the right paddle wheel is more mechanically stressed and experiences higher shear forces, more fines could appear due to attrition and the powder could potentially segregate.

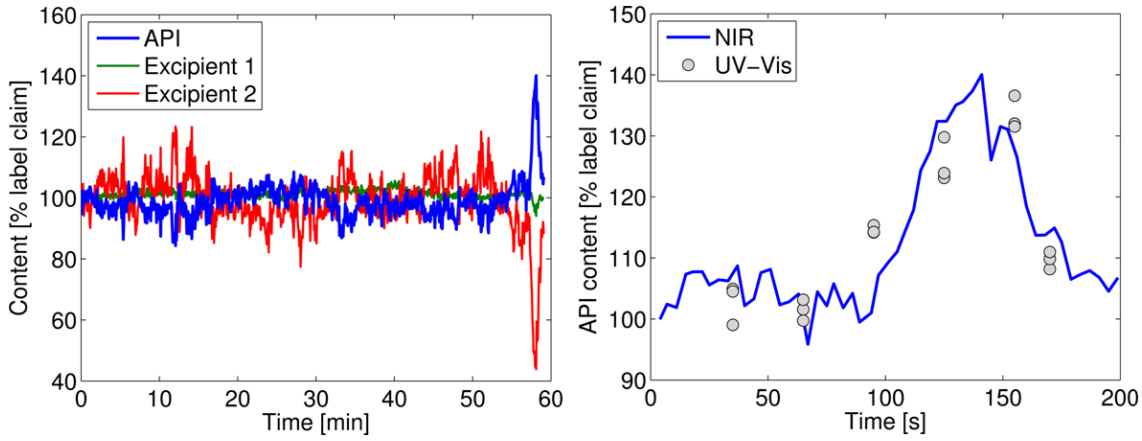

Figure 7. Left: Plot of the entire formulation over time, with strong API deviations towards the end of the process. Right: Comparison of UV-Vis and NIR results at the process end (UV-Vis data shifted by 30s to compensate for the time delays between the NIR measurement and sampling).

This effect, alongside with the segregation in the hopper, might have been root causes for content deviations towards the process end.

A typical plot of the three component concentrations during the last hour of the process is shown in Figure 7, left. All components are stated relative to the nominal content of the formulation. Note that the API excess (blue), e.g., occurring between 10 and 20 minutes, is compensated by the reduction in only one excipient (red, EX2), which may be a useful observation with regard to future improvements to the formulation. Additionally, out-of-spec tablets could possibly be identified selected and removed, which would drastically increase the overall quality. Figure 7, right, presents a comparison of inline (NIR) and offline (UV-Vis) methods. A time delay of on average 30s between NIR and UV-Vis data was observed and corrected for in the Figure for comparison purposes. During the timeframe of 30s further (de-)mixing could have occurred, but clearly there is strong correlation between inline and offline results. This confirms that the composition of the tablets can be predicted via NIR monitoring of the powder.

5.3.4 Quality Improvement Opportunities by Inline Analysis

According to the U.S. Pharmacopoeia (USP 905 “Uniformity of Dosage Units”), a batch of tablets is considered “in-spec” with regard to content uniformity, if the acceptance

value (AV) of the sampled tablets is smaller than 15. The AV is calculated as $AV = |M - \bar{X}| + ks$, with the reference value M, the mean API content of the analyzed tablets $\bar{X}$, the acceptability constant k and the RSD s. Assuming that the deviations in the mean API content are less than 1.5%, the formula can be simplified as $AV = ks$, with k=2.4 for n=10 tablets and k=2.0 for n=30 tablets analyzed. For the analyzed batch (Figure 6, right, and Figure 7) the acceptance value for the reference samples analyzed via UV-Vis ($RSD_{process,UV\text{-}Vis}$ = 5.4%, 10 tablets: k =2.4) was $AV = 2.4 * 5.3 = 12.72$ and for the inline NIR analysis (RSD_{NIR} = 3.3%, >30 unit doses: k = 2.0) it was $AV = 2.0 * 3.3 = 6.6$. Hence, the batch was "in-spec" according to the reference and the inline measurements.

Moreover, no tablet should deviate from the label claim by more than 25%. Thus, the analyzed batches could fail if a tablet was drawn at the very end of the process, when the API content was above 125% of the label claim. This critical timeframe of about 30s constituted only 0.064% of the overall process time of 13h. The chance of sampling at least one of these tablets was calculated by $p = 1 - (1 - 0.00064)^n$ with values of 0.64% for n=10 tablets and 1.91% for n=30 tablets. Thus, even assuming a totally random sampling, it would be unlikely that classical thief sampling schemes of reference tablets would detect high frequency process upsets. However, inline methods (e.g., spectroscopy) can resolve such events.

5.4 Conclusion

A staged approach for optimizing an existing tablet production was proposed. Inline NIR spectroscopy indicated that the end of the process was critical: a significant peak in the API content was observed, which was probably caused by segregation effects. Further comparison of drawn samples and inline predicted powder composition confirmed the findings, and corrective actions were suggested.

In our case, inline analysis proved to have distinct advantages because it created a more complete picture of the process than the AV, which is only a single statistical number. Since sampling a few tablets may not provide sufficient information about

process events that lead to product quality deviations, conventional process and quality control may fail to determine the significance and effects of those critical events. Process analytical technologies, such as NIRS, are key enablers of the next step in quality and process understanding in the pharmaceutical industry.

Comparing the drawn samples and inline data raised important questions. How should the USP 905 criteria "no tablet is allowed to deviate more than 25%" be handled with regard to inline measurements? For example, if out-of-spec tablets are successfully identified and diverted, the batch should be accepted and the diverted tablets should be removed from the SD calculations. In this case, what is the correct way to calculate the AV? Moreover, a k-factor in the AV calculation would be dispensable since there is no need to compensate for statistical uncertainties associated with drawing only 10 to 30 tablets. The most important question regarding quality is "Does drawing a handful of tablets still constitute the state of the art for quality control or would it be wise to demand inline measurements?"

Extensive further research is required, for example, reducing the time delay between the measurement and compression, taking corrective actions such as diversion of tablets and identifying the right position (e.g., the distance to the paddle wheel) for ideal sample presentation [20]. Moreover, comparison of models developed offline (e.g., via a rotating dish) and inline (e.g., via feeding of known premixes) should be performed concerning the robustness of LC as a calibration transfer method. Offline modeling, such as the presented approach, dramatically reduces both the experimental and the financial efforts, are clearly preferable.

Acknowledgements

This work has been funded by the Austrian COMET Program under the auspices of the Austrian Federal Ministry of Transport, Innovation and Technology (bmvit), the Austrian Federal Ministry of Economy, Family and Youth (bmwfj) and by the State of Styria (Styrian Funding Agency SFG). COMET is managed by the Austrian Research Promotion Agency FFG. The authors would like to thank GL Pharma for supplying the materials and providing the opportunity to work together with their experienced team.

5.5 References

[1] U.S. Food and Drug Administration, "Guidance for Industry. PAT - a framework for innovative pharmaceutical development, manufacturing, and quality assurance," US Department of Health, Rockville, MD., 2004.

[2] ICH, "ICH Q8(R2) (Pharmaceutical Development), ICH Q9 (Quality Risk Management), ICH Q10 (Pharmaceutical Quality System) and ICH Q11 (Development and Manufacture of Drug Substances)." [Online]. Available: http://www.ich.org/products/guidelines/quality/article/quality-guidelines.html.

[3] S. Adam, D. Suzzi, C. Radeke, and J. G. Khinast, "An integrated Quality by Design (QbD) approach towards design space definition of a blending unit operation by Discrete Element Method (DEM) simulation.," *Eur. J. Pharm. Sci.*, vol. 42, no. 1–2, pp. 106–15, Jan. 2011.

[4] M. Blanco, J. Coello, H. Iturriaga, S. Maspoch, and C. De Pezuela, "Near-infrared spectroscopy in the pharmaceutical industry," *Analyst*, vol. 123, no. August, pp. 135–150, 1998.

[5] T. De Beer, A. Burggraeve, M. Fonteyne, L. Saerens, J. P. Remon, and C. Vervaet, "Near infrared and Raman spectroscopy for the in-process monitoring of pharmaceutical production processes.," *Int. J. Pharm.*, vol. 417, no. 1–2, pp. 32–47, Sep. 2011.

[6] J. Luypaert, D. L. Massart, and Y. Vander Heyden, "Near-infrared spectroscopy applications in pharmaceutical analysis.," *Talanta*, vol. 72, no. 3, pp. 865–83, May 2007.

[7] G. Reich, "Near-infrared spectroscopy and imaging: basic principles and pharmaceutical applications.," *Adv. Drug Deliv. Rev.*, vol. 57, no. 8, pp. 1109–43, Jun. 2005.

[8] W. Li, L. Bagnol, M. Berman, R. A. Chiarella, and M. Gerber, "Applications of NIR in early stage formulation development. Part II. Content uniformity evaluation of low dose tablets by principal component analysis," *Int. J. Pharm.*, vol. 380, no. 1, pp. 49–54, 2009.

[9] P. Schoenmakers, R. Smits, A. Townshend, M. Blanco, and M. Alcalá, "Content uniformity and tablet hardness testing of intact pharmaceutical tablets by near infrared spectroscopy," *Anal. Chim. Acta*, vol. 557, no. 1, pp. 353–359, 2006.

[10] M. Blanco, M. Alcalá, J. M. González, and E. Torras, "A process analytical technology approach based on near infrared spectroscopy: tablet hardness, content uniformity, and dissolution test measurements of intact tablets.," *J. Pharm. Sci.*, vol. 95, no. 10, pp. 2137–44, Oct. 2006.

[11] R. P. Cogdill, C. A. Anderson, M. Delgado-Lopez, D. Molseed, R. Chisholm, R. Bolton, T. Herkert, A. M. Afnán, and J. K. Drennen, "Process analytical technology case study, part I: feasibility studies for quantitative near-infrared method development.," *AAPS PharmSciTech*, vol. 6, no. 2, pp. E262–72, Jan. 2005.

[12] R. P. Cogdill, C. A. Anderson, M. Delgado, R. Chisholm, R. Bolton, T. Herkert, A. M. Afnan, and J. K. Drennen, "Process analytical technology case study, part II: development and validation of quantitative near-infrared calibrations in support of a process analytical technology application for real-time release.," *AAPS PharmSciTech*, vol. 6, no. 2, pp. E273–83, Jan. 2005.

[13] S. H. Tabasi, R. Fahmy, D. Bensley, C. O'Brien, and S. W. Hoag, "Quality by design, part I: application of NIR spectroscopy to monitor tablet manufacturing process.," *J. Pharm. Sci.*, vol. 97, no. 9, pp. 4040–51, Sep. 2008.

[14] J. J. Moes, M. M. Ruijken, E. Gout, H. W. Frijlink, and M. I. Ugwoke, "Application of process analytical technology in tablet process development using NIR spectroscopy: blend uniformity, content uniformity and coating thickness measurements," *Int. J. Pharm.*, vol. 357, no. 1, pp. 108–118, 2008.

[15] S. H. Tabasi, R. Fahmy, D. Bensley, C. O'Brien, and S. W. Hoag, "Quality by design, part II: application of NIR spectroscopy to monitor the coating process for a pharmaceutical sustained release product.," *J. Pharm. Sci.*, vol. 97, no. 9, pp. 4052–66, Sep. 2008.

[16] M.-J. Lee, D.-Y. Seo, H.-E. Lee, I.-C. Wang, W.-S. Kim, M.-Y. Jeong, and G. J. Choi, "In line NIR quantification of film thickness on pharmaceutical pellets during a fluid bed coating process," *Int. J. Pharm.*, vol. 403, no. 1, pp. 66–72, 2011.

[17] J. D. Pérez-Ramos, W. P. Findlay, G. Peck, and K. R. Morris, "Quantitative analysis of film coating in a pan coater based on in-line sensor measurements.," *AAPS PharmSciTech*, vol. 6, no. 1, pp. E127–36, Jan. 2005.

[18] M. Andersson, S. Folestad, J. Gottfries, M. O. Johansson, M. Josefson, and K.-G. Wahlund, "Quantitative Analysis of Film Coating in a Fluidized Bed Process by In-Line NIR Spectrometry and Multivariate Batch Calibration," *Anal. Chem.*, vol. 72, no. 9, pp. 2099–2108, May 2000.

[19] A. D. Karande, P. W. S. Heng, and C. V. Liew, "In-line quantification of micronized drug and excipients in tablets by near infrared (NIR) spectroscopy: Real time monitoring of tabletting process.," *Int. J. Pharm.*, vol. 396, no. 1–2, pp. 63–74, Aug. 2010.

[20] H. W. Ward, D. O. Blackwood, M. Polizzi, and H. Clarke, "Monitoring blend potency in a tablet press feed frame using near infrared spectroscopy," *J. Pharm. Biomed. Anal.*, vol. 80, pp. 18–23, 2013.

[21] S. S. Sekulic, H. W. Ward II, D. R. Brannegan, E. D. Stanley, C. L. Evans, S. T. Sciavolino, P. A. Hailey, and P. K. Aldridge, "On-line monitoring of powder blend homogeneity by near-infrared spectroscopy," *Anal. Chem.*, vol. 68, no. 3, pp. 509–513, 1996.

[22] O. Scheibelhofer, N. Balak, P. R. Wahl, D. M. Koller, B. J. Glasser, and J. G. Khinast, "Monitoring Blending of Pharmaceutical Powders with Multipoint NIR Spectroscopy.," *AAPS PharmSciTech*, vol. 14, no. 1, pp. 234–44, Mar. 2013.

[23] O. Scheibelhofer, N. Balak, D. M. Koller, and J. G. Khinast, "Spatially Resolved Monitoring of Powder Mixing Processes via Multiple NIR-Probes," *Powder Technol.*

[24] Y. Sulub, B. Wabuyele, P. Gargiulo, J. Pazdan, J. Cheney, J. Berry, A. Gupta, R. Shah, H. Wu, and M. Khan, "Real-time on-line blend uniformity monitoring using near-infrared reflectance spectrometry: A noninvasive off-line calibration approach," *J. Pharm. Biomed. Anal.*, vol. 49, no. 1, pp. 48–54, 2009.

[25] C. V. Liew, A. D. Karande, and P. W. S. Heng, "In-line quantification of drug and excipients in cohesive powder blends by near infrared spectroscopy," *Int. J. Pharm.*, vol. 386, no. 1, pp. 138–148, 2010.

[26] M. C. Hennigan and A. G. Ryder, "Quantitative polymorph contaminant analysis in tablets using Raman and near infra-red spectroscopies," *J. Pharm. Biomed. Anal.*, vol. 72, pp. 163–171, 2013.

[27] D. Pan, G. Crull, S. Yin, and J. Grosso, "Low level drug product API form analysis – avalide tablet NIR quantitative method development and robustness challenges," *J. Pharm. Biomed. Anal.*, 2013.

[28] J. M. Amigo and C. Ravn, "Direct quantification and distribution assessment of major and minor components in pharmaceutical tablets by NIR-chemical imaging," *Eur. J. Pharm. Sci.*, vol. 37, no. 2, pp. 76–82, 2009.

[29] J. M. Prats-Montalbán, J. I. Jerez-Rozo, R. J. Romañach, and A. Ferrer, "MIA and NIR chemical imaging for pharmaceutical product characterization," *Chemom. Intell. Lab. Syst.*, vol. 117, pp. 240–249, 2012.

[30] A. Palou, J. Cruz, M. Blanco, J. Tomàs, J. de los Ríos, and M. Alcalà, "Determination of drug, excipients and coating distribution in pharmaceutical tablets using NIR-CI," *J. Pharm. Anal.*, vol. 2, no. 2, pp. 90–97, Apr. 2012.

[31] M. Blanco, R. Cueva-Mestanza, and A. Peguero, "NIR analysis of pharmaceutical samples without reference data: Improving the calibration," *Talanta*, vol. 85, no. 4, pp. 2218–2225, 2011.

[32] R. P. Cogdill, C. A. Anderson, and J. K. Drennen, "Process analytical technology case study, part III: calibration monitoring and transfer.," *AAPS PharmSciTech*, vol. 6, no. 2, pp. E284–97, Jan. 2005.

[33] S. Pieters, W. Saeys, T. Van den Kerkhof, M. Goodarzi, M. Hellings, T. De Beer, and Y. Vander Heyden, "Robust calibrations on reduced sample sets for API content prediction in tablets: Definition of a cost-effective NIR model development strategy," *Anal. Chim. Acta*, vol. 761, pp. 62–70, 2013.

[34] S. Sharma, M. Goodarzi, L. Wynants, H. Ramon, and W. Saeys, "Efficient use of pure component and interferent spectra in multivariate calibration," *Anal. Chim. Acta*, vol. 778, pp. 15–23, 2013.

[35] R. N. Feudale, N. A. Woody, H. Tan, A. J. Myles, S. D. Brown, and J. Ferré, "Transfer of multivariate calibration models: a review," *Chemom. Intell. Lab. Syst.*, vol. 64, no. 2, pp. 181–192, 2002.

[36] C. F. Pereira, M. F. Pimentel, R. K. H. Galvão, F. A. Honorato, L. Stragevitch, and M. N. Martins, "A comparative study of calibration transfer methods for determination of gasoline quality parameters in three different near infrared spectrometers," *Anal. Chim. Acta*, vol. 611, no. 1, pp. 41–47, 2008.

[37] E.-L. Bergman, H. Brage, M. Josefson, O. Svensson, and A. Sparén, "Transfer of NIR calibrations for pharmaceutical formulations between different instruments," *J. Pharm. Biomed. Anal.*, vol. 41, no. 1, pp. 89–98, 2006.

[38] W. R. Ketterhagen, J. S. Curtis, C. R. Wassgren, A. Kong, P. J. Narayan, and B. C. Hancock, "Granular segregation in discharging cylindrical hoppers: A discrete element and experimental study," *Chem. Eng. Sci.*, vol. 62, no. 22, pp. 6423–6439, 2007.

[39] N. Standish, "Studies of size segregation in filling and emptying a hopper," *Powder Technol.*, vol. 45, no. 1, pp. 43–56, 1985.

[40] A. D. Rosato, D. L. Blackmore, N. Zhang, and Y. Lan, "A perspective on vibration-induced size segregation of granular materials," *Chem. Eng. Sci.*, vol. 57, no. 2, pp. 265–275, 2002.

[41] D. Huerta and J. Ruiz-Suárez, "Vibration-Induced Granular Segregation: A Phenomenon Driven by Three Mechanisms," *Phys. Rev. Lett.*, vol. 92, no. 11, p. 114301, Mar. 2004.

The scientific man does not aim at an immediate result.
He does not expect that his advanced ideas will be readily taken up...
His duty is to lay the foundation for those who are to come, and point the way.

Nikola Tesla

6. Summary and Outlook

6.1 Summary of Major Findings

The chapters 2-4 comprise the application of NIR spectroscopy, photometric stereo image analysis and process data monitoring to hot melt extrusion.

In chapter 2 monitoring of the API content in the die section was shown. The die section was modified to allow representative monitoring of the melt. Using this setup the criticality of the influential factors (feeders, screw design and screw speed) on CU were determined. The findings are:

- The die section was designed according to the theory of sampling. The shear rate in the vicinity of the NIR probe was increased by forcing the melt in an annular flow, resulting in higher material exchange rates.
- A chemometric model was developed in a range of 0% to 60% API content. Predictions were in good agreement with the pre-set API content (as determined via feeding rates) and with the offline HPLC reference measurements.
- Designed experiments were performed to evaluate the influential factors on CU. By analyzing the SD of the API profile the screw design was identified having the highest impact on CU. Employing two feeders simultaneously caused a higher SD, probably due to the superposition of the feeder fluctuations.

A broader view, how PAT tools are integrated in an HME process, its downstream processes and into computerized systems, was presented in chapter 3. In this book chapter the requirements and challenges for continuous manufacturing and process monitoring have been discussed:

- Continuous extrusion: Development of a stable process, including feeding, extrusion and downstream processes, depends on the specific formulation. Feeding performance strongly impacts CU.
- Downstream: There is a strong coupling between upstream and downstream processes. Thus control strategies for process disturbances are needed.
- PAT analyzers: A wide variety of analyzers is available, but they need to be carefully adapted to the process. A suitable sensor position needs to be determined. Use cases for monitoring of process parameters, qualitative and quantitative process analysis are given.
- Computerized systems: PAT analyzers and process data need to be integrated into a central system. Therefore GMP requirements for computerized systems need to be met.

In chapter 4 four different implementations of a photometric stereo imaging system to monitor pellets produced by HME and die-face pelletizing are compared. The findings are:

- Challenges regarding the low volume fraction of particles in the transportation air and a random orientation of particles had to be overcome. Therefore several implementation approaches were compared. Monitoring of pellets separated from the transportation air, immediately after falling off the edge of a vibratory conveyor, showed the best results.
- The reduction in the volume mean particle size of the pellets by increasing the pelletizer rotational speed could be accurately monitored and was verified offline with QICPIC.
- Photometric stereo image analysis is a suitable tool to monitor the particle size distribution and shape of pellets produced by hot melt extrusion with hot die-face pelletizing.

Chapter 5 encompasses a staged approach for optimizing an existing tablet production. Therefore inline NIR measurements were compared to UV-Vis analysis of sampled tablets, resulting in the following findings:

- Analyzing the spectroscopic data of a tableting process with PCA indicated that the end of the process was critical. Further comparison of drawn samples and inline predicted powder composition confirmed the findings, and corrective actions were suggested.
- A PLS model was created in the laboratory using a mixture design, varying API and the two main excipients by ± 20% relative to their nominal value. The model was transferred to inline monitoring using local centering and a calculated transfer sample.
- Inline analysis proved to have distinct advantages because it created a more complete picture of the process than the AV, which is only a single statistical number.
- Conventional process and quality control may fail to determine the significance and effects of those critical events. Comparing the drawn samples and inline data raised important questions regarding USP 905 “Uniformity of Dosage Units”, including: “Does drawing a handful of tablets still constitute the state of the art for quality control or would it be wise to demand inline measurements?”

6.2 Outlook

PAT has received significant attention in the scientific literature. Also a necessary shift from proof of concept studies to real-life implementations in pharmaceutical manufacturing has clearly begun. A driver for this shift is the growing up of PAT, from laboratory tools for rare specialists to delivering business value. The number of successful PAT implementations will strongly depend on the robustness of the PAT methods under (varying) process conditions. Low robustness would notably drive the costs for model maintenance and PAT implementations likely would not pay off.

One aspect, which can improve robustness, is the separation of scattering and absorption effects for spectroscopic measurements. But a common approach of acquiring reflectance and transmittance spectra is not a feasible option for inline measurements. Several possible solutions for this problem have been proposed: EMSC, MCR-ALS and SRS. EMSC, a preprocessing method, allows using prior-knowledge about the spectra of the analytes and interference effects [1], [2]. For MCR-ALS reflection and transmission measurement of a single tablet with an integrating sphere are performed once [3]. The scattering and absorption spectra are then used as hard model constraints of an MCR-ALS modeling algorithm. For SRS the probe needs to be in contact with the sample to collect spectra as a function of the distance, which light propagated in the sample. The setup consists of one illuminating fiber and several detection fibers in varying distances, as proposed by Nguyen Do Trong *et al.* [4]. Additionally simulating the penetration of light into scattering media can help to gain deeper understanding.

The scattering and adsorption behavior might be altered, if process parameters are changed to a new set point. Exemplarily, in hot melt extrusion the influences of material temperature, moisture and pressure on spectroscopic and ultrasound measurements is known, but not yet fully understood or systematically measured. Therefore attention should be paid when using chemometric models. Finding *any* correlation using PLS between spectra and a target value usually is fairly simple. But if process parameters change significantly, it is quite likely to get wrong estimations. The crucial point is to really understand the sources of scattering and adsorption in order to separate them, as well as knowing the influence of other process parameters on the spectrum. Only by then chemometric models are more than “just correlations”. Alternatively hierarchical models can be developed, which include the spectra, as well as important process parameters, which might influence the result (e.g. temperature). Thus, by taking into account the influential factors, the predictions can be corrected. In this field extensive further research will be required to ensure accurate model performance across a larger operating space.

Low dose monitoring poses another challenge for spectroscopy. NIR monitoring of contents around or below 1% with good accuracy is extremely difficult or not possible at all. Raman and LIF show potential to shift the limits of detection down to the sub-percentage region. The demand of the pharmaceutical industry for inline low dose monitoring is obvious, because many APIs are highly potent (e.g., hormones, cancer treatments).

Finally in the author's opinion, a combination of multi- and univariate data will be of major interest for future developments and might be called a must-have for advanced process control strategies.

By ensuring robust measurements as reliable inputs for a whole process-chain control strategy, the future of PAT in the pharmaceutical industry is assured. But, as mentioned in the chapter "Motivation", there is still a long road ahead to *Plantopia* [5]. Let's keep on walking.

6.3 References

[1] H. Martens and E. Stark, "Extended multiplicative signal correction and spectral interference subtraction: new preprocessing methods for near infrared spectroscopy," *J. Pharm. Biomed. Anal.*, vol. 9, no. 8, pp. 625–635, 1991.

[2] H. Martens, J. P. Nielsen, and S. B. Engelsen, "Light scattering and light absorbance separated by extended multiplicative signal correction. Application to near-infrared transmission analysis of powder mixtures," *Anal. Chem.*, vol. 75, no. 3, pp. 394–404, Feb. 2003.

[3] N. K. Afseth and A. Kohler, "Extended multiplicative signal correction in vibrational spectroscopy, a tutorial," *Chemom. Intell. Lab. Syst.*, vol. 117, pp. 92–99, Aug. 2012.

[4] N. Nguyen Do Trong, C. Erkinbaev, M. Tsuta, J. De Baerdemaeker, B. Nicolaï, and W. Saeys, "Spatially resolved diffuse reflectance in the visible and near-infrared wavelength range for non-destructive quality assessment of 'Braeburn' apples," *Postharvest Biol. Technol.*, vol. 91, pp. 39–48, May 2014.

[5] A. Gonce and U. Schrader, "Plantopia? A mandate for innovation in pharma manufacturing," in *Operations for the Executive Suite*, D. Keeling and U. Schrader, Eds. 2012, pp. 9–22.

7. Publications

Peer-Refereed Journals

P.R. Wahl, G. Fruhmann, S. Sacher, G. Straka, S. Sowinski, and J.G. Khinast, "PAT for Tableting: Inline Monitoring of API and Excipients via NIR Spectroscopy.," Eur. J. Pharm. Biopharm., submitted 2014

D. Treffer, P.R. Wahl, T. Hörmann, D. Markl, S. Schrank, I. Jones, P. Cruise, R.-K. Mürb, G. Koscher, E. Roblegg and J.G. Khinast, "In-line Quality Analysis of Continuously-Produced Pharmaceutical Pellets.," Int. J. Pharm., submitted, 2013.

P.R. Wahl, D. Treffer, S. Mohr, E. Roblegg, G. Koscher, and J.G. Khinast, "Inline monitoring and a PAT strategy for pharmaceutical hot melt extrusion.," Int. J. Pharm., vol. 455, no. 1–2, pp. 159–68, 2013.

O. Scheibelhofer, N. Balak, P. R. Wahl, D. M. Koller, B. J. Glasser, and J. G. Khinast, "Monitoring Blending of Pharmaceutical Powders with Multipoint NIR Spectroscopy.," *AAPS PharmSciTech*, vol. 14, no. 1, pp. 234–44, Mar. 2013.

D. Markl, P. R. Wahl, J. C. Menezes, D. M. Koller, B. Kavsek, K. Francois, E. Roblegg, and J. G. Khinast, "Supervisory control system for monitoring a pharmaceutical hot melt extrusion process.," *AAPS PharmSciTech*, vol. 14, no. 3, pp. 1034–44, Sep. 2013.

Book Chapter

D. Treffer, P.R. Wahl, D. Markl, G. Koscher, E. Roblegg, and J.G. Khinast, "Hot Melt Extrusion as a Continuous Pharmaceutical Manufacturing Process.," in *Melt Extrusion: Equipment and Pharmaceutical Applications*, M. Repka, Ed. Springer Publishers, 2013, pp. 363–396.

Conference Proceedings

P.R. Wahl, D. Markl, D. Treffer, G. Koscher, E. Roblegg, and J.G. Khinast, "PAT Solution for Inline Content Homogeneity Monitoring with NIR for Pharmaceutical Hot Melt Extrusion.," in *Book of Abstracts 8. Minisymposium,* JKU Linz, 2012, pp. 71 – 74

P.R. Wahl, O. Scheibelhofer, D.M. Koller, J.G. Khinast, J, "Application of Process Analytical Technology (PAT) in Pharmaceutical Production.," in *Book of Abstracts 7. Minisymposium*, TU Graz, 2011, pp. 197 – 199

Talks

P.R. Wahl, D. Markl, D. Treffer, S. Sacher, G. Koscher, E. Roblegg and J.G. Khinast, "PAT for Pharmaceutical Extrusion: In-line Monitoring of Drug Content with NIR.," in *PAT & QbD Meeting 2013*, Dresden, 2013

P.R. Wahl, D. Markl, D. Treffer, S. Sacher, J.C. Menezes, G. Koscher, E. Roblegg and J.G. Khinast, "PAT for Pharmaceutical Extrusion Monitoring and Supervisory Control.," in *AIChE 2012 Annual Meeting*, Pittsburgh, 2012

D. Markl, P.R. Wahl, J.G. Khinast, B. Kavsek, K. Francois and P. Lederer, "Continuous Pharmaceutical Manufacturing with Hot Melt Extrusion.," in *EuPAT 5 – Continuous Innovation in Process Analytics & Control*, Ghent, 2012

D. Markl, B. Kavsek, P.R. Wahl, D.M. Koller, K. Francois and J.G. Khinast, "Demonstration of a Pharmaceutical Hot Melt Extrusion Process with SIPAT.," in *IFPAC 12 Annual Meeting*, Baltimore, 2012

P.R. Wahl, D. Markl, D. Treffer, G. Koscher, E. Roblegg and J.G. Khinast, "PAT Solution for Inline Content Homogeneity Monitoring with NIR for Pharmaceutical Hot Melt Extrusion.," in *8. Minisymposium der Verfahrenstechnik*, Linz, 2012

P.R. Wahl, D. Markl, D. Treffer, D.M. Koller, G. Koscher, E. Roblegg and J.G. Khinast, "Full PAT Solution for Real-Time Process Control of a Pharmaceutical Hot Melt Extruder (HME).," in *8th WorldMeeting on Pharmaceutics, Biopharmaceutics and Pharmaceutical Technology*, Istanbul, 2012

Posters

D. Treffer, P.R. Wahl, T.R. Hörmann, D. Markl, A. Eitzlmayr, S. Schrank, G. Koscher, E. Roblegg and J.G. Khinast, "Implementation of a Novel Particle Size Measurement Tool to Monitor Pellet Produced by Hot Melt Extrusion and Die Face Pelletizing.," in *AIChE Annual Meeting 2013*, San Francisco, 2013

P.R. Wahl, D. Treffer, D. Markl, G. Koscher, E. Roblegg and J.G. Khinast, "Developing a PAT Strategy for Pharmaceutical Hot Melt Extrusion.," in *EuPAT 5 Continuous Innovation in Process Analytics & Control*, Ghent, 2012

P.R. Wahl, O. Scheibelhofer, D.M. Koller, G. Straka, F. Reiter, M. Schlingmann and J.G. Khinast, "Industrial PAT Use Cases.," in *5th International Congress on Pharmaceutical Engineering*, Graz, 2011

D. Markl, P.R. Wahl, D.M. Koller, J.G. Khinast, B. Kavsek, P. Lederer and K. Francois, "SIPAT for Monitoring of a Pharmaceutical Hot Melt Extrusion Process.," in *7. Kolloquium Prozessanalytik*, Linz, 2011

P.R. Wahl, O. Scheibelhofer, D.M. Koller, G. Straka, F. Reiter, M. Schlingmann and J.G. Khinast, "NIR as a PAT Tool in Pharmaceutical Manufacturing.," in *7. Kolloquium Prozessanalytik*, Linz, 2011

P.R. Wahl, O. Scheibelhofer, D.M. Koller and J.G. Khinast, "Application of Process Analytical Technology (PAT) in Pharmaceutical Production.," in *7. Minisymposium Verfahrenstechnik*, Graz, 2011